INVESTIGATION OF REACTIONS BETWEEN BARIUM COMPOUNDS AND TUNGSTEN IN A SIMULATED RESERVOIR HOLLOW CATHODE ENVIRONMENT

A Thesis
Presented to
The Academic Faculty

By

Laura Schoenbeck

In Partial Fulfillment
Of the Requirements for the Degree
Master of Science in Materials Science and Engineering

Georgia Institute of Technology

February 2005

INVESTIGATION OF REACTIONS BETWEEN BARIUM COMPOUNDS AND TUNGSTEN IN A SIMULATED RESERVOIR HOLLOW CATHODE ENVIRONMENT

Approved by:

Dr. D. Norman Hill, Advisor
School of Materials Science & Engineering
Georgia Institute of Technology

Dr. Joe K. Cochran, Jr.
School of Materials Science & Engineering
Georgia Institute of Technology

Dr. Robert F. Speyer
School of Materials Science & Engineering
Georgia Institute of Technology

Date Approved: February 25, 2005

ACKNOWLEDGEMENTS

I would like to express my gratitude to the many people who have helped me to complete this work. First of all, I would also like to acknowledge the support of Dr. James E. Polk in the Advanced Propulsion Technology Group at the Jet Propulsion Laboratory for his support of this research.

I would like to thank my advisor, Dr. D. Norman Hill, for all of his support over the past couple of years. Not only did his direction help to broaden my knowledge of materials science and the research process, but the guidance he gave me on my career and life was also invaluable.

I would also like to thank Dr. Joe Cochran, Dr. Wayne Ohlinger, and Dr. Robert Speyer for serving on my committee. I am very grateful for the time they took to read my thesis, and their valuable suggestions and revisions truly helped to improve the quality of this document. In addition, I would like to thank Dr. Robert Snyder for taking time out of his busy schedule to offer me guidance on the quantitative x-ray diffraction work.

None of this work would have been possible without Richard Shafer who assisted me with semi-quantitative analysis, set up the furnace and TGA systems used in these experiments, and taught me many valuable skills in the laboratory that I will be able to use throughout my career. Richard was always willing to help out whenever I needed him (even on weekends!), and for that I am deeply grateful.

I want to thank all of my fellow graduate students in the School of Materials Science & Engineering at Georgia Tech for making my time in Atlanta very enjoyable and

truly unforgettable. I would especially like to thank Jelila Mohammed, Erin Campone-schi, and Jeremy Walker for being such wonderful friends.

I owe my deepest gratitude to my parents for providing me with the support I needed in order to pursue this opportunity. The constant love and encouragement they have provided me throughout my life is truly an inspiration to me.

Finally, I would like to thank my wonderful fiancé R.J. for being there for me during this whole process. I am truly grateful to him for his patience and for helping me to keep everything in my life in perspective.

TABLE OF CONTENTS

LIST OF TABLES

LIST OF FIGURES

NOMENCLATURE

311	$3BaO{\cdot}CaO{\cdot}Al_2O_3$ or $Ba_3CaAl_2O_7$
411	$4BaO{\cdot}CaO{\cdot}Al_2O_3$ or $Ba_4CaAl_2O_8$
532	$5BaO{\cdot}3CaO{\cdot}2Al_2O_3$ or $Ba_5Ca_3Al_4O_{14}$
612	$6BaO{\cdot}CaO{\cdot}2Al_2O_3$ or $Ba_6CaAl_4O_{13}$
BCA	$BaO{\cdot}CaO{\cdot}Al_2O_3$ or $BaCaAl_2O_5$
B_2CA	$2BaO{\cdot}CaO{\cdot}Al_2O_3$ or $Ba_2CaAl_2O_6$
B_3A	$3BaO{\cdot}\ Al_2O_3$ or $Ba_3Al_2O_6$
B_4A	$4BaO{\cdot}\ Al_2O_3$ or $Ba_4Al_2O_7$
B_4A_{SSL}	Substitutional solid solution limit of Ca in B_4A, or $Ba_{2.9}Ca_{1.1}Al_2O_7$
$B_{11}C_6A_4$	$11BaO{\cdot}6CaO{\cdot}4Al_2O_3$ or $Ba_{11}Ca_6Al_8O_{29}$

SUMMARY

Reservoir-type dispenser hollow cathodes are currently being developed for use on NASA's Prometheus 1 mission. In these cathodes, the reaction between a barium source material and tungsten powder contained in a cavity surrounding a porous tungsten emitter produces barium vapor which is crucial to operation of the cathode.

The primary objective of this research was to investigate the reactions between tungsten and a commercial barium source material in a simulated reservoir hollow cathode environment. Mixtures of tungsten and a barium calcium aluminate material were sealed inside molybdenum capsules with porous tungsten closures and heated to 1000ºC, 1200ºC, and 1300ºC for 100, 200, and 400 hours. Based on the reaction products, which were identified to be $BaAl_2O_4$ and Ba_2CaWO_6, a reaction was proposed for the barium calcium aluminate material with tungsten. The bottom pellets in the capsules were found to have reacted to a much further extent than the top pellets in all of the samples, possibly due to a temperature gradient or excessive moisture in the base of the capsules. Quantitative and semi-quantitative x-ray analysis results did not show a clear trend as to how the concentrations of $BaAl_2O_4$ and Ba_2CaWO_6 vary with time.

Most of the barium source materials are hygroscopic, and hydration of the materials would substantially reduce the performance of the cathode. Therefore, the environmental stability of several barium compounds, $3BaO\cdot Al_2O_3$ (B_3A), $6BaO\cdot CaO\cdot 2Al_2O_3$ (612), $4BaO\cdot CaO\cdot Al_2O_3$ (411), $Ba_{2.9}Ca_{1.1}Al_2O_7$ (B_4A_{SSL}), and $Ba_3Sc_4O_9$, were investigated in order to evaluate their suitability for use as barium source materials. A microbalance was used to measure weight gain of the materials as they were exposed to dew

points of –15ºC and 11ºC at room temperature. The results showed that B_3A hydrated more extensively than any of the other materials tested in the low- and intermediate-humidity environments, while the 612, 411, and B_4A_{SSL} materials were all reasonably stable in the low-humidity environment. The $Ba_3Sc_4O_9$ was extremely stable compared to the barium aluminates in the intermediate-humidity conditions.

CHAPTER 1

INTRODUCTION

For over thirty years, NASA has relied on chemical systems for propulsion on deep-space missions; however, chemical propulsion cannot meet velocity change (ΔV) requirements consistent with reasonable trip times nor provide spacecraft maneuverability capabilities consistent with future complex missions. Therefore, NASA has been investigating the use of nuclear power systems coupled with electric propulsion which would not only vastly increase the amount of power available for advanced experimental payloads and reduce transit times associated with outer planet and Kuiper Belt missions, but it would also enable multi-destination missions that aren't currently possible using chemical propulsion.

In nuclear electric propulsion, the spacecraft is launched from Earth by a traditional chemical rocket; then once in space, the spacecraft is powered by a small nuclear reactor. Nuclear fission in the reactor generates heat that is converted to electrical power. This power is then used by the electric propulsion system to produce xenon ions, which are accelerated to extremely high velocities by potentials applied to a grid system, thus expelling the ions from the engine to generate thrust. NASA's first proposed mission that would use nuclear electric propulsion is the Jupiter Icy Moons Orbiter (JIMO) which will orbit three moons of Jupiter to investigate their makeup and their potential for sustaining life.

Each thruster on the spacecraft will contain a dispenser cathode that produces electrons to ionize the xenon gas. A critical component of the cathode is the barium

source material that reacts with a reducing agent, typically tungsten, to form free barium which diffuses to the surface of the porous tungsten emitter forming an adsorbed monolayer of barium-oxygen dipoles. The dipoles significantly lower the work function of the tungsten surface, from about 4.5 eV to approximately 2.0 eV, and hence the operating temperature of the cathode, which can significantly impact cathode lifetime.

The only previous NASA mission which utilized ion propulsion, Deep Space 1, made use of an impregnated-type dispenser cathode insert fabricated by infiltrating molten barium source material into the pores of the tungsten insert. Unfortunately, the build up of reaction products in the pores can limit the life of the cathode by precluding the diffusion of barium vapor to the surface of the emitter. An impregnated-type dispenser cathode insert identical to that used on NASA's Deep Space 1 mission demonstrated a lifetime of 32,000 hours during a ground based test of a flight spare engine. Because the JIMO mission will require a lifetime of at least 100,000 hours and because the anticipated power demand of about 30 kW per engine will require high operating temperatures, it is expected that the impregnated-type cathodes will not be able to meet these needs.

Therefore, reservoir-type dispenser hollow cathodes are being developed to replace the impregnated-type dispenser cathode inserts. These reservoir hollow cathodes consist of an annular reservoir or cavity filled with a mixture of the barium source material and tungsten powder which surrounds the thin-walled cylindrical porous tungsten emitter. The source material reacts with the tungsten within the reservoir to form free barium which diffuses to the surface of the porous tungsten emitter. The reservoir hollow cathodes will allow provision of a larger supply of the barium source material than that of

the impregnated-type cathodes, and the configuration should prevent the build up of reaction products which are believed to play a role in limiting impregnated cathode life.

Several reservoir-type cathodes of the configuration typically used in microwave tubes are currently on long-term life test at Crane Division, Naval Surface Warfare Center. These cathodes employ BaO powder as the barium source material in the reservoir. Upon heating, the BaO evaporates and flows through a porous tungsten plug welded to the top of the reservoir where it is reduced to Ba, which then diffuses to the surface of the cathode to reduce the work function of the tungsten. While the use of BaO as the source material would seem to be a more straightforward solution to creating the barium monolayer on the cathode, BaO is, unfortunately, extremely hygroscopic. Because the cathodes for the JIMO mission could potentially be exposed to a high-humidity environment prior to launch, it is necessary to use environmentally stable materials in the hollow cathode reservoir of each ion thruster. Thus, the reservoir hollow cathodes must rely upon the reaction between a more complex barium source material and tungsten powder in order to produce the necessary barium vapor.

The rate of reaction between the barium compound and tungsten to form Ba/BaO vapor is critically important to the life of the cathode. While the reaction must proceed rapidly enough to provide sufficient Ba to maintain a monolayer on the surface of the emitter, exhaustion of the available barium within the source material will mark the end of cathode life. While previous studies have examined the reaction of commercial cathode impregnant materials and tungsten powder, there has never been a study of the reactions under conditions similar to the actual operating conditions in a microwave tube or ion thruster. Furthermore, it is virtually impossible to extract the reaction products from

the tungsten matrix in order to determine the extent of reaction in impregnated cathodes that have been operated to end of life.

The primary objective of this research was to investigate the reactions between tungsten and a commercial barium calcium aluminate source material in a simulated reservoir hollow cathode environment. Experiments were designed to identify the reaction products and to study how the reaction products affected the barium supply. By studying the reactions for varying time periods under isothermal conditions, a diffusion-couple model could be employed to predict extended life time of a hollow cathode using the barium calcium aluminate source material.

Mixtures of tungsten and a barium calcium aluminate material were sealed inside molybdenum capsules with porous tungsten closures. The samples were heated to elevated temperatures for extended periods of time under vacuum. Quantitative x-ray diffraction analysis was performed to determine the reaction products, which provided a means to model the reaction kinetics between the barium source material and tungsten.

Most barium source materials are hygroscopic, and there is anecdotal evidence which indicates that hydration of the source materials would substantially reduce the performance of the cathode. Hydration of the materials could lead to release of water vapor upon heating during activation of the cathode and subsequent oxidation of the tungsten emitter, which would increase the work function of the tungsten and thus, at least, increase the operating temperature and, at worst, render the cathode inoperable. Furthermore, since hydration of the materials results in a substantial increase in their volume, the source materials could potentially expand sufficiently to crack the welds sealing the reservoir or fracture the porous tungsten emitter.

Thus, a secondary objective of this research was to investigate the sensitivity of various barium source materials to atmospheric moisture. A microbalance was used to measure weight gain of several barium compounds as they were exposed to low- and intermediate-humidity environments, and the results allowed direct comparison of the materials and evaluation of their suitability for use as barium source materials.

CHAPTER 2

LITERATURE REVIEW

In order to study the reactions between barium compounds and tungsten in a reservoir hollow cathode environment, it is first necessary to understand the phase equilibria in the $BaO\text{-}Al_2O_3$, $BaO\text{-}CaO\text{-}Al_2O_3$ and $BaO–Sc_2O_3$ systems. This survey will also include some previously reported information on reactions in thermionic dispenser cathodes, and several solid-state reaction kinetics models will be introduced in order to aid in the analysis of cathode lifetime. The vapor pressure of barium inside the cathode and the evaporation rate of barium from the cathode also play an important role in determining the lifetime of the cathode. Therefore, various vapor pressure measurement techniques will be discussed along with a summary of previous work on barium and barium oxide vapor pressures. Finally, evaporation rate values will be presented for dispenser cathodes impregnated with various barium compounds.

The $BaO\text{-}Al_2O_3$ Binary System

Wartenberg & Reusch[1] discovered the first compound in the $BaO\text{-}Al_2O_3$ system: $BaAl_2O_4$. Shortly after, Toropov[2] discovered two additional barium aluminate compounds: $Ba_3Al_2O_6$ and $BaAl_{12}O_{19}$. Toropov and Galakhov[3] created the first phase diagram for the $BaO\text{-}Al_2O_3$ system which is shown in Figure 2.1. Toropov and Galakhov reported the melting points of $BaAl_2O_4$, $Ba_3Al_2O_6$, and $BaAl_{12}O_{19}$ to be 1830ºC, 1750ºC, and 1900ºC, respectively.

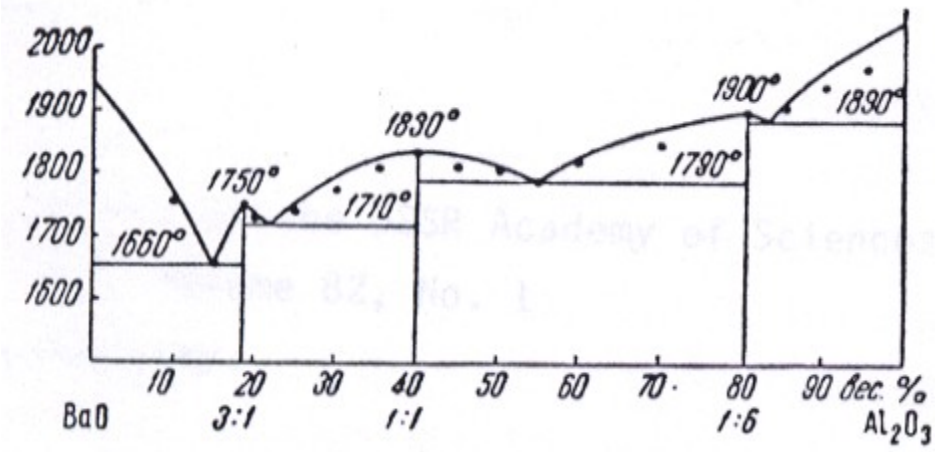

Figure 2.1. Binary Phase Diagram of the BaO-Al_2O_3 System by Toropov and Galakhov.[3]

Appendino[4] studied the high-baria portion of the binary system between BaO and $Ba_3Al_2O_6$. He identified five new phases by x-ray diffraction: $Ba_4Al_2O_7$, stable above 940º C; $Ba_5Al_2O_8$, stable at 940ºC; $Ba_7Al_2O_{10}$, stable at 1050ºC; $Ba_8Al_2O_{11}$, stable above 1050ºC; and $Ba_{10}Al_2O_{13}$, stable at 1130ºC. The portion of the phase diagram developed by Appendino is shown in Figure 2.2.

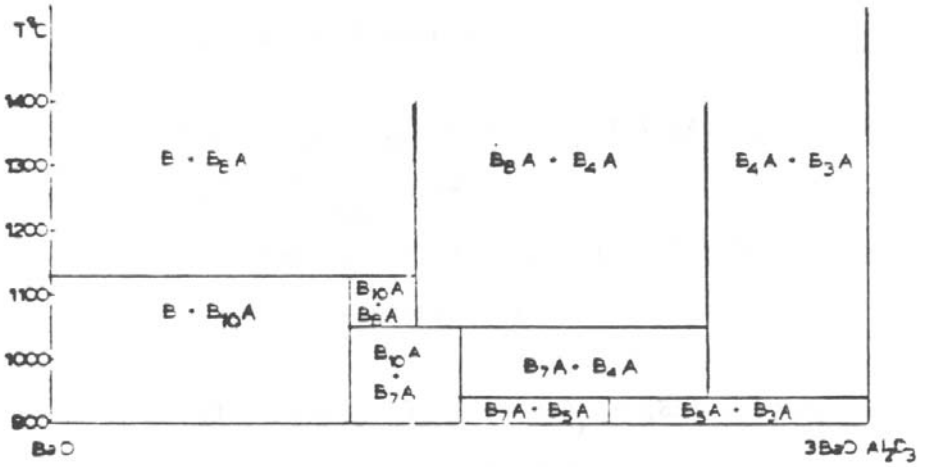

Figure 2.2. High-Baria Portion of the BaO-Al_2O_3 System by Appendino.[4]

The High-Baria Portion of the $BaO–CaO–Al_2O_3$ Ternary System

Early investigators of the BaO-CaO-Al_2O_3 system encountered difficulties in studying the high-baria portion. Samples totaling more than 75 mol% CaO and BaO were difficult to prepare because they reacted with platinum crucibles, atmospheric moisture, and carbon dioxide. Appendino[5] was the first individual to successfully study the high-baria portion of the BaO-CaO-Al_2O_3 ternary system, creating the isothermal section of this system at 1250ºC, illustrated in Figure 2.3. Appendino reported the substitution limits of Ca ions for Ba in BaO, $Ba_8Al_2O_{11}$, $Ba_4Al_2O_7$, and $Ba_3Al_2O_6$ to be 0%, 2.5%, 10%, and 25%, respectively. While investigating the solid solubility of CaO in $Ba_4Al_2O_7$, Appendino reported the existence of a new ternary phase: $Ba_3CaAl_2O_7$.

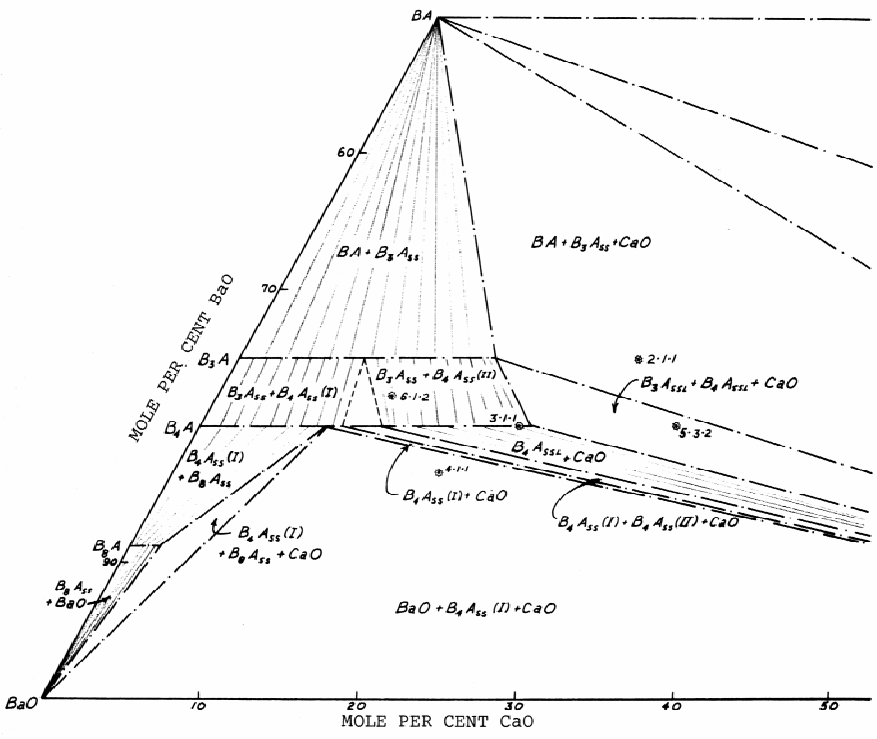

Figure 2.3. Isothermal Section of the High-BaO Portion of the BaO-CaO-Al_2O_3 Phase Diagram at 1250ºC by Appendino.[5]

Wolten[6] suggested that $Ba_3CaAl_2O_7$ may not be a unique compound but one of a series of solid solution compositions along the $Ba_4Al_2O_7 – B_{4-x}Ca_xAl_2O_7$ ($0<x<?$) join.

Asselanis[7] used the classical thermal arrest method to determine the solidus and liquidus temperatures for compositions in the high-baria portion of the $BaO\text{-}CaO\text{-}Al_2O_3$ system, including those corresponding to the common commercial impregnants $3BaO\cdot CaO\cdot Al_2O_3$ (311), $5BaO\cdot 3CaO\cdot 2Al_2O_3$ (532), and $4BaO\cdot CaO\cdot Al_2O_3$ (411). In this region, he found that the solidus temperatures ranged from 1650ºC - 1800ºC, and the liquidus temperatures ranged from 1750ºC - 1900ºC.

Tarter[8] refined the measurements of the solidus and liquidus temperatures of 311, 532, and 411. In addition, he determined the melting characteristics of five additional commercial impregnant compositions: $6BaO\cdot CaO\cdot 2Al_2O_3$ (612), $11BaO\cdot 6CaO\cdot 4Al_2O_3$ ($B_{11}C_6A_4$), $2BaO\cdot CaO\cdot Al_2O_3$ (B_2CA), & $BaO\cdot CaO\cdot Al_2O_3$ (BCA). Tarter reported that the solidus temperatures for the seven compositions ranged from 1490ºC – 1585ºC, while the liquidus temperatures ranged from 1690ºC - 1835ºC.

Hill, Hann, and Suitch[9] studied the melting characteristics of forty compositions in the high-baria portion of the $BaO\text{-}CaO\text{-}Al_2O_3$ system. They constructed vertical sections that described the crystallization paths along the non-binary planes in the system and isothermal sections at 1100ºC and 1475ºC that described the sub-solidus equilibria. They determined the solubility limits of calcium in $Ba_3Al_2O_6$ and $Ba_4Al_2O_7$ to be 18.8 mol% and 20.5 mol%, respectively.

The $BaO–Sc_2O_3$ Binary System

In 1974, Kwestroo, van Hal, and Langereis[10] reported the existence of three compounds in the $BaO\text{-}Sc_2O_3$ system: $Ba_2Sc_2O_5$, $Ba_3Sc_4O_9$, and $BaSc_2O_4$. Persianova, Soloveichik, and Yudinskaya[11] proposed the existence of another compound, $Ba_3Sc_2O_6$, but further studies by Kovba, Lykova, Paromova, and Kalinina[12] concluded that $Ba_3Sc_2O_6$ does not exist in this system.

Magnus[13] found that $BaSc_2O_4$ decomposed in the range 1100-1200ºC, which did not agree with the previously published phase diagrams for the $BaO\text{-}Sc_2O_3$ binary system. Therefore, she proposed a new binary phase diagram, shown in Figure 2.4. Janowski[14] suggested the possible existence of a more baria rich compound than $Ba_2Sc_2O_5$, namely $Ba_4Sc_2O_7$. However, she reported that $Ba_3Sc_4O_9$ is the most baria rich phase that is stable at high temperatures.

Hydration of Barium Source Materials

Hydration of the barium source materials can seriously impact the performance of either a reservoir or impregnated dispenser cathode. Reactions between the barium compounds and the atmosphere can have several potentially damaging effects.[15] First of all, these reactions form a reaction product with a larger volume than the original materials. In extreme cases, this volume expansion can lead to cracking of the tungsten matrix in impregnated cathodes. Also, subsequent heating of the impregnant materials after hydration leads to decomposition of the hydrates, and the evolving gaseous products could potentially crack the tungsten matrix. Furthermore, the gaseous decomposition

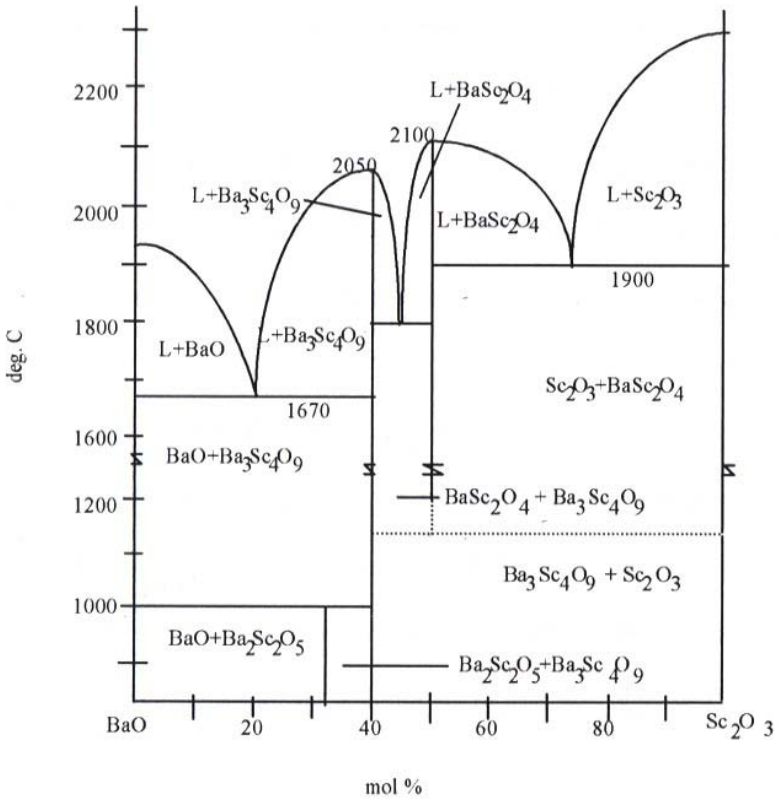

Figure 2.4. Binary Phase Diagram of the BaO-Sc_2O_3 System by Magnus.[13]

products can oxidize the tungsten matrix, causing it to react rapidly with the impregnant material to form complex tungstates.

Toropov,[2] who discovered $Ba_3Al_2O_6$, reported that it is very soluble in water and highly hygroscopic. While studying the BaO-Al_2O_3 system, Wallmark and Westgren[16] encountered difficulties in performing x-ray analysis on BaO and aluminates containing more than 50 mol. % BaO because they reacted so rapidly with moisture in the air. A number of people have studied the materials which form during the hydration of barium compounds, including $Ba(OH)_2$, $Ba(OH)_2 \cdot H_2O$, $Ba(OH)_2 \cdot 2H_2O$, and $Ba(OH)_2 \cdot 8H_2O$. Ahmed and Dent Glasser[17] reported the existence of a new barium aluminate hydrate: $Ba_2Al_2H_4O_7$.

Habashy and Kolta[18] studied the thermal dehydration of barium hydroxide octa-hydrate. They reported that initial heating leads to the formation of the dihydrate then the monohydrate which eventually decompose to anhydrous barium hydroxide at 375ºC. In an inert atmosphere, the anhydrous barium hydroxide then decomposes to BaO at 410ºC.

Ohlinger and Rebstock[15] studied the effects of exposing 411 to sea level ambient atmospheric conditions and characterized the decomposition behavior of the reaction products. After exposing 411 to atmospheric conditions for several hundred hours, they observed total weight gains of up to 40% of the anhydrous weight of the 411. They used x-ray diffraction to identify the reaction products between the 411 and the atmospheric water vapor and carbon dioxide as barium hydroxide octahydate, calcium hydroxide, and barium carbonate.

Ohlinger and Rebstock also used thermogravimetric analysis to observe the de-composition of 411 samples that had been exposed to atmospheric conditions. They ob-

served seven different weight loss events and were able to identify five of them. They reported that the first three weight loss events corresponded to the decomposition of barium hydroxide octahydrate to barium hydroxide dihydrate, the decomposition of the dihydrate to barium hydroxide monohydrate, and the decomposition of the monohydrate to anhydrous barium hydroxide. These results agreed with those reported by Habashy and Kolta. At higher temperatures, Ohlinger and Rebstock also observed the decomposition of the anhydrous barium hydroxide, anhydrous calcium hydroxide, and barium carbonate to form BaO, CaO, H_2O, and CO_2.

Reactions between Barium Compounds and Tungsten

Because thermionic dispenser cathodes rely on a monolayer of barium to lower the work function of the emitter, several authors have investigated the crucial reaction between the oxide impregnant that contains barium and the porous tungsten matrix that results in production of Ba and/or BaO. Brodie & Jenkins[19] proposed that this reaction actually takes place in two stages in impregnated cathodes. First, the source material dissociates to produce BaO vapor in the insterstices between the impregnant and the tungsten emitter, as shown below for $Ba_3Al_2O_6$:

$$3BaO{\cdot}Al_2O_3 \leftrightarrow 2BaO + BaO{\cdot}Al_2O_3.$$

The BaO vapor then reacts with the tungsten to form Ba vapor and a barium tungstate:

$$2BaO + 1/3\ W \leftrightarrow Ba + 1/3\ Ba_3WO_6.$$

The various barium tungstates can be observed on the binary phase diagram of the BaO-WO_3 system by Kreidler,[20] shown in Figure 2.5.

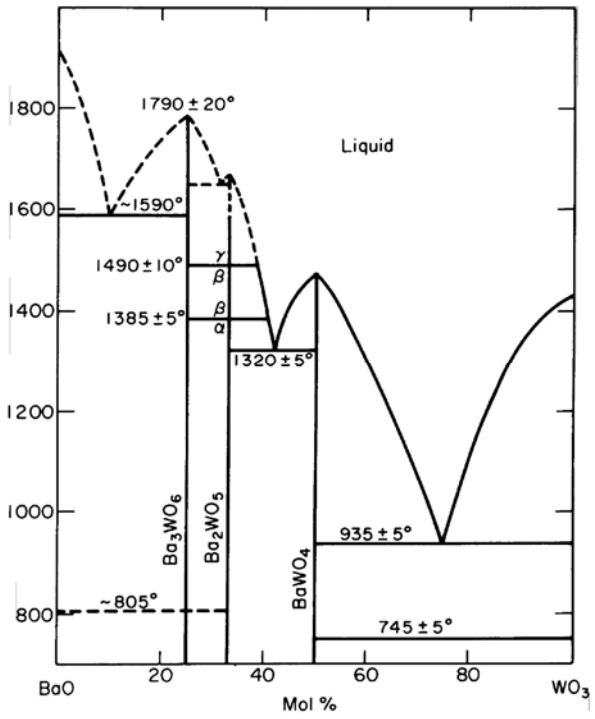

Figure 2.5. Binary Phase Diagram of the BaO-WO_3 System by Kreidler.[20]

Rittner, Rutledge and Ahlert[21] chose to impregnate their porous tungsten cathodes with $5BaO \cdot 2Al_2O_3$ because it is the lowest melting composition which does not contain free BaO. This composition is actually a eutectic mixture of $Ba_3Al_2O_6$ and $BaAl_2O_4$, but the $BaAl_2O_4$ is chemically inert and does not react to form barium vapor. Therefore, Rittner et al. proposed that the barium vapor is produced by the reaction of $Ba_3Al_2O_6$ and W:

$$2/3\ Ba_3Al_2O_6 + 1/3\ W \leftrightarrow 1/3\ BaWO_4 + 2/3\ BaAl_2O_4 + Ba$$

Using a manually operated polarograph, they identified only Ba and BaO evolving from the front of the cathode. The authors calculated the average content of BaO in the evaporant to be 33%, and they proposed that the BaO is produced by the oxidation of Ba as it passes through the tungsten matrix and by decomposition of the $Ba_3Al_2O_6$ as follows:

$$\tfrac{1}{2}\ Ba_3Al_2O_6 \leftrightarrow \tfrac{1}{2}\ BaAl_2O_4 + BaO.$$

Finally, Rittner et al. hypothesized that using a barium calcium aluminate impregnant (532) would yield a reaction product of Ca_2BaWO_6, as opposed to the $BaWO_4$ that forms from the reaction of barium aluminates. Kreidler's[22] phase diagram of the BaO-CaO-WO_3 system, displayed in Figure 2.6, shows that the ternary compound is Ba_2CaWO_6, not Ca_2BaWO_6 as Rittner et al. had proposed, thus rendering Rittner's hypothesis untenable.

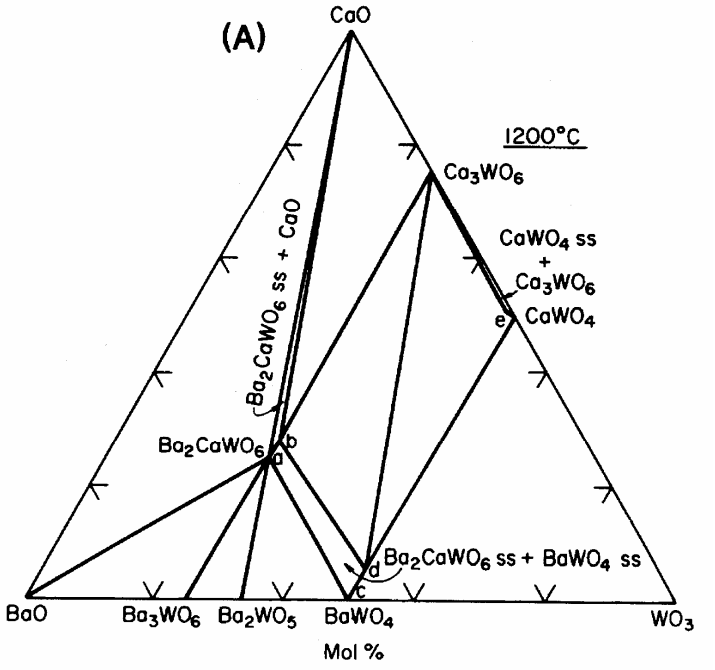

Figure 2.6. Ternary Phase Diagram of the BaO-CaO-WO_3 System by Kreidler.[22]

In an attempt to identify the reaction products in impregnated cathodes, Shroff, Palluel, and Tonnerre [23] impregnated barium calcium aluminate materials into thin tungsten filaments which they submitted to the same processes of activation and life tests as cathodes. After designated operating times, they analyzed fragments of the samples by x-

ray diffraction. They identified the major reaction products at the end of the test to be $BaAl_2O_4$, $BaWO_4$, and $CaWO_4$.

After running a xenon hollow cathode using a 411 impregnated insert for a 28,000 hour life test, Sarver-Verhey[24] used X-Ray Micro-diffraction Analysis (XRMA) to identify the two main compounds deposited on the porous tungsten emitter surface as Ba_2CaWO_6 and $BaWO_4$. He observed Ba_2CaWO_6 deposited 6.3 mm – 7.6 mm from the downstream end of the insert, while $BaWO_4$ was the dominant constituent 10 mm from the downstream end through to the upstream end of the insert (25 mm). Sarver-Verhey was unable to determine the identity and the quantity of Ba-containing compounds such as tungstates and aluminates remaining inside the emitter.

Solid-State Reaction Kinetics Models

In 1927, Jander[25] modeled the rate of reaction between powders using the geometry of a spherical particle as shown in Figure 2.7. Assuming that the rate of formation of the reaction layer depends on the rate of diffusion, Jander developed the following expression to describe the rate of reaction between spherical powder particles:

$$[1-(1-f)^{\frac{1}{3}}]^2 = \frac{kt}{R^2} \qquad (1)$$

where f = the fraction of the material which is unreacted, t = time, R = the radius of the original particle, and k is a constant.

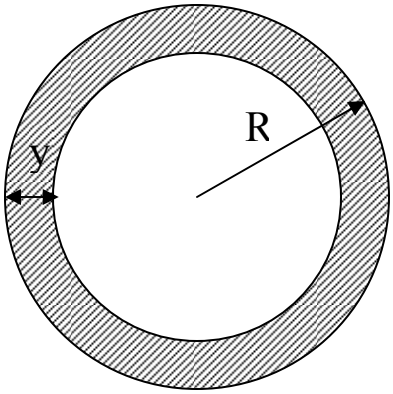

Figure 2.7. Sketch of the Cross Section of a Reacting Spherical Particle as used by Jander.

While the Jander equation has been found to hold for many solid-state reactions, several authors have discussed the limitations of the Jander equation.[26, 27, 28] Kingery, Bowen, and Uhlmann[26] pointed out that not only does Jander's model assume that particles are spherical and of uniform size, but it is also only valid when the reaction thickness is small and does not consider a change in molar volume between the reactants and product layer. Blum and Li[27] listed these additional assumptions made by the Jander equation: particles A must be effectively surrounded by particles B, only particles B diffuse into A, only Fick's law of diffusion applies, and the diffusion constant remains unchanged throughout the reaction.

In 1950, Ginstling and Brounshtein[29] developed a relationship for the rate of reaction of spheres which was not restricted to a constant diffusion constant:

$$\frac{2}{3}x + (1-x)^{\frac{2}{3}} = 1 - \frac{Kt}{r_0^{\,2}}, \qquad (2)$$

where x = the fraction of each sphere which has reacted, t = time, r_0 = the initial radius of each sphere, and K is a constant.

Carter[28] further modified the Jander equation in order to take into consideration the volume change during the reaction as shown in the equation below:

$$[1+(z-1)\,f]^{\frac{2}{3}}+(z-1)(1-f)^{\frac{2}{3}}=z+(1-z)\,\frac{kt}{R^2}, \tag{3}$$

where z = the volume of the product formed per unit volume of the spherical particle consumed, f = the fraction of the material which is unreacted, t = time, R = the radius of the original particle, and k is a constant.

Through their experimental work on nickel ferrite formation, Blum and Li observed that plotting the percent ferrite formation, "x," multiplied by the time in minutes, "t," vs. time produced a straight line with slope "a." Therefore, they proposed the following equation to model the rate of nickel ferrite formation:

$$\frac{dx}{dt}=\frac{a-x}{t}. \tag{4}$$

Blum and Li proposed that after extended time, the slope "a" provides an estimate of the maximum concentration of the reaction product that would form.

In 2003, He, Zhang, and Ling[30] used Jander's equation, Ginstling-Brounshtein's equation, and Blum-Li's equation to model the rate of ferrite formation in sol-gel derived composites. They found that their experimental data was best fit to a straight line by plotting xt vs. t. Therefore, He, Zhang, and Li determined that the rate of formation of ferrites by sol-gel processing could be best described by Blum-Li's equation.

In 1968, Bailey & Russell[31] validated the use of Blum-Li's equation in modeling the formation of spinel ceramics. They reported that Blum-Li's equation fit their experimental data better than the models by Jander, Carter, and Ginstling-Brounshtein.

Finally, Suitch[32] found that Blum-Li's equation could effectively model the reaction between tungsten and barium calcium aluminate materials at atmospheric pressure in flowing argon.

Vapor Pressure Measurement Techniques

Experimental techniques for measuring vapor pressures are commonly classified into three different categories: static, dynamic, and effusion methods. Common static methods include observing the rise of liquid in a manometer column, the stretching of a flexible diaphragm, or the distension of a Bourdon tube or a sickle gauge.[33] Dynamic methods include the boiling point method and the flow or transportation method.

In the first attempts at the boiling point method, Ruff and Bergdahl[34] put the material under investigation in a crucible suspended from a balance and observed the temperature at which the weight suddenly decreased as it reached its boiling point. At this temperature, it was known that the vapor pressure of the substance was equal to the pressure of the atmosphere with which it was in contact. In the flow or transportation method first applied by von Wartenberg,[35] a stream of inert gas is passed over or bubbled through the material under investigation at constant temperature. The flowing gas removes the vapor of the substance, which is condensed at a cooler part of the system. By measuring the weight gain from the condensation of the vapor, it is possible to calculate the vapor pressure of the material under investigation.

The Langmuir and Knudsen effusion methods allow the vapor pressure of a substance to be calculated from its rate of evaporation in vacuum. Langmuir[36] measured the

weight loss from wires of W, Ta, and Mo as they were heated in vacuum. He was able to relate the weight loss from the wires to the rate of evaporation, m, with the equation:

$$m = \sqrt{\frac{\rho}{\pi}} \cdot \frac{\sqrt{w_o} - \sqrt{w}}{t}, \tag{5}$$

where ρ = the density of the wire, w_0 = the original weight of the wire per unit length, w = the final weight of the wire per unit length, and t = time.

Knudsen developed an effusion method in which the substance was enclosed in a cylinder with a small hole in the top and then heated in vacuum.[33] The weight loss from the cell can be determined by weighing the cell before and after heating or by measuring the weight of gas that condenses on a target. Both Knudsen and Langmuir related the vapor pressure, p, from the rate of the evaporation using the following equation:

$$m = \sqrt{\frac{M}{2\pi RT}}\ p, \tag{6}$$

where M = the molecular weight of the vapor, R = the gas constant, and T = temperature in Kelvin. The vapor pressure in atm can then be calculated from the equation:

$$p = \frac{z(MT)^{\frac{1}{2}}}{44.33 \cdot a \cdot t} \tag{7}$$

where z = the number of moles lost from the Knudsen cell per second, a = the area of the hole in the Knudsen cell in cm^2, and t = the time during which effusion occurred.

The Knudsen technique requires that the sample area must be large compared with the orifice area, and the mean free path of the atoms in the vapor inside the cell must be at least ten times larger than the diameter of the orifice.[37] The identity of the vapor species must also be known in order to enter the molecular weight of the vapor into equation (6). Because this is not always known, numerous people have made use of Knudsen

cell mass spectrometry over the past fifty years to identify the gaseous species in equilibrium inside the cells and to obtain corresponding vapor pressure values and thermodynamic data.[38, 39, 40] In this method, a sample of the vapor effusing from the cell enters a mass spectrometer where it is ionized and the resulting ion intensities are recorded. Knudsen cell mass spectrometry is particularly valuable because it can be used to study all classes of materials over a pressure range of 10^{-4}-10^{-11} bar and temperatures from 500-2800 K.[41]

Another adaptation of the Knudsen technique involves continous weighing of the cell with thermogravimetric analysis (TGA). Goodrum and Siesel[42] equipped a TGA with a Knudsen effusion cell attachment and heated each cell at constant pressure. By plotting the weight loss due to the effusing vapor vs. temperature, they could determine the boiling temperature. Margrave[33] and Zavitsanos[43] took a different approach by weighing Knudsen cells with and without effusion taking place in order to measure the force exerted on the microbalance pan by the effusing molecules. They calculated the vapor pressure, P, using the equation:

$$P = 2 \cdot \Delta W \cdot g / \pi r^2 \ \ dynes / cm^2, \tag{8}$$

where ΔW = the increase in weight of the cell caused by effusion, g = the acceleration of gravity, and r = the radius of the effusion hole.

Vapor Pressure of Ba

Over the past 80 years, people have used various experimental techniques to develop expressions to describe the vapor pressure of barium. Table I gives a summary of

some of the key investigators, their experimental methods, and their corresponding vapor pressure values.

Table 2.1. Literature Values of the Vapor Pressure of Barium

Investigators	Year	Method	Vapor Pressure of Ba	Temp. Range (K)
Ruff and Hartmann[44]	1924	Boiling point	log p(atm) = 16.1-18750/T	1203-1403
Hartmann and Schneider[45]	1929	Boiling point	log p(atm) = 6.95 – 7824/T	1333-1419
Rudberg and Lempert[46]	1935	Molecular effusion target	log p(mm Hg) = 6.99-8980/T	798-1023
Zavitsanos[43]	1968	Knudsen	log p(atm) = 5.145 – 9597/T	1100-1215
Karmyshin, Totskii, and Shpil'rain[47]	1972	Static	log p(mm Hg) = 6.711 – 7850.5/T	1309-1539
Jacob and Waseda[48]	1988	Knudsen	log p(Pa) = 9.733 - 9304/T	700-1200

It is commonly believed that the vapor pressures measured by Ruff and Hartmann[44] appear too high because of error in the weight measurements caused by condensation of the barium vapor on a cold filament supporting the sample.[47] Disregarding this set of data, the vapor pressure expressions developed by the other investigators all appear to be in relatively close agreement.

Vapor pressure of BaO

The vapor pressure of BaO has also been widely studied. While Claassen and Veenemans[49] used the Langmuir method to collect their vapor pressure values, most of the work done on this topic has made use of the Knudsen effusion method. A summary

of some of the previous investigations into the vapor pressure of BaO is shown in Table 2.2:

Table 2.2. Literature Values of the Vapor Pressure of Barium Oxide

Investigators	Year	Method	Vapor Pressure of BaO	Temp. Range (K)
Claassen and Veenemans[49]	1933	Langmuir	log p(mm Hg) = 8.87-19700/T	1200-1500
Blewett, Liebhafsky, and Hennelly[50]	1939	Knudsen	log p(mm Hg) = 8.63 – 19400/T	1200-1800
Inghram, Chupka, and Porter[38]	1955	Knudsen cell mass spec.	$1.4x10^{-6}$ atm $7.9x10^{-6}$ atm	1664 K 1758 K
Newbury, Barton, and Searcy[51]	1968	Knudsen cell mass spec. and TGA	log p(atm) = 7.90 – 22610/T	1365-1917 K
Hilpert and Gerads[39]	1975	Knudsen cell mass spec.	log p(atm) = (7.19 ± 0.30) -21730/T	1332-1681 K

Inghram, Chupka, and Porter[38] were the first to study the evaporation of BaO with the Knudsen cell mass spectrometry method. They heated alumina Knudsen cells filled with BaO solid and used the mass spectrometer to measure the ion currents of Ba^+, BaO^+, Ba_2O^+, $Ba_2O_2^+$, and $Ba_2O_3^+$ effusing from the cells. While Inghram, Chupka, and Porter selected Al_2O_3 as the cell material to prevent reduction of the BaO vapor, Hilpert and Gerads[39] speculated that reaction between the Al_2O_3 and BaO to form barium aluminates could introduce error into the results. Therefore, they experimented with several alternative cell materials to determine their suitability for studying the evaporation of BaO. They found that molybdenum cells and molybdenum cells lined with Al_2O_3 or Pt all showed similar ion intensities of the species Ba^+, BaO^+, Ba_2O^+, and $Ba_2O_2^+$, while graphite cells showed varied results due to extensive reduction of the BaO to form Ba.

Vapor Pressures of Ba and BaO over Barium Source Materials

Hilpert, Beske, and Naoumidis[40] studied the evaporation of BaO from barium aluminate compounds by means of Knudsen cell mass spectroscopy. They loaded molybdenum Knudsen cells with the sample materials and then used a mass spectrometer to measure the BaO produced by heating $Ba_3Al_2O_6$ in the range of 1469-1745 K and $BaAl_{12}O_{19}$ in the range of 1897-2170 K. After calibrating the system with silver, they were able to establish relationships for the vapor pressures of BaO over the two barium aluminate materials. They calculated the vapor pressure of BaO over $Ba_3Al_2O_6$ to be log p(atm) = 7.90 - 23620/T and the vapor pressure of BaO over $BaAl_{12}O_{19}$ to be log p(atm) = 9.14 - 28300/T.

The two barium aluminate compositions studied by Hilpert, Beske, and Naoumidis are single-phase materials. For an impregnant composition consisting of multiple phases, Lipeles and Kan[52] predicted that the vapor pressure would be determined by thermal decomposition of the least chemically stable phase. Therefore, the BaO vapor pressure of the impregnant would correspond to the BaO vapor pressure of the least chemically stable phase. They also hypothesized that solid solutions are ideal solutions, so the vapor pressure of a solid solution should be equal to the sum of the partial pressures of the component phases.

Lipeles and Kan used thermodynamic modeling to predict the equilibrium vapor pressures of BaO over several barium aluminates and several CaO solid solutions in the BaO-CaO-Al_2O_3 system. Their results are summarized in Table 2.3:

Table 2.3. Thermodynamic Data used to Calculate the Vapor Pressure of BaO by Lipeles and Kan[52]

Thermal decomposition	ΔH (kcal/mole)	ΔS (eu)	P_{BaO} at 1100ºC (atm)	Reference
$BaO \rightarrow BaO(g)$	99.4	32.9	8×10^{-9}	39
$\frac{1}{4}\ Ba_8Al_2O_{11} \rightarrow BaO(g) + \frac{1}{4}\ Ba_4Al_2O_7$	101.8	31.2	4×10^{-10}	52
$Ba_4Al_2O_7 \rightarrow BaO(g) + Ba_3Al_2O_6$	105.3	29.3	7×10^{-11}	52
$\frac{1}{2}\ Ba_3Al_2O_6 \rightarrow BaO(g) + \frac{1}{2}\ BaAl_2O_4$	107.2	29.9	3×10^{-11}	53
$6/5\ BaAl_2O_4 \rightarrow BaO(g) + 1/5\ BaAl_{12}O_{19}$	129.0	29.8	1×10^{-14}	54
$\frac{1}{2}\ Ba_3WO_6 \rightarrow BaO(g) + \frac{1}{2}\ BaWO_4$	131.0	38.2	3×10^{-13}	55
$Ba_{7.8}Ca_{0.2}Al_2O_{11}$	101.8	31.14	4×10^{-10}	52
$Ba_{2.9}Ca_{1.1}Al_2O_7$	105.3	29.13	4×10^{-11}	52
$Ba_{2.25}Ca_{0.75}Al_2O_6$	107.2	29.34	2×10^{-11}	52

Lipeles and Kan predicted that the phase composition of the impregnant determines the ratio of Ba and BaO in the vapor. For a more active phase, they predicted a higher ratio of Ba vapor to BaO vapor. For example, the substitution of Ca^{2+} for Ba^{2+} in the crystal structure forms more stable, less active phases so the ratio of Ba/BaO vapor decreases. Lipeles and Kan also reported that increasing the BaO content in the impregnant forms higher-vapor pressure Ba-rich phases. They suggested selecting lower vapor pressure impregnant materials in order to extend the life of the cathodes at high temperatures.

Evaporation Rates from Dispenser Cathodes

The evaporation of barium from the impregnant or reservoir is crucial to the operation of all barium dispenser cathodes. A minimum rate is required in order to maintain activation, but exhaustion of the available barium within the source material will eventu-

ally lead to the end of cathode life.[19] Therefore, it is important to be aware of the rate of evaporation of barium from the various barium source materials in order to understand how they will perform.

Zalm and van Stratum[56] reported unpublished measurements by C.A.M van den Broek and A. Venema on barium evaporation rates from L (reservoir-type) cathodes utilizing porous tungsten emitters with a given porosity. These results show that the quantity of Ba (and BaO) evaporating per unit time and per unit cathode surface depends only on the cathode temperature, as shown in Figure 2.8.

In 1957, Brodie and Jenkins[19] studied evaporation rates for cathodes impregnated with the compounds $Ba_3Al_2O_6$ and $BaAl_2O_4$, the eutectic mixture of $Ba_3Al_2O_6$ and $BaAl_2O_4$, and the eutectic mixture of BaO and $Ba_3Al_2O_6$. By measuring the time necessary to deposit a monolayer of barium on a tungsten wire adjacent to the cathode, they were able to estimate the barium evaporation rates. A graph of their measured evaporation rates for the barium aluminates is shown in Figure 2.9. Brodie and Jenkins found the barium evaporation rate to be lower for the mixture of $Ba_3Al_2O_6$ and $BaAl_2O_4$ than the pure $Ba_3Al_2O_6$, which was expected because $BaAl_2O_4$ reacts with tungsten at a negligible rate. However, they found that increasing the ratio of $BaO:Al_2O_3$ in the impregnant above 3, as in the eutectic mixture of BaO and $Ba_3Al_2O_6$, was undesirable because it led to very rapid reaction of the free BaO phase with tungsten.

Brodie and Jenkins also measured the evaporation rates from cathodes impregnated with barium calcium aluminate materials. They found that adding ½ molar proportion of CaO to $Ba_3Al_2O_6$ decreased the evaporation rate of the $Ba_3Al_2O_6$ by a

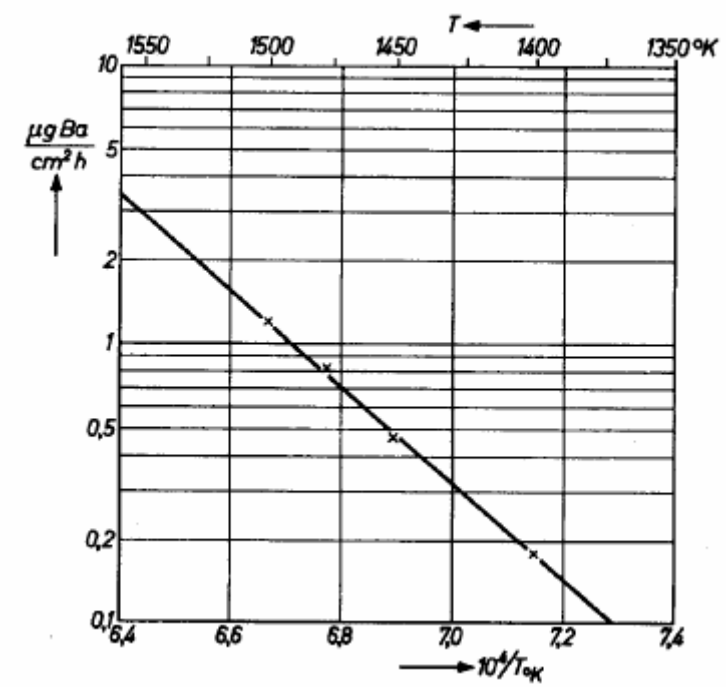

Figure 2.8. Evaporation of Ba per Unit Time and per Unit Cathode Surface for Tungsten L Cathodes, Based on Unpublished Measurements by van den Broek and Venema.[56]

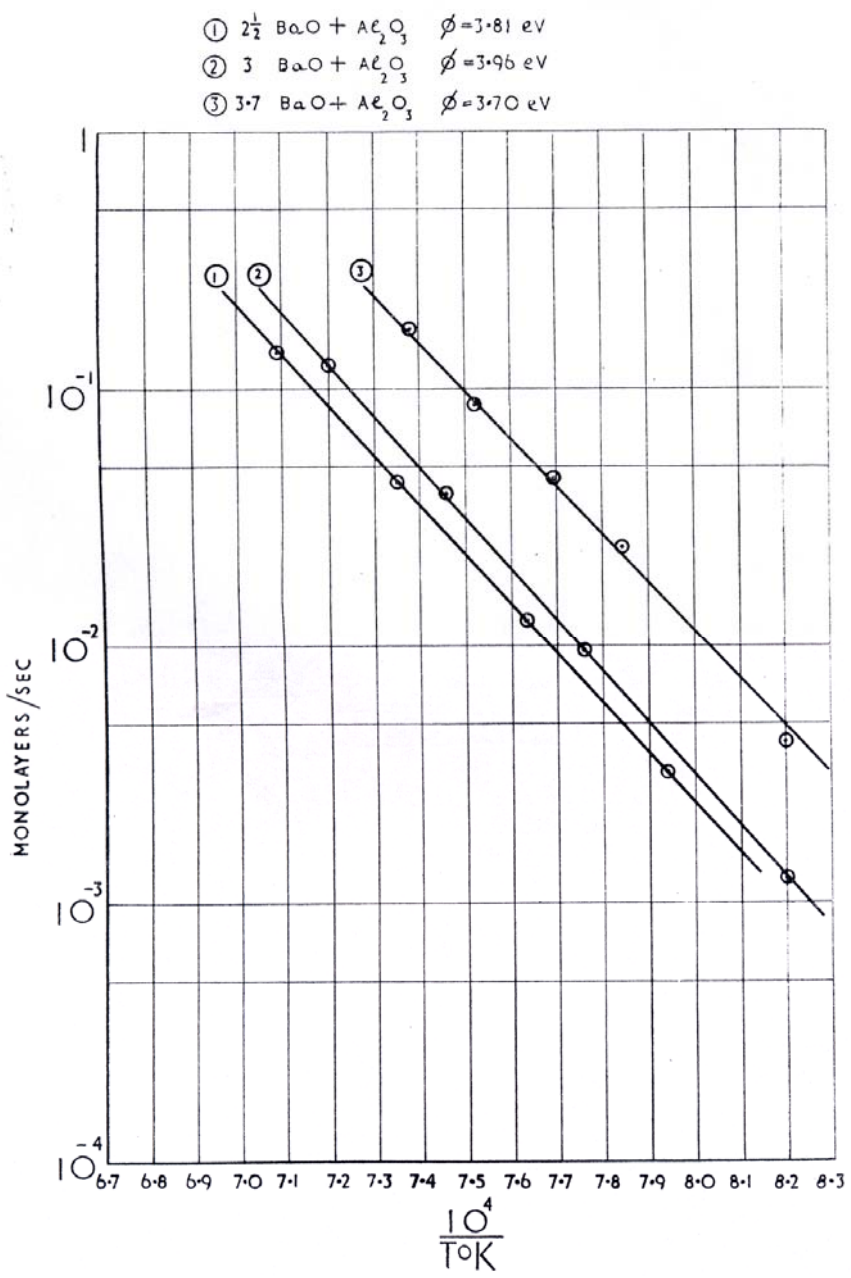

Figure 2.9. Evaporation of Barium from Cathodes Impregnated with Barium Aluminates by Brodie and Jenkins.[19]

factor of 5. Brodie and Jenkins hypothesized that the addition of the CaO may lead to the formation of a compound with few interstices, which impedes the escape of vapor.

In 1981, Shroff, Palluel, and Tonnerre[23] measured the evaporation rates for several of the common commercial impregnant materials in the early stages of life. Their results are show in Figure 2.10. Like Brodie and Jenkins, Shroff et al. also found that the cathodes impregnated with barium calcium aluminate materials generally had lower evaporation rates than those impregnated with barium aluminate materials. Lipeles and Kan[52] pointed out that increasing the CaO concentration beyond the point where its solid solubility limit has been reached has little effect on lowering the evaporation rate, because it starts to segregate out as a CaO phase.

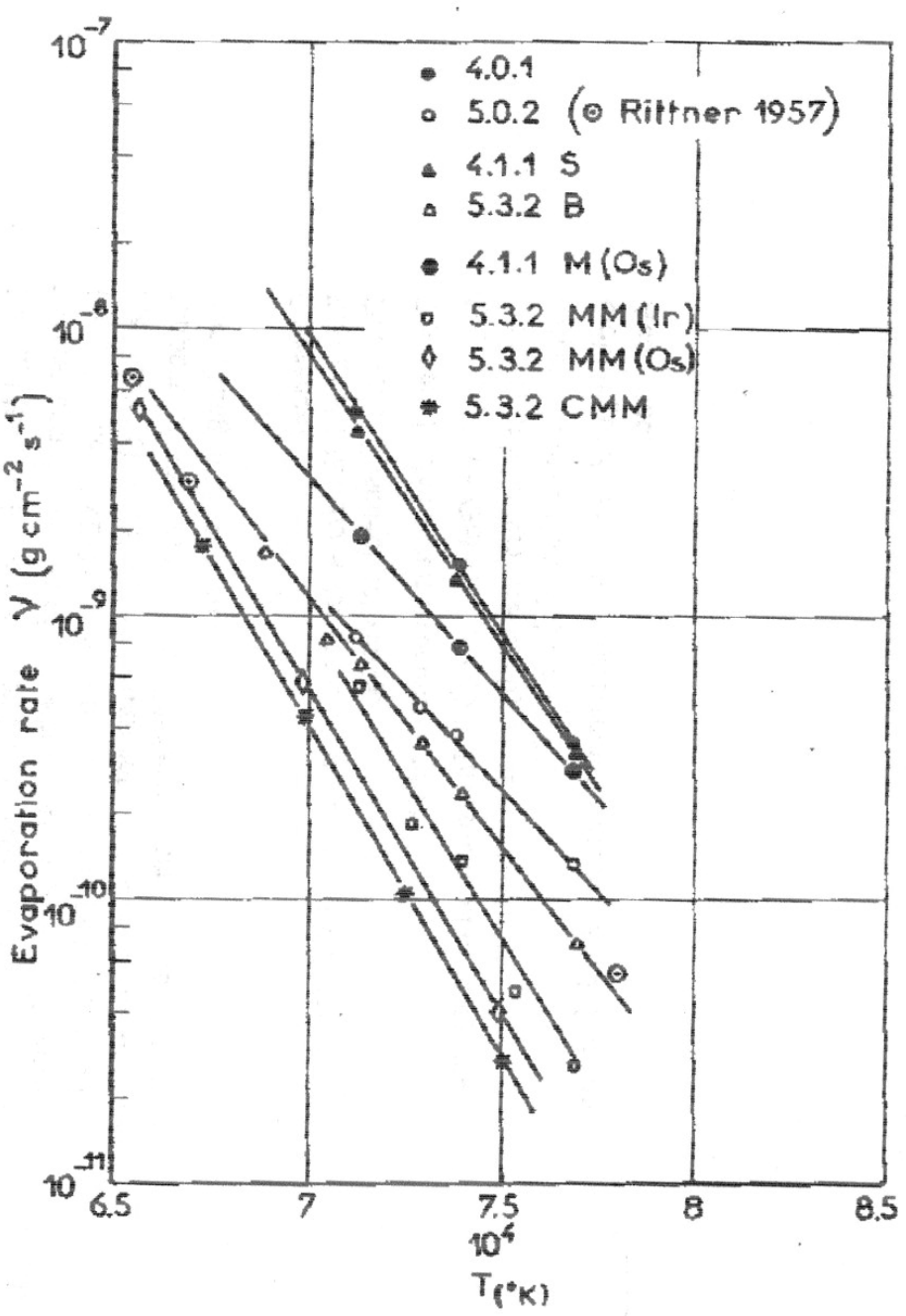

Figure 2.10. Evaporation Rates of Different Types of Cathodes at Early Stages of Life by Shroff, Palluel, and Tonnerre.[23]

CHAPTER 3

EXPERIMENTAL PROCEDURE

Two types of experiments were performed to evaluate the behavior of barium source materials in potential handling and storage environments and to ascertain the reaction characteristics with tungsten in typical reservoir hollow cathode operating environments, respectively. First, the environmental stability of several barium materials was studied using thermogravimetric analysis (TGA) in controlled atmospheres. The masses of five barium source materials were measured as they were exposed to air with dew points of –15ºC and 11ºC, and the percent weight gain vs. time was plotted for the various materials to compare their environmental stability.

Also, a series of experiments were run to investigate the reactions between a barium calcium aluminate compound, typically used as a commercial cathode impregnant, and tungsten by sealing the materials inside capsules with porous tungsten closures and heating them to elevated temperatures for extended periods of time. Quantitative x-ray analysis was then used to identify and quantify the reaction products, which provided a means to study the reaction kinetics between the barium compound and tungsten.

Preparation of the Barium Source Materials

The barium source materials were formed by combining the raw materials $BaCO_3$ (Alfa-Aesar), Al_2O_3 (Linde B), $CaCO_3$ (J. T. Baker), and Sc_2O_3 (Alfa-Aesar). Before the raw materials were mixed, they were placed in separate alumina crucibles and heated to 400ºC for 15 hours to remove moisture. After removing any adsorbed water, it was pos-

sible to weigh out accurate amounts of the raw materials so that they could be combined in the proper ratios to form the desired products.

Looking at the formation reactions for the barium compounds, shown in Table 3.1, it was possible to determine the molar percentages of the raw materials needed for the various reactions. Using the molar percentages and the molecular weights of the raw materials, it was possible to calculate the weight percents of the raw materials needed to form the barium compounds.

Table 3.1. Formation Reactions for Four Barium Compounds

Material	Formation reaction	wt% $BaCO_3$	wt% Al_2O_3	wt% $CaCO_3$	wt% Sc_2O_3
$3BaO \cdot Al_2O_3$ (B_3A)	$3BaCO_3 + Al_2O_3 \rightarrow Ba_3Al_2O_6 + 3CO_2$	85.3	14.7	0	0
$6BaO \cdot CaO \cdot 2Al_2O_3$ (612)	$6BaCO_3 + CaCO_3 + 2Al_2O_3 \rightarrow Ba_6Al_4CaO_{13} + 7CO_2$	79.6	13.7	6.7	0
$Ba_{2.9}Ca_{1.1}Al_2O_7$ (B_4A_{SSL})	$2.9BaCO_3 + 1.1CaCO_3 + Al_2O_3 \rightarrow Ba_{2.9}Al_2Ca_{1.1}O_7 + 4CO_2$	73	13	14	0
$Ba_3Sc_4O_9$	$3BaCO_3 + 2Sc_2O_3 \rightarrow Ba_3Sc_4O_9 + 3CO_2$	68.2	0	0	31.8

The $4BaO \cdot CaO \cdot Al_2O_3$ (411) material used in these experiments was prepared by Semicon Associates in Lexington, Kentucky.

The powders were combined in the proper ratio in a molybdenum mill with tungsten rods and dry milled for two hours at a speed appropriate for optimum mixing. The powder was then transferred to alumina boats for calcining. Because some sintering occurs during the calcination process, the powder was lightly tamped into the boat, then scribed into one-centimeter squares with a razor blade; this allowed each section of calcined powder to be easily removed for further processing. Flat pieces of alumina were

placed on top of alumina spacers on the boats to cover the powder yet still permit adequate air circulation during calcination.

The boats were placed in a Keith bottom-loading furnace, equipped with $MoSi_2$ elements, where they were heated at 10°C/min to 1200°C, held at temperature for 50 hours, and cooled at 5°C/min to 200°C. To minimize water absorption, the boats were removed from the furnace at 200°C and stored in a vacuum desiccator. X-ray analysis was used to confirm that the desired products formed during the calcination reactions.

X-Ray Analysis of Barium Source Materials

The barium compounds used in this project are hygroscopic, so they tend to pick up a significant amount of moisture during a typical two-hour x-ray diffraction run. Because the absorption of water leads to displacement in the height of the x-ray sample, this causes shifts in the locations of the peaks in the x-ray pattern. Absorption also tends to cause broadening of the peaks which also reduces peak intensities. While shortening the time of the run could allow the sample to be scanned before there was significant hydration, this would also reduce the resolution of the peaks. Therefore, it was desired to find a way to prevent hydration of the material so that a longer run could be performed. Coating the barium compounds with mineral oil prevented hydration of the material and therefore led to a higher quality x-ray diffraction pattern.

While the mineral oil was beneficial in preventing hydration of the sample, excess oil could decrease the resolution of the peaks by absorbing the x-ray beam. Therefore, it was necessary to determine the minimum amount of mineral oil needed to prevent hydration of the sample. After several trials, it was discovered that the best quality diffraction

pattern was obtained by adding 8 drops of mineral oil for every 1 gram of the sample powder. The barium compound was ground with a mortar and pestle, the desired amount of mineral oil was added, and then the mixture was stirred by hand. The mixture was then coated on a cover glass placed in a bulk x-ray sample holder, and x-ray diffraction analysis was performed using a Philips PW 1800 Automated Powder Diffractometer.

Environmental Stability of Barium Source Materials

The candidate barium source materials were analyzed using thermogravimetric analysis in controlled atmospheres consisting of air with dew points of –15ºC and 11ºC, corresponding to a RT (circa 22ºC) relative humidity of 7% and 50%, respectively. The five barium source materials selected for study in this experiment were B_3A, 612, B_4A_{SSL}, 411, and $Ba_3Sc_4O_9$.

Pellets were formed on a Carver press by applying ~15,000 psi of pressure to approximately 0.4 g of the barium compound in a ¼" die. The pellet was placed on a platinum boat that was set inside a wire stirrup. The stirrup was then hung from a platinum suspension wire that was connected to the Cahn D-200 Digital Recording Balance as shown in Figure 3.1. The port on the balance used during the experiments has the following characteristics: 1.5 g capacity, 0.1 μg sensitivity, and 150 mg weight change. A picture of the TGA used for the environmental experiments is shown in Figures 3.2.

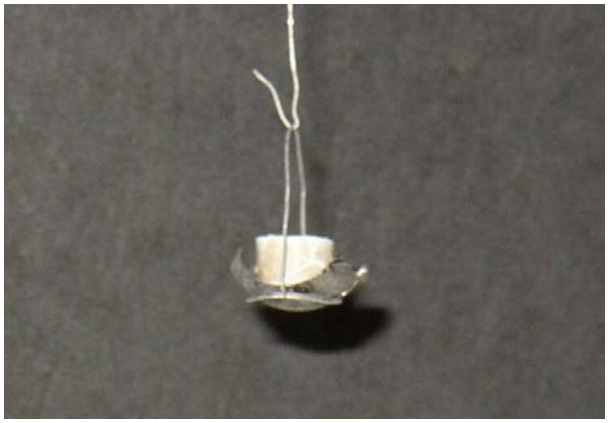

Figure 3.1. Sample Placed on a Pt Boat Hung with a Wire Stirrup.

Figure 3.2. Picture of the TGA Setup for the Environmental Experiments

Before starting the experiment, the pellet, boat, and wire stirrup were weighed on a Denver Instrument balance having a sensitivity of 0.1 mg. After the pellet, boat, and stirrup were suspended from the Cahn balance, the furnace was moved up around the sample. Glass tubing was secured with clamps to seal the system. Ceramic fiber insulation was placed between the top of the furnace and the structural frame in order to provide thermal isolation. An aluminum heat exchanger was placed on the structural frame in order to prevent temperature fluctuations that could introduce instrumental error into the results.

Compressed air (ultra zero grade), with a dew point of -15ºC (~ 7% relative humidity at room temperature), was used to provide a low-humidity environment, while the same air, flowed through a bubbler, was mixed with the "dry" air to achieve a controlled, intermediate-humidity environment with a dew point of 11ºC (~ 50% relative humidity at room temperature). The total gas flow rate in each case was maintained at a level of 230 ml/min. The dew point was continually monitored throughout each run with an hygrometer in the exit gas stream. In order to remove any moisture that was already present in the material, the sample was heated to 700ºC for 8 hours before the weight gain measurements began. Each sample was then cooled and held at room temperature for approximately 60 hours while weight measurements were recorded.

Accelerated Reactions Between the 612 Material and W

The rate of reaction between a barium calcium aluminate material and tungsten was studied in a reservoir hollow cathode environment. Mixtures of the 612 material and W were sealed inside molybdenum capsules with porous tungsten closures and heated to

1000ºC, 1200ºC and 1300ºC for extended periods of time. Quantitative x-ray diffraction analysis was then used to determine the amount of reaction products present in the samples, which was used to study the reaction kinetics. Short pieces of W wire were also placed in the capsules, surrounded by the powder mixtures. By viewing cross sections of the wires with the Scanning Electron Microscope, it was desired to study the reaction layer between the W wires and barium source material.

Sample Preparation

A schematic and picture of the molybdenum capsules that were used for the accelerated test studies are shown in Figures 3.3 and 3.4:

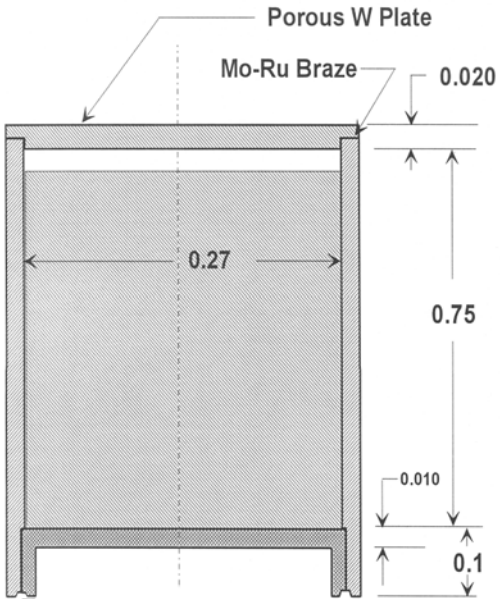

Figure 3.3. Schematic of the Capsule used for Accelerated Testing.

The tungsten closures on top of the capsules had a density of 80%.

Figure 3.4. Picture of the Capsule used for Accelerated Testing.

To prepare the materials to put inside the reaction capsules, equal weights of the 612 material and W were mixed with a mortar and pestle in order to make a mixture that was 50 wt% of the 612 material and 50 wt% W. Tungsten wire of 0.005" diameter was cut into 3/16" lengths, and the pieces of wire were then soaked in acetone for approximately 1 hour.

Pellets were formed using a Carver press by applying ~1500 lbs of force (30,000 psi) to approximately 0.87 g of the powder mixture in a ¼" die. Additional pellets were also formed in the same manner with six pieces of the W wire interspersed throughout the powder. Seven of the molybdenum reaction capsules were filled by stacking one 612/W powder pellet, one 612/W pellet with wires, and then one 612/W powder pellet on top of one another inside the capsule. The bottom closures were snapped into place, and then the parts were vacuum-sealed and sent to Semicon Associates where the bottom closures were laser welded to the capsules. Because there was oxidation around the site of the welds, the parts were then heat treated by firing them at 1000ºC for 1 min. in H_2.

Furnace Operation

A tube furnace with silicon carbide heating elements was used for the reaction-rate experiments, shown below in Figure 3.5:

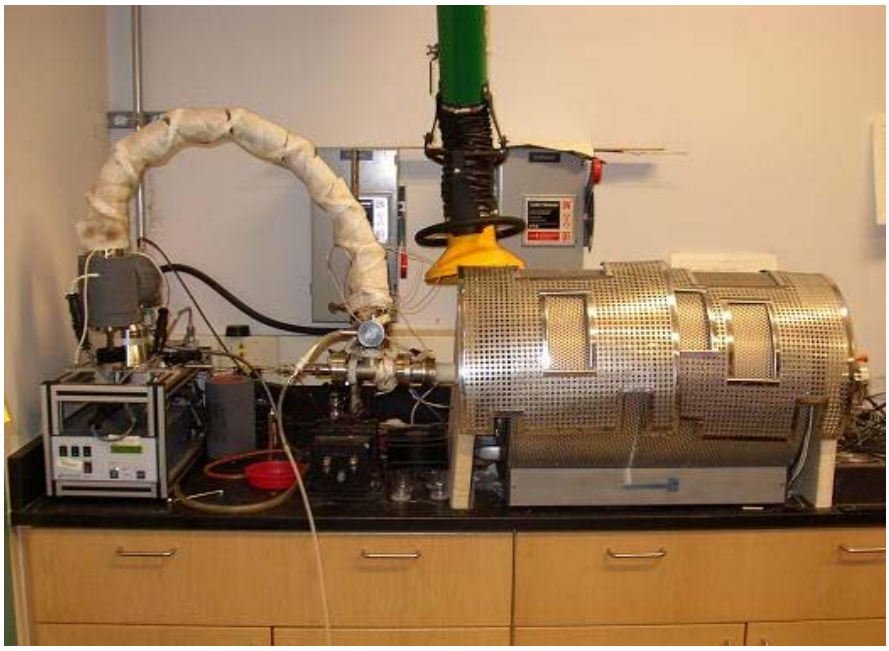

Figure 3.5. Photograph of the Furnace System used for the Accelerated Reaction Tests.

The samples were placed inside a 36” long mullite tube with an inner diameter of 1 ¼” which was inserted into the furnace and sealed with end-plates on both ends. On one end-plate, there was a gas outlet which led to an Alcatel turbo pump with a diaphragm backing pump. A Varian 880 RS ion gauge was used to monitor pressure in the system. A Type-S thermocouple was placed in the center of the furnace and used to monitor the temperature of the sample.

Samples 1-6 were loaded into the furnace upright in a carrier fashioned from a piece of molybdenum foil, while Sample 7 was loaded on its side in a molybdenum carrier as shown in Figure 3.6:

Figure 3.6. Sample 7 Loaded on its Side in a Molybdenum Carrier.

Ceramic insulators were placed on either side of the sample inside the furnace to act as heat shields, and then the end plate was put into place to seal the system. A vacuum was then drawn on the furnace tube, and the pressure in the system eventually stabilized around $2x10^{-6}$ torr.

The samples were heated at 3ºC/min to 200ºC where they were held for 480 minutes to remove water and CO_2 from the samples so they did not react with the W at elevated temperatures. The samples were then heated at 2ºC/min up to 700 ºC and then 5ºC/min up to the desired temperature where they were held for 100, 200, or 400 hours. Table 3.3 shows the experimental parameters for the various accelerated tests:

Table 3.3. Experimental Parameters for the Accelerated Tests

Sample	Temperature (ºC)	Time (hrs)
1	1300	100
2	1300	400
3	1300	200
4	1200	100
5	1200	400
6	1200	200
7	1000	100

At the end of the experiments, the samples were first cooled at 10ºC to 800ºC and then at the natural cooling rate to prevent cracking of the alumina tube. After the samples were cooled, they were removed from the furnace. A pair of pliers was used to remove the end closure from the reaction capsule, and the pellets were stored in a vacuum desiccator until characterization was performed.

Qualitative X-ray Diffraction Analysis

A portion of each of the pellets in the reaction capsules was analyzed using qualitative analysis. The material was mixed with a proper amount of mineral oil to prevent hydration and then spread on a cover glass set in a bulk sample holder. X-ray diffraction analysis was performed using a Philips PW1800 Automated Diffractometer with a Cu radiation source. The samples were scanned from 15º - 85º 2θ for 2 seconds per step, with a step size of 0.015º 2θ.

Preparation of Materials for the X-Ray Standards

Before quantitative analysis could be performed on the samples, it was necessary to create samples of the reaction products $BaAl_2O_4$ and Ba_2CaWO_6. As with the barium

source materials, it was necessary to look at the formation reactions in order to determine the percentage of the raw materials needed to form the desired end product. The following reaction occurs to form $BaAl_2O_4$:

$$BaCO_3 + Al_2O_3 \rightarrow BaAl_2O_4 + CO_2.$$

As shown in the reaction, the ratio of moles of $BaCO_3$ to moles of Al_2O_3 must be 1:1. The weight percents of the raw materials needed to form $BaAl_2O_4$ are calculated to be 65.9 wt% $BaCO_3$ and 34.1 wt% Al_2O_3. The $BaAl_2O_4$ was processed in the same way as the barium source materials using an identical heating schedule.

The following reaction occurs to form Ba_2CaWO_6:

$$2BaCO_3 + CaCO_3 + W + 3/2O_2 \rightarrow Ba_2CaWO_6 + 3CO_2.$$

The ratio of the moles of $BaCO_3$ to $CaCO_3$ to W must be 2:1:1, and the corresponding weight percents of the raw materials needed to form Ba_2CaWO_6 are calculated to be 58.1 wt% $BaCO_3$, 14.7 wt% $CaCO_3$, and 27.2 wt% W.

Rather than using the molybdenum mill, the raw materials for the barium calcium tungstate were mixed by hand with a mortar and pestle. The samples were held at 750ºC for six hours in order for the tungsten to oxidize, and then they were heated to 1100ºC for 36 hours. Once again, x-ray analysis was used to confirm that the desired products formed during the calcination reactions.

Quantitative X-Ray Diffraction Analysis

After heating, quantitative x-ray diffraction analysis was used to determine the amount of reactants and products that were present in the samples. In quantitative analysis, the intensity of a diffraction peak corresponding to a particular phase in a mixture is

used to determine the concentration of that phase in the mixture. In this case, the internal standard method of quantitative analysis was utilized in which a known concentration of an internal standard is mixed with each powder sample. The integrated intensity of one of the internal standard peaks is compared to the integrated intensity of a diffraction peak corresponding to the phase of interest A. The weight fraction of A in the original sample (w_A) is calculated using the following equation:

$$\frac{I_A}{I_S} = K \cdot w_A$$

where I_A is the intensity of a particular peak from phase A, I_S is the intensity of a particular peak from the standard phase, and K is a constant.

In selecting a material for a standard, there are two important factors to consider. The standard material should have a similar mass absorption coefficient (MAC) to the MAC of the phases being identified, and the standard must contain a diffraction peak that does not overlap peaks in the phases of interest. It was therefore necessary to find a standard material with a MAC value close to those of the reaction products $BaAl_2O_4$, $BaWO_4$, and Ba_2CaWO_6. In order to calculate the MAC of a compound (μ/ρ), the weight fraction of each element 1, 2, etc., is multiplied by the element's MAC:

$$\frac{\mu}{\rho} = w_1\left(\frac{\mu}{\rho}\right)_1 + w_2\left(\frac{\mu}{\rho}\right)_2 + \cdots.$$

Using this equation and the MAC values for the elements using Cu Kα radiation listed in Appendix 8 of Cullity's *Elements of X-Ray Diffraction*,[57] the MAC's for $BaAl_2O_4$, $BaWO_4$, and Ba_2CaWO_6 were calculated to be 194.2 cm^2/g, 203.0 cm^2/g, and 226.21 cm^2/g, respectively. The standard material which was selected for these experiments is Ag, whose MAC is listed in Appendix 8 as 218.1 cm^2/g for Cu Kα radiation. Not only is its

MAC value similar to those of the predicted reaction products, but Ag has a peak with a relative intensity of 50% at a 2θ value of 81.506º which does not overlap a peak in any of the predicted reaction products, the 612 material, or W.

Before quantitative analysis can be performed, it is necessary to create calibration sets by running samples with known quantities of analyte and standard. From qualitative analysis of the samples, the reaction products were identified to be $BaAl_2O_4$ and Ba_2CaWO_6. It was decided to quantify the amount of the starting materials, the 612 material and W, and the reaction products, $BaAl_2O_4$ and Ba_2CaWO_6, present in the samples. The desired amounts of the 612 material, $BaAl_2O_4$, Ba_2CaWO_6, and W were weighed out and then ground with a mortar and pestle. Preliminary results showed that grinding the Ag caused strain in the powder that broadened its x-ray peaks, so 20 wt% Ag was mixed into the sample by hand at the end. Eight drops of mineral oil was added per gram of powder to prevent hydration of the materials.

Using the APD software, quantitative analysis programs and corresponding calibration sets were made for $BaAl_2O_4$, Ba_2CaWO_6, W, and the 612 material. The following diffraction peaks were selected to identify the starting materials and reaction products: $BaAl_2O_4$ – 19.45º, Ba_2CaWO_6 – 53.51º, W – 40.42º, and the 612 material – 31.38º. Each quantitative analysis program scanned the sample from 44.2º - 44.7º with a step size of 0.01 and measurement time of 5 s per step in order to obtain the silver peak. Each program also scanned a range of ~0.8º 2θ around the peak of interest for that phase with a step size of 0.01º 2θ and measurement time of 5 s per step. Samples were run with four different concentrations of the 612 material, $BaAl_2O_4$, Ba_2CaWO_6, and W and 20% Ag. Using this information, it was possible to create calibration sets by plotting the relative

integrated intensity (integrated intensity of the peak of interest divided by the integrated intensity of the Ag peak) vs. the relative concentration (concentration of the phase of interest divided by the concentration of Ag, 20%). The calibration sets for the four materials are shown in Figures 3.7-3.10.

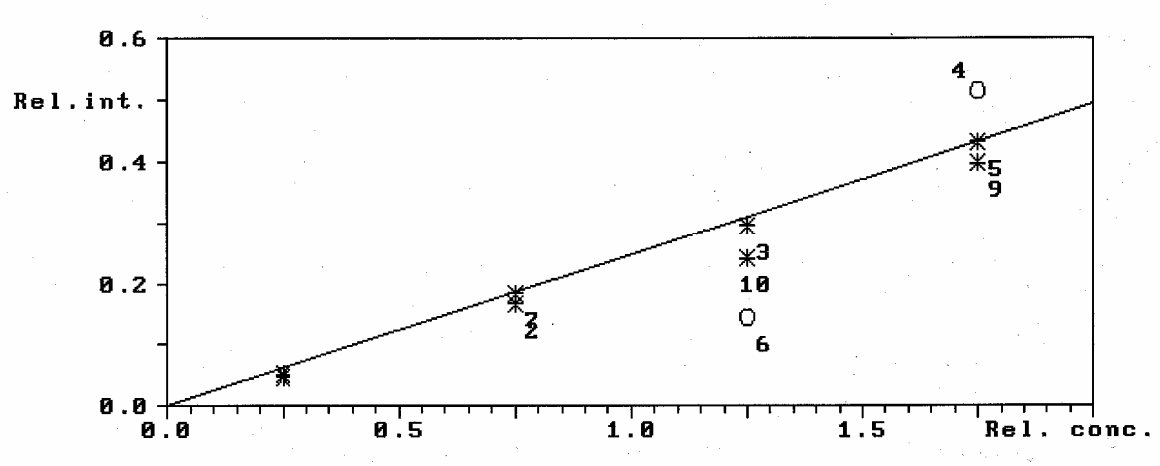

Figure 3.7. Calibration Set for $BaAl_2O_4$.

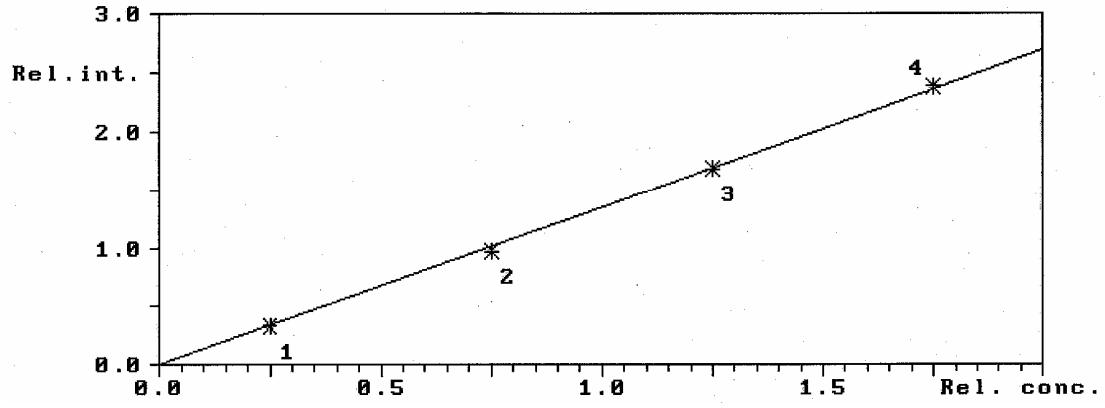

Figure 3.8. Calibration Set for Ba_2CaWO_6.

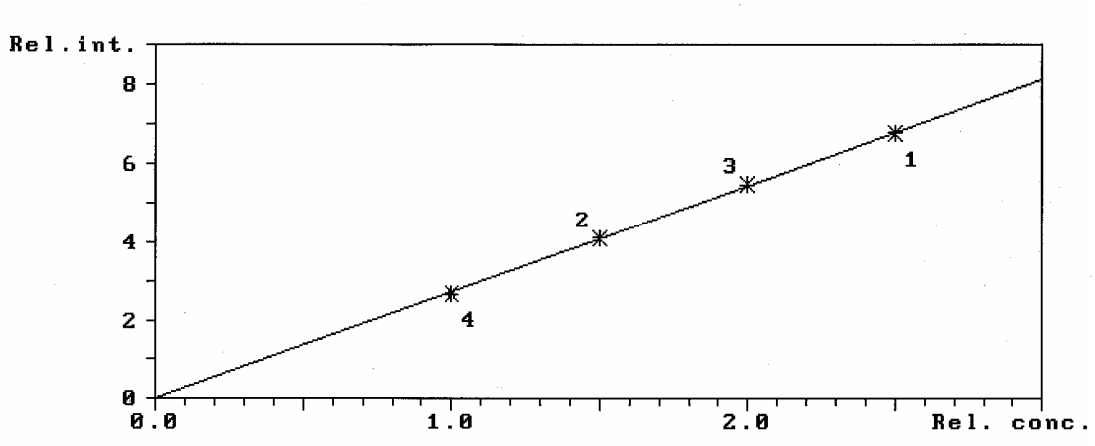

Figure 3.9. Calibration Set for W.

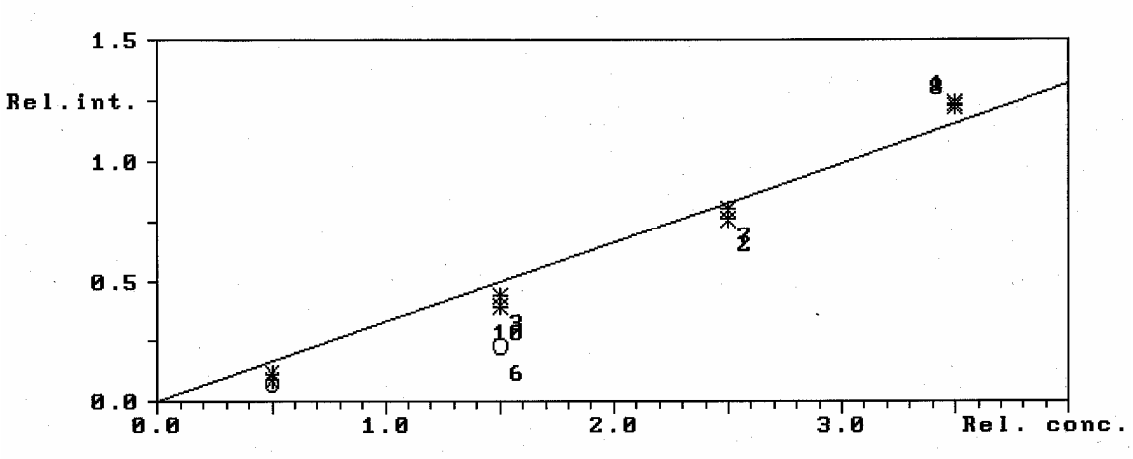

Figure 3.10. Calibration Set for the 612 Material.

Once the samples were heated in the reaction capsules, a portion of each pellet was mixed with 20 wt% Ag and mineral oil. The quantitative analysis programs were run in order to calculate the concentrations of $BaAl_2O_4$, Ba_2CaWO_6, W, and the 612 material in each of the samples.

Semi-Quantitative Analysis

Semi-quantitative analysis was used as an additional means to quantify the reaction products of the accelerated tests. In semi-quantitative analysis, the intensity of the strongest peak in the phase of interest was compared to the intensity of the strongest line of alumina, forming the Reference Intensity Ratio (RIR). Using this method, it was possible to estimate the mass fractions of the phases present, assuming that the sum of all identified phases was 100%.

First, qualitative scans of samples of 50 wt% Al_2O_3 and 50 wt% of the phases of interest were obtained in order to calibrate the system. Then, the X'Pert HighScore software was used to perform the semi-quantitative analysis using the qualitative x-ray scans for the different samples which were described previously. Before the analysis began, the software was used to convert the data from adjustable to fixed aperture, and the $\alpha 2$ peaks were stripped from the patterns.

Scanning Electron Microscopy

By viewing cross sections of the wires with the Scanning Electron Microscope, it was desired to study the reaction layer between the W wires and the the 612 material. The wires were placed inside thermocouple tubing and then mounted in epoxy. The samples were ground with kerosene on 320, 600, and 1200 grit papers and then polished with 3 mm diamond paste (Struers). After the samples were initially viewed in the Hitachi S-800 SEM, further polishing and etching of the surface was obtained with a dilute mixture of Murakami's reagent and alumina powder. The Murakami's reagent was made

with 10 parts distilled water, 1 part $K_3Fe(CN)_8$, and 1 part NaOH. The samples were then viewed again in the Hitachi S-800 SEM for further analysis.

CHAPTER 4

RESULTS AND DISCUSSION

In this chapter, the results of the thermogravimetric analysis of the barium source materials are presented as plots of percent weight gain vs. time in both the low- and intermediate-humidity environments. In addition, the results of the qualitative, quantitative, and semi-quantitative x-ray diffraction analyses are presented, along with proposed reaction sequences for the mixture of the 612 material and tungsten in the cathode. Finally, the data is fit to a reaction rate model; several factors are discussed which could affect the rate of reaction in the capsules; and published evaporation rates of Ba are used to predict cathode lifetime.

Environmental Stability of Barium Source Materials

Thermogravimetric analysis was used to study the sensitivity of several barium compounds to moisture in the atmosphere in order to evaluate their suitability for use as barium source materials. Weight gain of the samples was measured as they were exposed to both low- and intermediate-humidity environments.

During each experiment, the temperature and mass lost were recorded as a function of time. Figure 4.1 shows temperature and mass lost plotted as a function of time for the $4BaO{\cdot}CaO{\cdot}Al_2O_3$ material (411) at a dew point of –15ºC. It is evident that the 411 material lost mass as it was heated and held at 700°C, and then gained mass as it was cooled and held at room temperature. Figure 4.2 is a plot of the rate of change in the mass of the 411 material as it was heated to 700°C.

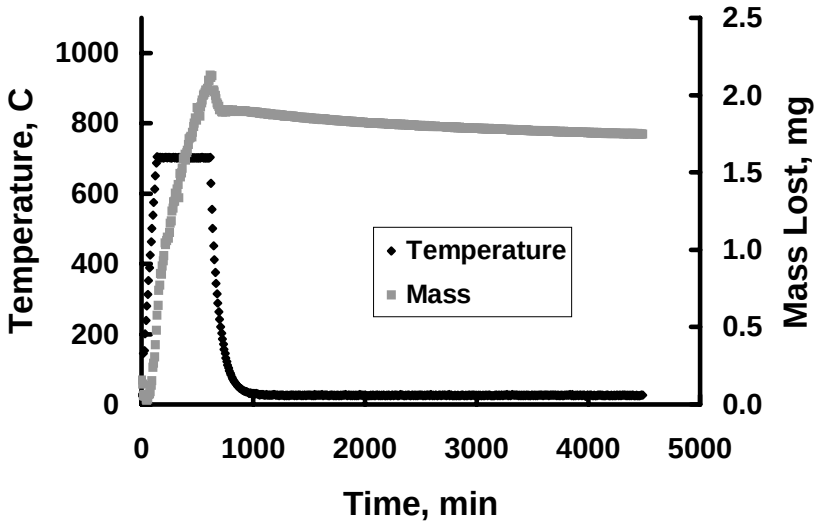

Figure 4.1. Temperature and Mass Lost vs. Time for the 411 Material at a Dew Point of -15ºC.

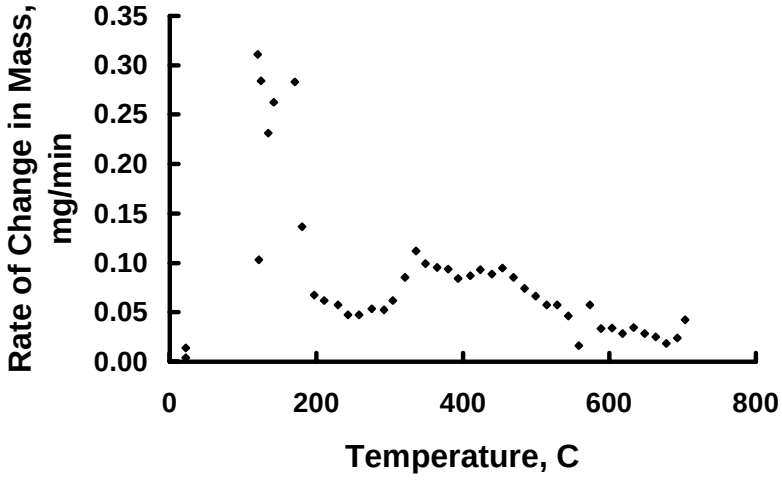

Figure 4.2. Rate of Change in Mass vs. Temperature During Heat Up for the 411 Material.

Because the material had been exposed to some atmospheric moisture during handling prior to the start of the experiment, dehydration of the 411 material could be observed as it was heated to 700°C. The material appeared to lose water in several stages, which agrees with results reported by Ahmed and Glasser[17] as well as Habashy and Kolta.[18] Based on results reported by Habashy and Kolta, the initial peak in the dm/dt curve at approximately 140°C corresponds to the decomposition of $Ba(OH)_2 \cdot 8H_2O$ to $Ba(OH)_2 \cdot 2H_2O$ or $Ba(OH)_2 \cdot H_2O$. The second peak in the dm/dt curve at approximately 335°C corresponds to the decomposition of the $Ba(OH)_2 \cdot 2H_2O$ or $Ba(OH)_2 \cdot H_2O$ to form anhydrous barium hydroxide. Finally, the peak at 450ºC corresponds to the dehydration of anhydrous barium hydroxide to form BaO.[16]

Even after the sample was held at 700°C for 8 hours, the sample was still losing mass. Therefore, the experiment was repeated holding the sample at 700°C for 30 hours to determine at what point the weight loss might stabilize. Figure 4.3 shows temperature and mass lost plotted as a function of time for the 411 material at a dew point of –15ºC.

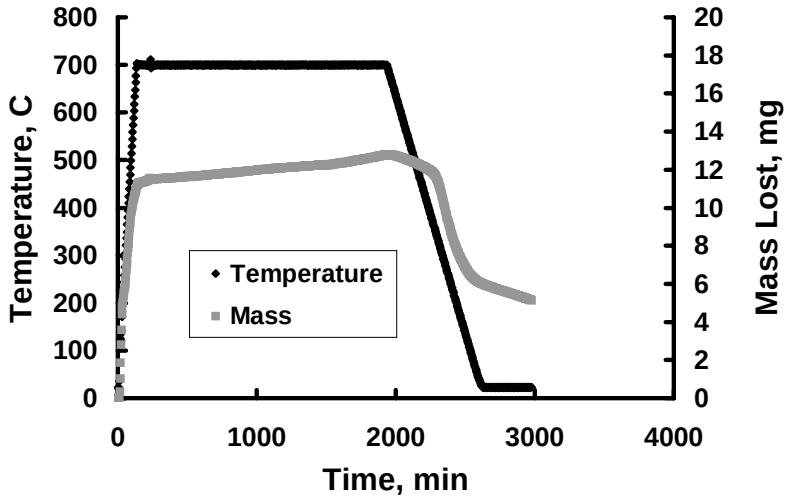

Figure 4.3. Temperature and Mass Lost vs. Time for the 411 Material at a Dew Point of -15ºC.

Even after holding at 700°C for 30 hours, the sample was still losing mass. At this point one would expect that all of the water of hydration had been removed from the material, so the continued weight loss was attributed to evaporation of barium oxide. Based on these results, it was deemed sufficient to hold the samples for just 8 hours at 700ºC in subsequent experiments in order to insure that the material was fully dehydrated.

The sample began to pick up moisture as it was cooled from 700°C to room temperature. Figure 4.4 shows the rate of change in mass upon cooling plotted as a function of temperature.

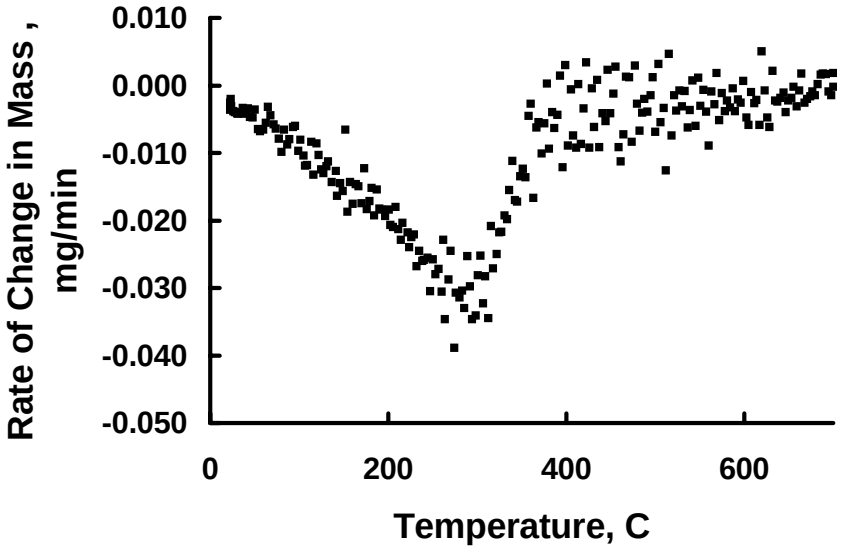

Figure 4.4. Rate of Change in Mass Plotted vs. Temperature During Cooling for the 411 Material at a Dew Point of –15ºC.

The 411 material picked up moisture at the greatest rate at a temperature of approximately 300°C. The amount of mass gained while the material was cooled and held at room temperature was calculated as a percentage of the original mass of the material. Figure 4.5 shows temperature and percent weight gain plotted as a function of time for the 411 material at a dew point of –15ºC.

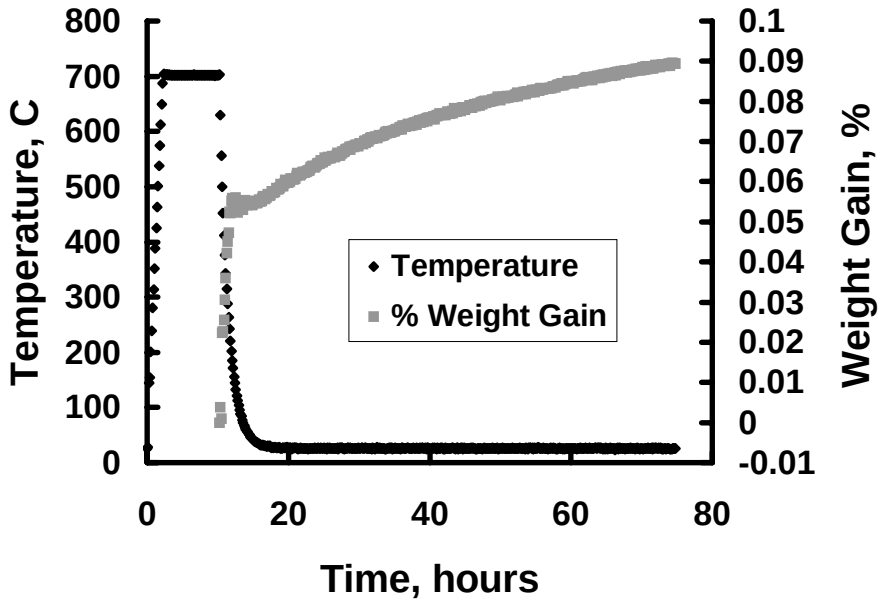

Figure 4.5. Temperature and Percent Weight Gain Plotted vs. Time for the 411 Material at a Dew Point of –15ºC.

The experiment was repeated for the other four source materials, and the percent weight gain vs. time for all five materials is plotted in Figure 4.6. An expanded view of the percent weight gain for the barium source materials at a dew point of –15ºC is shown in Figure 4.7.

It is evident in Figure 4.6 that B_3A was the least stable in the presence of water vapor, having gained 1.68% by 60 hours. The other four barium source materials all gained less than 0.4% in a similar time frame. The difference between the performance of the B_3A and the barium calcium aluminates (612, 411, and B_4A_{SSL}) is evidently attributable to the presence of calcium. The addition of calcium in solid solution form apparently decreases the reactivity of the material, and thus reduces the hydration effects.

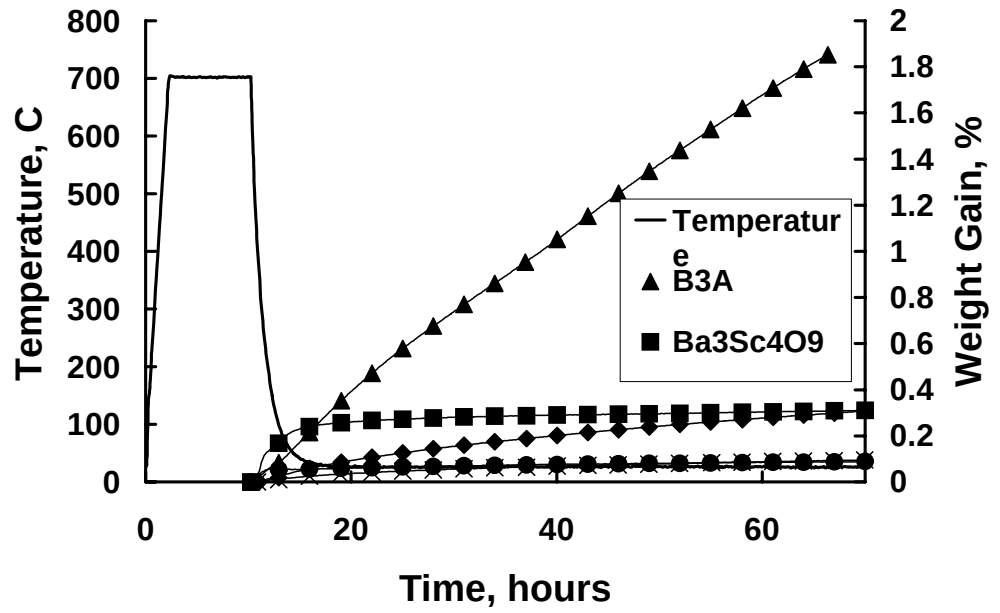

Figure 4.6. Temperature and Percent Weight Gain Plotted vs. Time for Five Barium Source Materials at a Dew Point of –15ºC.

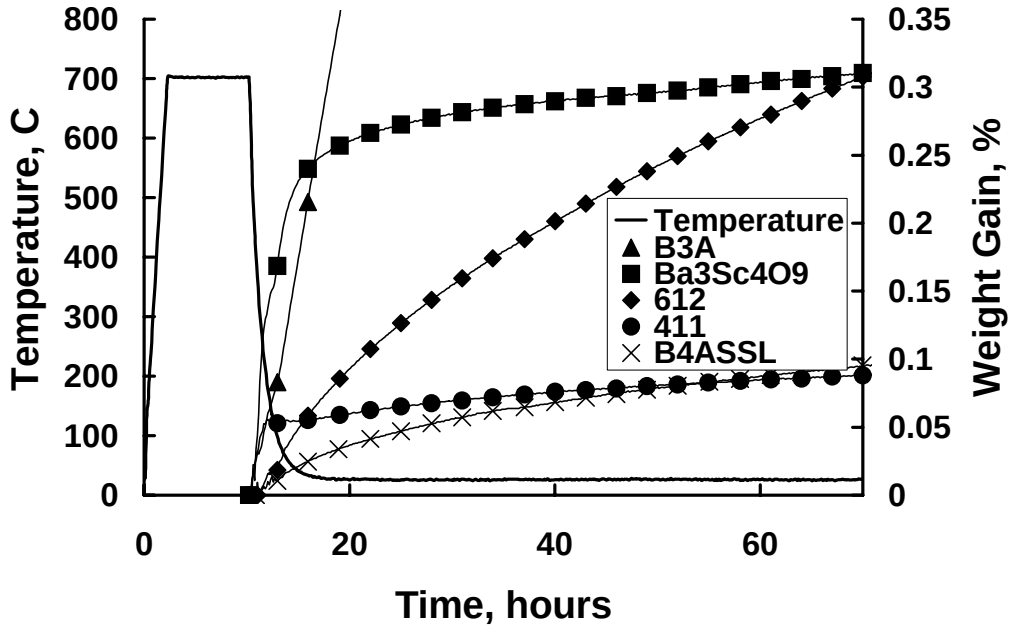

Figure 4.7. Expanded View of the Temperature and Percent Weight Gain Plotted vs. Time for Five Barium Source Materials at a Dew Point of –15ºC.

In the case of the three barium calcium aluminates, the percent weight gain decreases with increasing calcium content, suggesting that additional calcium as solid solution increased the stability of the material. Unlike the other barium calcium aluminates, the 411 material initially gained weight at a rapid rate and then leveled off at a much slower rate. This difference in behavior can be explained by the presence of free BaO in the 411 material. The BaO is extremely reactive and hydrates quickly, which led to the initial rapid weight gain. Once the BaO had completely hydrated, the remaining solid solution materials hydrated at a much slower rate, similar to that of the 612 and B_4A_{SSL} solid solutions.

The experiment was repeated at a dew point of 11ºC for each of the barium source materials. Figure 4.8 shows the percent weight gain plotted as a function of time for the source materials at a dew point of 11ºC.

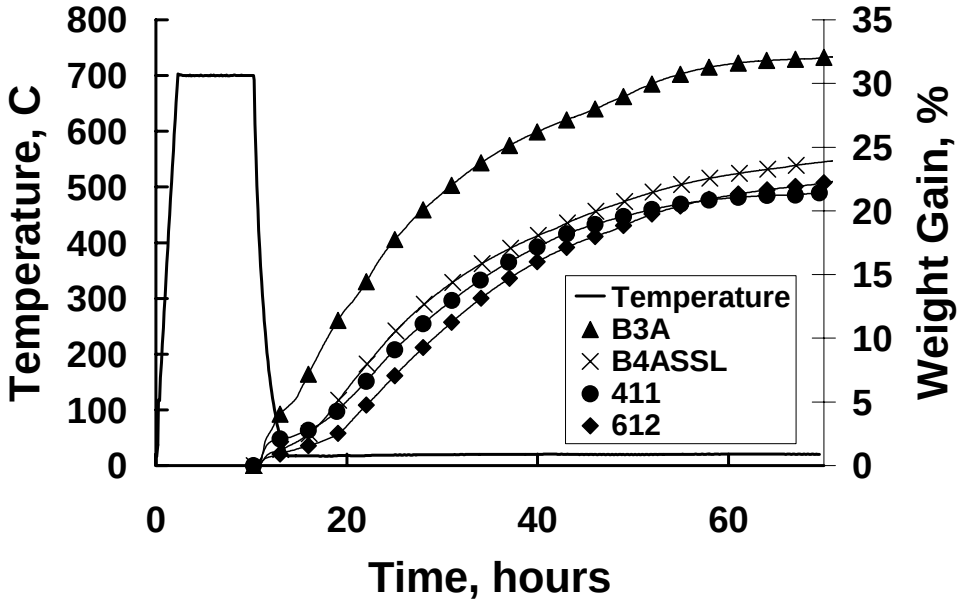

Figure 4.8. Temperature and Percent Weight Gain Plotted vs. Time for Five Barium Source Materials at a Dew Point of 11ºC.

While the materials had gained between 0.4-1.7% at 60 hours at a dew point of –15ºC, the weight gain increased to 21-32% over 60 hours at a dew point of 11ºC. This significant weight gain after exposure to an intermediate-humidity shows the importance of handling the source material in a controlled environment prior to use in the cathode. Again, the behavior of the B_3A varied from the behavior of the barium calcium aluminates. The presence of calcium increased the stability of the B_4A_{SSL}, 411, and the 612 material which reduced their percent weight gain significantly compared to that of the B_3A. Note that the $Ba_3Sc_4O_9$ was only moderately stable at low-humidity, but was extremely stable, relative to the barium calcium aluminates, in intermediate-humidity conditions. While this material appears to be an excellent choice from an environmental standpoint, more work needs to be done to determine if it is reactive enough with W to produce an adequate Ba supply.

Accelerated Reactions Between the 612 Material and W

As discussed in Chapters 1 and 3, experiments were performed to study the reaction between the 612 material and tungsten in a simulated reservoir hollow cathode environment. The reaction products were analyzed by qualitative, quantitative, and semi-quantitative x-ray diffraction.

Qualitative X-ray Diffraction Analysis Results for the 1000ºC Sample

X-ray analysis of the sample run at 1000ºC for 100 hours showed the contents of the capsule to be W, $BaAl_2O_4$, Ba_2CaWO_6, Ba_3WO_6, and a B_3A solid solution with 10% CaO. At temperatures below 1200ºC, the 612 material is composed of three phases: a

B_3A solid solution phase with 10% CaO which has the formula $Ba_{2.6}Ca_{0.4}Al_2O_6$ and two B_4A solid solution phases. However, the solid solubility of CaO changes as the temperature is increased, and at temperatures above 1200ºC the 612 material is composed of the B_3A solid solution phase and only one B_4A solid solution phase with 12% CaO which has the formula $Ba_{3.4}Ca_{0.6}Al_2O_7$.

While all of the B_4A solid solution phase appears to have reacted in the various samples, some of the B_3A solid solution still remained. As a general rule, the reactivity of barium calcium aluminate materials increases with increasing BaO content. Conversely, the substitution of Ca for Ba atoms tends to create more stable compounds which are less reactive.[52] Because the B_4A solid solution had a higher BaO content than the B_3A solid solution, while both had similar calcium contents, the B_4A solid solution reacted more rapidly than the B_3A solid solution.

The x-ray diffraction patterns for the bottom pellet of the capsule heated to 1000ºC for 100 hours is shown in Figures 4.9. An expanded view of the diffraction pattern showing the presence of the 100% intensity peak for the Ba_3WO_6 phase is shown in Figure 4.10. A proposed reaction sequence for the reaction of the 612 material with W to form $BaAl_2O_4$, Ba_2CaWO_6, and Ba_3WO_6 in the 1000 ºC sample will be presented under the discussion of the 2000 hour test cathode.

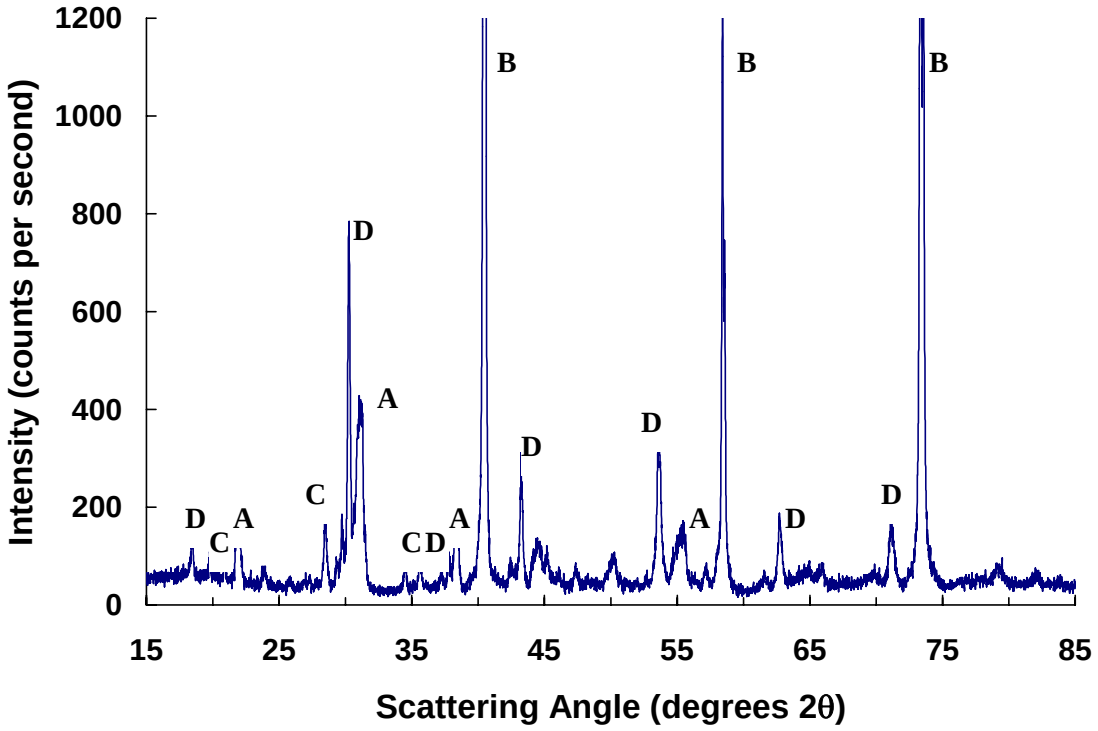

Figure 4.9. Diffraction Pattern for the Bottom Pellet of the Capsule Heated to 1000ºC for 100 Hours where A = the B_3A solid solution with 10% CaO, B = W, C = $BaAl_2O_4$, and D = Ba_2CaWO_6.

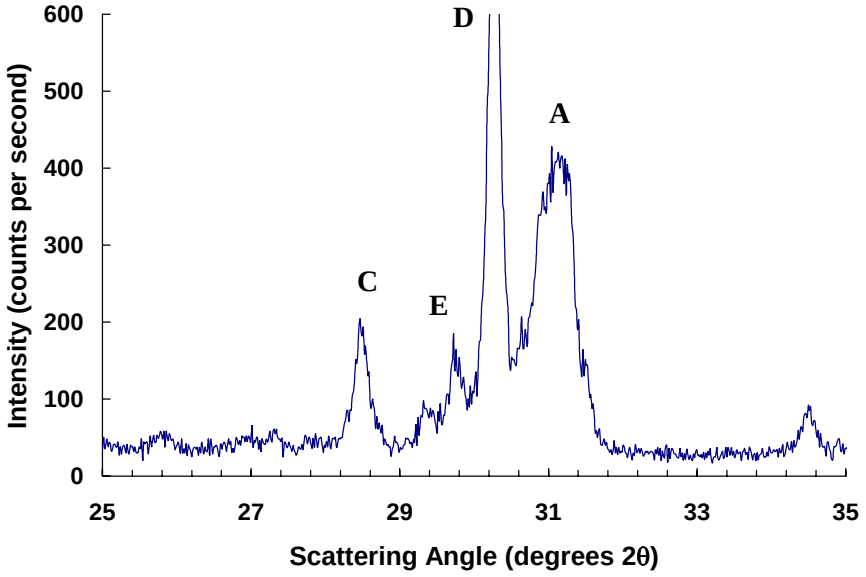

Figure 4.10. Expanded View of the Diffraction Pattern for the Bottom Pellet of the Capsule Heated to 1000ºC for 100 Hours where A = the B_3A solid solution with 10% CaO, C = $BaAl_2O_4$, and D = Ba_2CaWO_6, and E = Ba_3WO_6.

Qualitative X-ray Diffraction Analysis Results for the 1200ºC and 1300ºC Samples

X-ray analysis of the samples run at 1200ºC and 1300ºC for 100, 200, and 400 hours showed the contents of the capsules to be W, $BaAl_2O_4$, Ba_2CaWO_6, and a B_3A solid solution with 10% CaO. The x-ray diffraction patterns for the bottom and top pellets of the capsule heated to 1200ºC for 400 hours are shown in Figures 4.11 - 4.12.

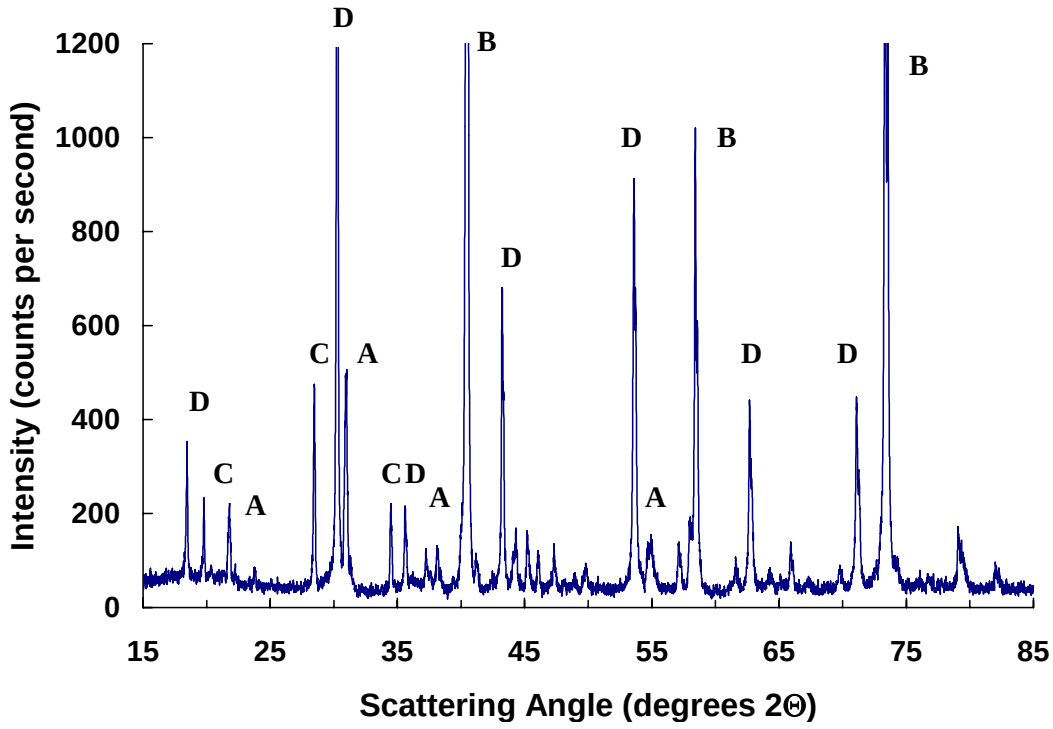

Figure 4.11. Diffraction Pattern for the Bottom Pellet of the Capsule Heated to 1200ºC for 400 Hours where A = the B_3A solid solution with 10% CaO, B = W, C = $BaAl_2O_4$, and D = Ba_2CaWO_6.

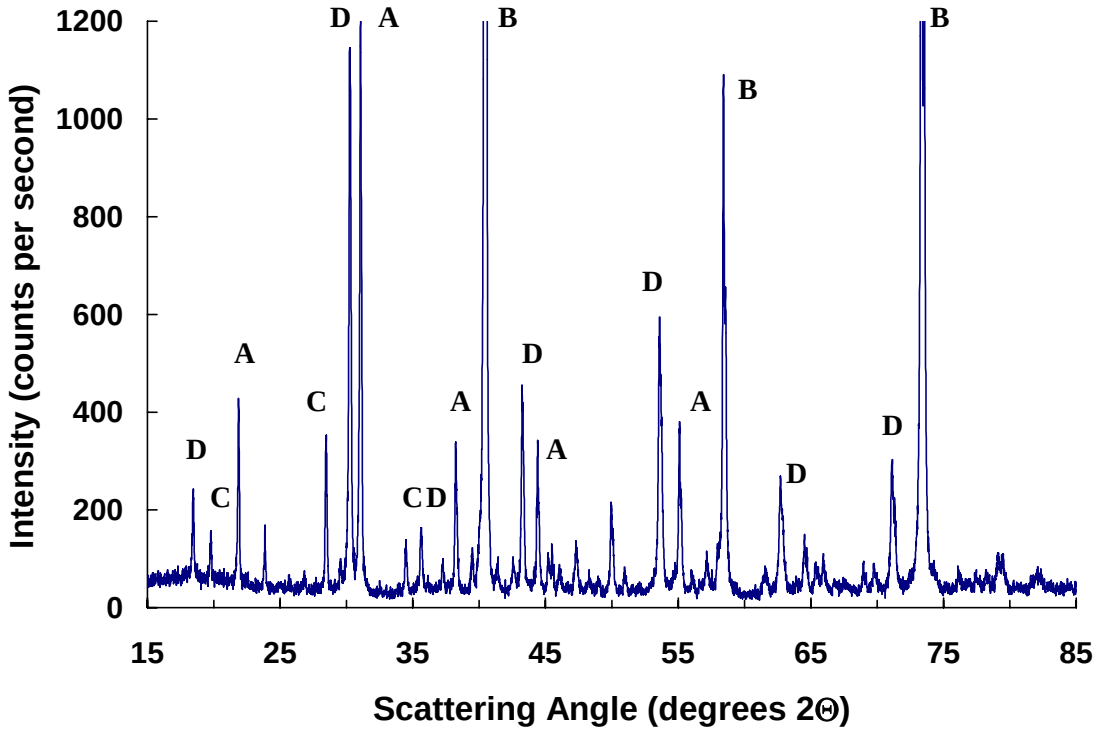

Figure 4.12. Diffraction Pattern for the Top Pellet of the Capsule Heated to 1200ºC for 400 Hours where A = the B_3A solid solution, B = W, C = $BaAl_2O_4$, and D = Ba_2CaWO_6.

A comparison between the 100% intensity peaks for the $BaAl_2O_4$, Ba_2CaWO_6, and B_3A solid solution phase with 10% CaO for the bottom and top pellets of the sample heated at 1200ºC for 400 hours is shown in Figure 4.13. It is apparent from Figure 4.13 that after heating, the top pellet contained a higher concentration of the starting material, the B_3A solid solution, while the bottom pellet contained a higher concentration of the reaction products, $BaAl_2O_4$ and Ba_2CaWO_6. The x-ray diffraction patterns for the top pellets of five other samples are shown in Figures 4.14 - 4.18.

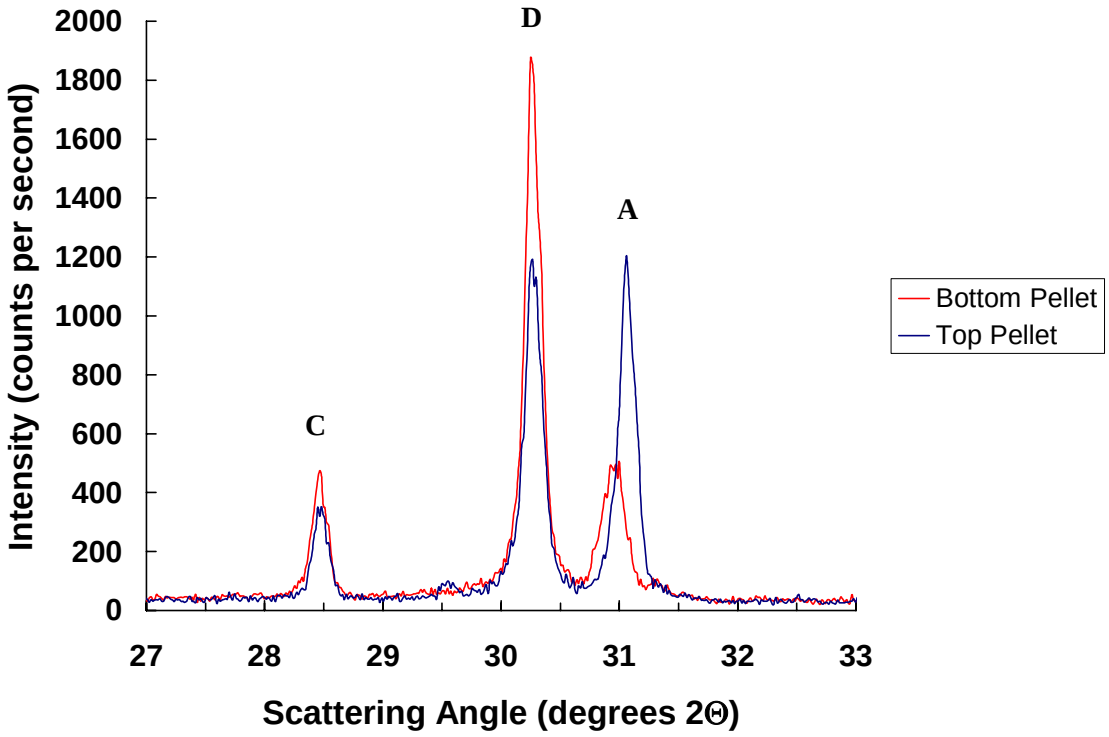

Figure 4.13. Comparison Between the Bottom and Top Pellets of the Capsule Heated to 1200ºC for 400 Hours where A = the B_3A solid solution with 10% CaO, B = W, C = $BaAl_2O_4$, and D = Ba_2CaWO_6.

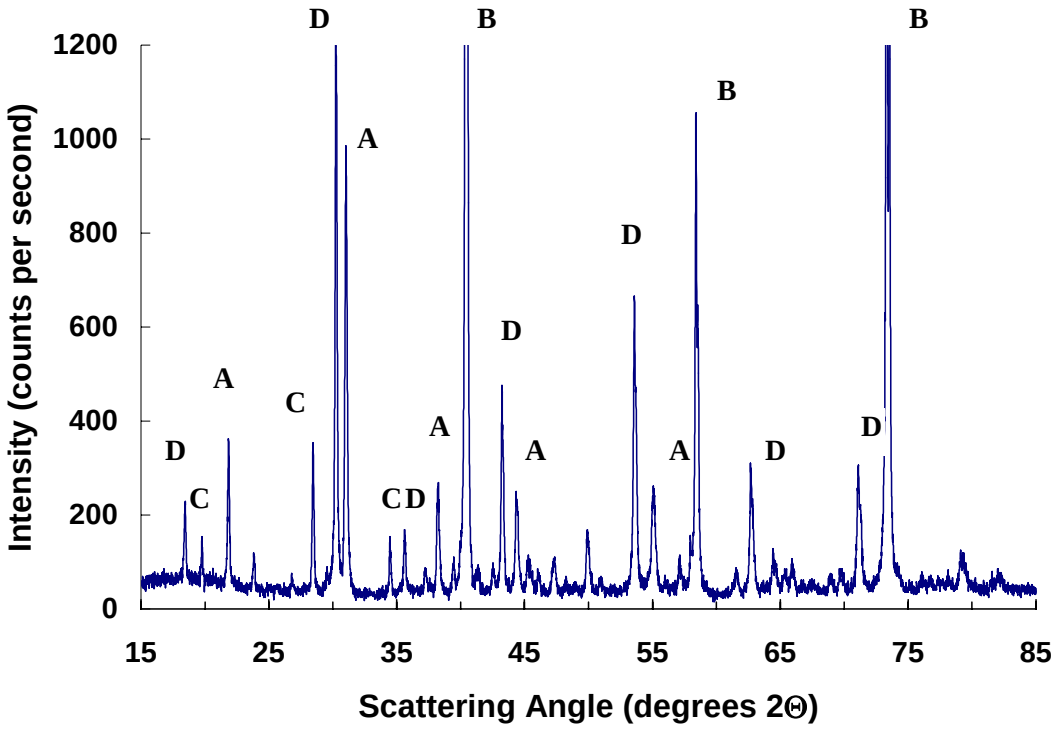

Figure 4.14. Diffraction Pattern for the Top Pellet of the Capsule Heated to 1200ºC for 100 Hours where A = the B_3A solid solution, B = W, C = $BaAl_2O_4$, and D = Ba_2CaWO_6.

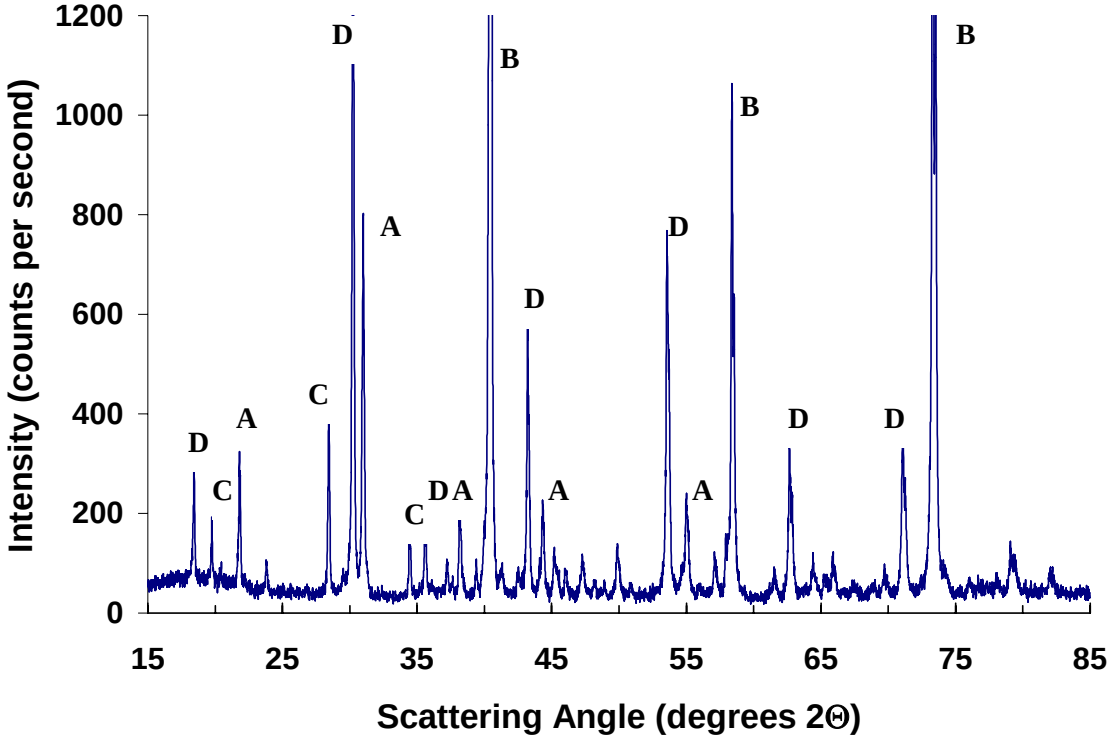

Figure 4.15. Diffraction Pattern for the Top Pellet of the Capsule Heated to 1200ºC for 200 Hours where A = the B_3A solid solution, B = W, C = $BaAl_2O_4$, and D = Ba_2CaWO_6.

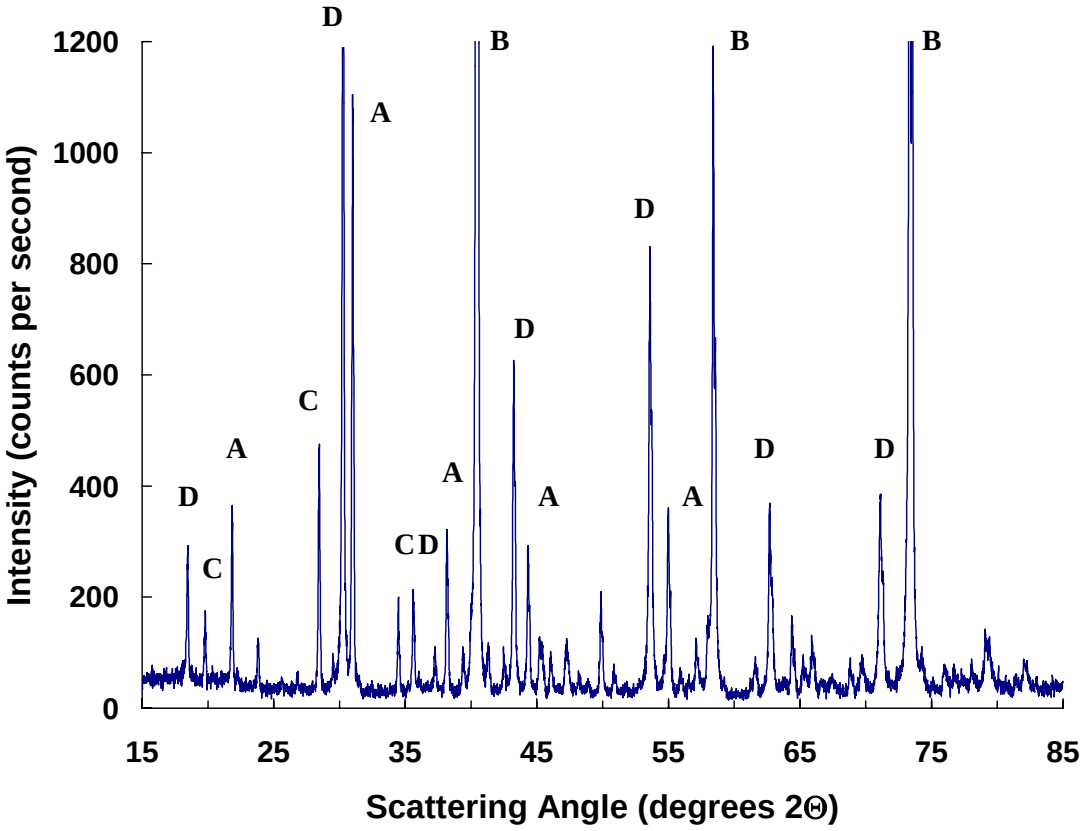

Figure 4.16. Diffraction Pattern for the Top Pellet of the Capsule Heated to 1300ºC for 100 Hours where A = the B_3A solid solution, B = W, C = $BaAl_2O_4$, and D = Ba_2CaWO_6.

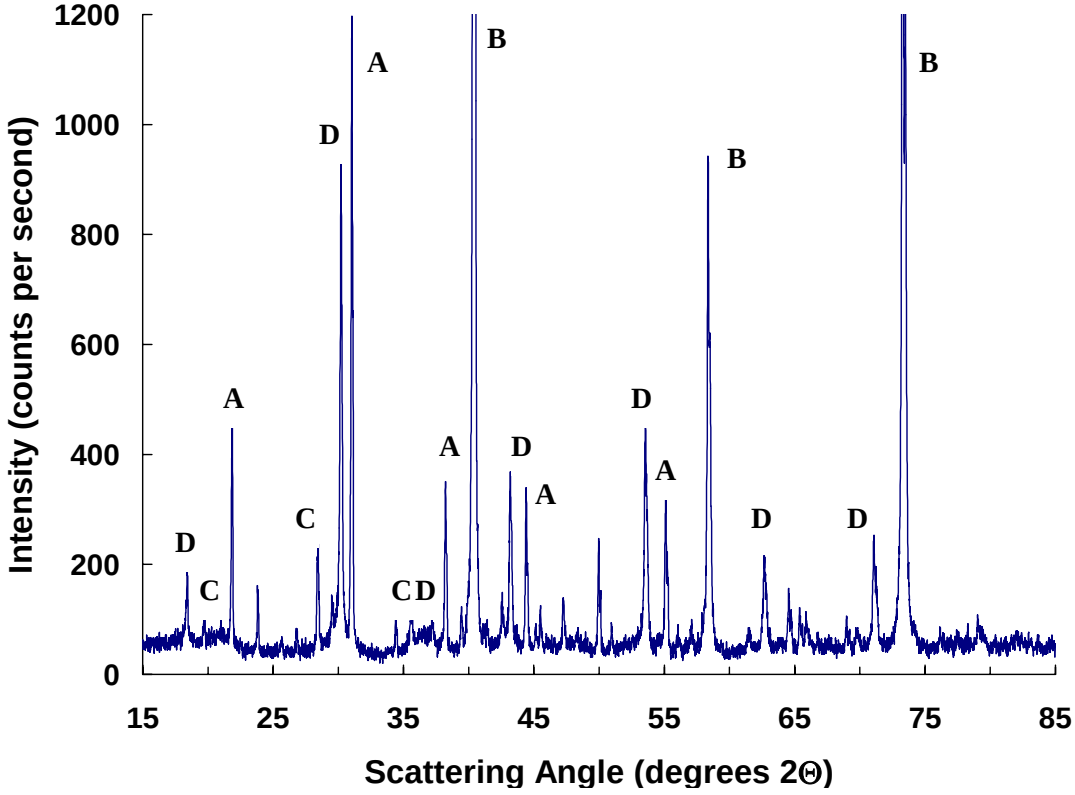

Figure 4.17. Diffraction Pattern for the Top Pellet of the Capsule Heated to 1300ºC for 200 Hours where A = the B_3A solid solution, B = W, C = $BaAl_2O_4$, and D = Ba_2CaWO_6.

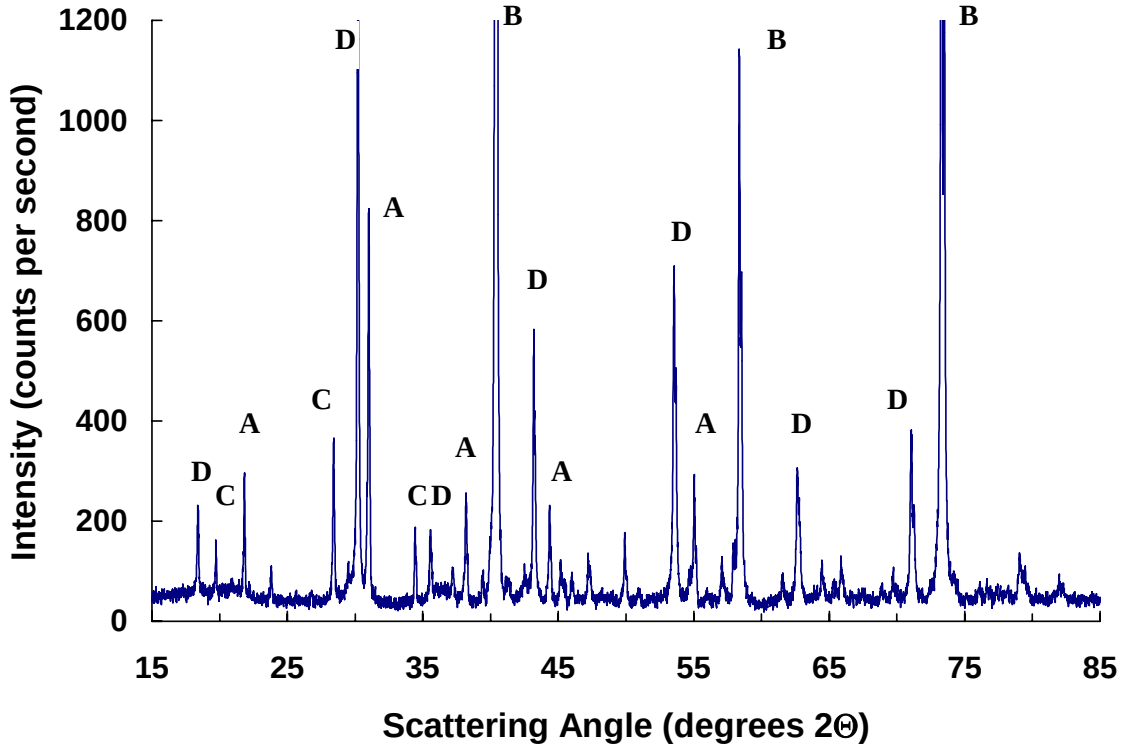

Figure 4.18. Diffraction Pattern for the Top Pellet of the Capsule Heated to 1300ºC for 400 Hours where A = the B_3A solid solution, B = W, C = $BaAl_2O_4$, and D = Ba_2CaWO_6 .

Proposed Reactions for the 1200ºC and 1300ºC Samples

Based on the qualitative x-ray diffraction analysis results for the samples heated to 1200ºC and 1300ºC, the following reaction is proposed for the 612 material and tungsten:

$$Ba_6CaAl_4O_{13} + W + 0.5O_2 \rightarrow Ba_2CaWO_6 + 2BaAl_2O_4 + 2Ba(g).$$

The reaction can also be broken down between the two solid solution phases of the 612 material:

$$Ba_{3.4}Ca_{0.6}Al_2O_7 + 0.6W + 0.3O_2 \rightarrow BaAl_2O_4 + 0.6Ba_2CaWO_6 + 1.2Ba(g)$$

$$Ba_{2.6}Ca_{0.4}Al_2O_6 + 0.4W + 0.2O_2 \rightarrow BaAl_2O_4 + 0.4Ba_2CaWO_6 + 0.8Ba(g)$$

It is believed that $BaAl_2O_4$ is a final reaction product which will not continue to react to produce barium vapor. This assumption is based on the activation energy for the thermal decomposition of $BaAl_2O_4$ to form BaO and $BaAl_{12}O_{19}$ which is reported by Lipeles and Kan[52] to be 129 kcal/mole over the 900 – 1250ºC range of cathode operation. Because it would require such a high activation energy to decompose $BaAl_2O_4$, it has been assumed that at the estimated service temperature of 1100-1200ºC, $BaAl_2O_4$ is a final reaction product.

The proposed reactions require a source of O_2 in order to proceed. Because the reactions were run in vacuum, there should not have been sufficient O_2 in the atmosphere to contribute to the reactions. There are two possible sources that could have provided the O_2 necessary for the reactions. First of all, it is assumed that there was O_2 adsorbed on the surface of the tungsten powder in the capsules. Also, there may have been water vapor in the hygroscopic 612 material that supplied oxygen to the reaction.

The following reaction is proposed for Ba_2CaWO_6 and W:

$$Ba_2CaWO_6 + O_2 + W \rightarrow BaWO_4 + CaWO_4 + Ba(g).$$

There are several reasons to believe that Ba_2CaWO_6 is an intermediate phase which reacts further with the tungsten to produce barium vapor. First of all, Suitch[32] observed $BaWO_4$ as a major reaction product after heating mixtures of 15 wt% of the 612 material and 85 wt% W at 1100ºC in air. Also Shroff et al.[23] heated tungsten filaments impregnated with barium calcium aluminates and identified the major reaction products to be $BaAl_2O_4$, $BaWO_4$, and $CaWO_4$. While the samples run in these experiments don't show any evidence of the formation of $BaWO_4$ and $CaWO_4$, it is believed that these reaction products would eventually have formed after an extended period of time.

Quantitative X-Ray Diffraction Analysis Results

Quantitative analysis was performed in order to determine the amount of the 612 material, $BaAl_2O4$, Ba_2CaWO_6, and W that were present in the reacted samples. Examples of the x-ray diffraction scans for the peaks of $BaAl_2O_4$, Ba_2CaWO_6, W and Ag which were used to calculate the percentages of $BaAl_2O_4$, Ba_2CaWO_6, and W in the bottom pellet of the sample heated to 1200ºC for 400 hours are shown below in Figures 4.19 - 4.22.

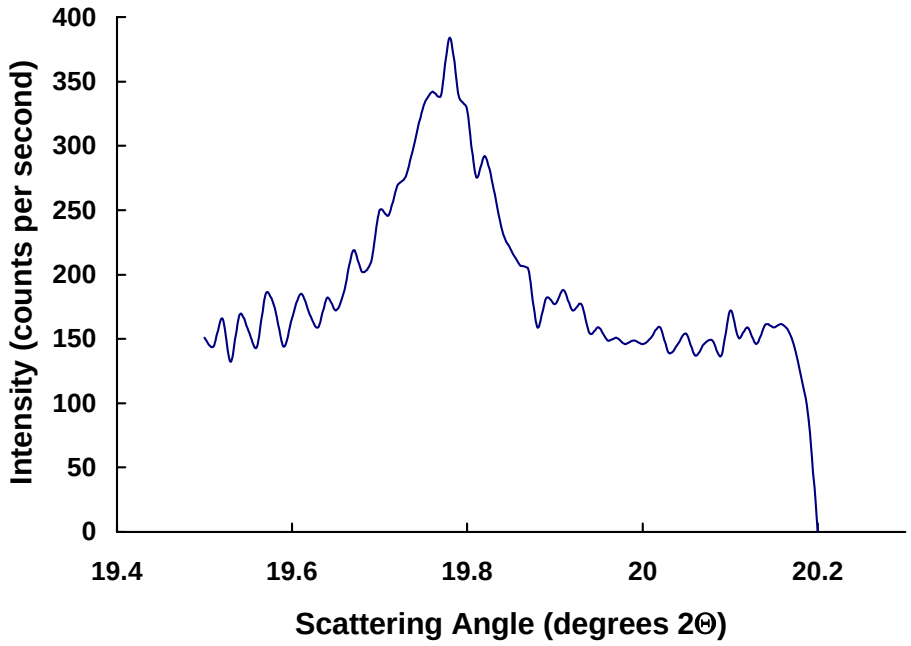

Figure 4.19. X-Ray Scan for the $BaAl_2O_4$ Peak in the Bottom Pellet of the Capsule Heated to 1200ºC for 400 Hours

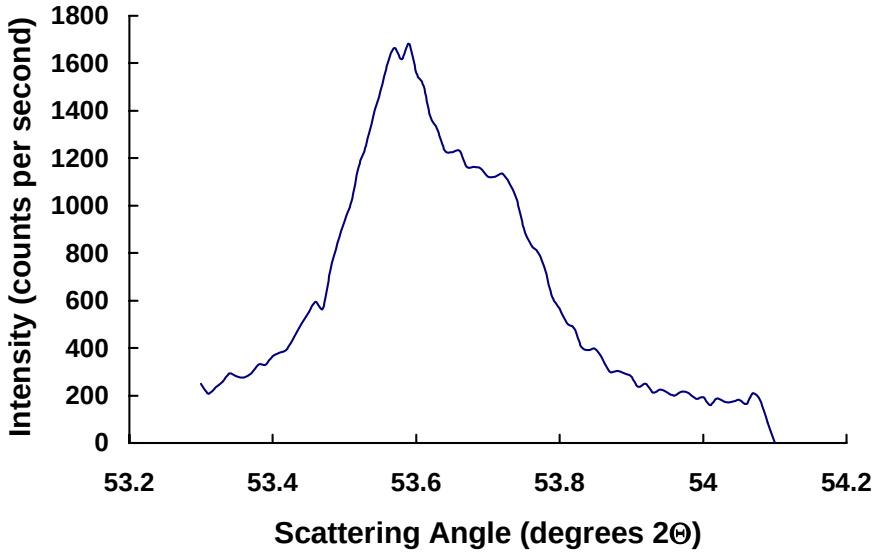

Figure 4.20. X-Ray Scan for the Ba_2CaWO_6 Peak in the Bottom Pellet of the Capsule Heated to 1200ºC for 400 Hours

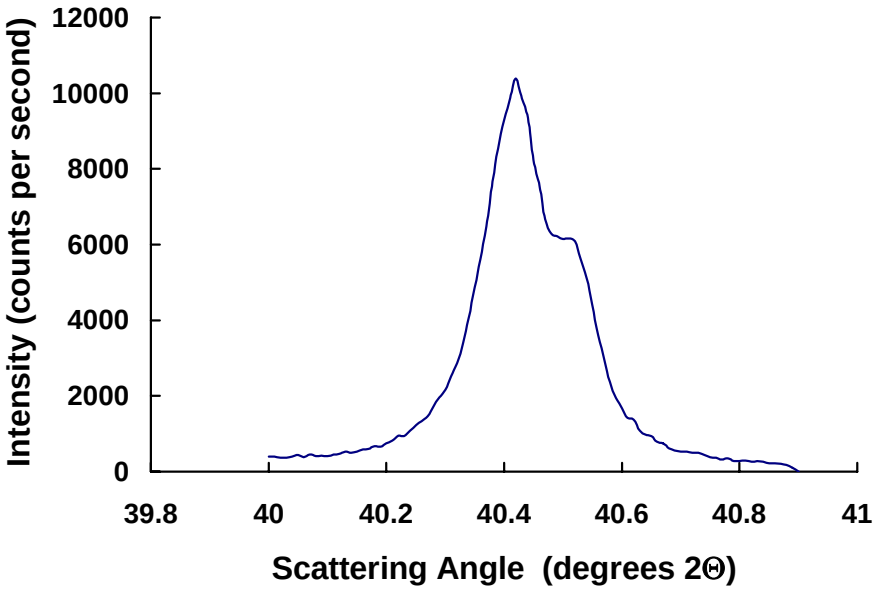

Figure 4.21. X-Ray Scan for the W Peak in the Bottom Pellet of the Capsule Heated to 1200ºC for 400 Hours

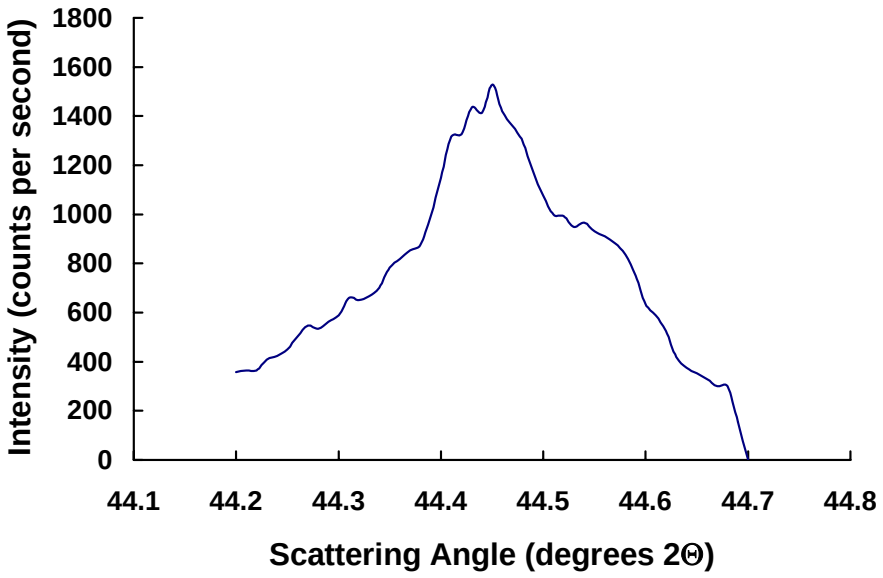

Figure 4.22. X-Ray Scan for the Ag Peak in the Bottom Pellet of the Capsule Heated to 1200ºC for 400 Hours

Two samples were run for each of the three pellets in the seven molybdenum capsules, and the average values are given in Table 4.1. The measured phase intensities and background intensities used to calculate these percentages for all of the quantitative analysis runs are shown in Appendix A.

While quantitative analysis was performed on the 612 material, these results have not been included in this analysis. The peak selected to identify the 612 material in the formation of the calibration set corresponded to a peak of the B_4A solid solution phase in the 612 material. Because all of the B_4A solid solution reacted in the accelerated test samples, the quantitative analysis program indicated that no 612 material remained in the samples. However, it is known that some of the B_3A solid solution actually remained in the samples. Quantitative analysis was also performed on the $BaWO_4$ phase, and these results have likewise been excluded from this analysis because the material was not found to be present in any of the samples.

Table 4.1 Quantitative Analysis Results for the Accelerated Reaction Tests

Temp. (ºC)	Time (hrs)	Pellet	% $BaAl_2O_4$	% Ba_2CaWO_6	%W
1000	100	Bottom	5.1	9.4	67.5
		Middle	4.4	12.8	12.8
		Top	2.3	10.0	83.2
1200	100	Bottom	9.2	18.1	45.4
		Middle	5.6	10.8	27.8
		Top	4.1	10.6	41.3
1200	200	Bottom	16.3	31.4	69.7
		Middle	11.7	21.1	54.0
		Top	7.6	13.9	42.6
1200	400	Bottom	11.5	20.8	58.1
		Middle	7.3	19.5	49.6
		Top	6.9	15.6	48.1
1300	100	Bottom	10.6	21.6	46.4
		Middle	10.1	20.6	47.9
		Top	6.0	12.6	27.0
1300	200	Bottom	7.9	18.0	25.8
		Middle	4.6	11.1	35.9
		Top	2.0	7.9	20.4
1300	400	Bottom	11.3	23.4	36.5
		Middle	9.9	19.3	49.4
		Top	6.3	16.4	30.9

While the quantitative results did appear to be fairly consistent for the runs performed on the same samples, there was natural variation due to the fact that each x-ray scan only analyzed a small amount of powder spread on a cover glass. Another factor that surely contributed to the variations is the fact that the analysis was being used to quantify small amounts of material in the presence of large amounts of tungsten which is a strong absorber of x-rays.

Inconsistencies in the calculated tungsten concentrations may be attributed to overlap of the tungsten peak selected for quantitative analysis at 40.3º 2θ by a 25% intensity $BaAl_2O_4$ peak at 40.1º 2θ. When the calibration set for the W was originally established, it was believed that the $BaAl_2O_4$ phase would be present in such small amounts in

the reaction products that a 25% intensity peak would not significantly contribute to the measured W peak. However, the reaction proceeded to a further extent than was originally anticipated, and it is possible that the presence of the $BaAl_2O_4$ peak introduced error into the calculation of the W concentrations.

Variations Between the Pellets in the Molybdenum Capsules

For most of the samples, it appears that the bottom pellet reacted to the furthest extent while the top pellet reacted to the least extent. Once again, the "bottom" pellet refers to the pellet closest to the laser-welded end, while the "top" pellet refers to the pellet closest to the porous tungsten plate.

There are at least two possible explanations for the variable composition of the pellets in the capsules. First of all, it is possible that there was a radial temperature gradient in the furnace, which placed the bottom pellet at a higher temperature than the top pellet. The top pellet in the capsule was located near the center of the furnace tube near the thermocouple monitoring temperature in the system, while the bottom pellet in the capsule was sitting very close to the alumina tube. If the temperature of the tube itself was higher than the temperature at the center of the tube, this may help to explain why the bottom pellets reacted to a further extent than the top pellets.

In order to test this theory, sample 7 was loaded into the furnace on its side in a carrier which placed it directly in the center of the tube. The results in Table 4.1 show that even when the pellets were placed in this configuration, the same trend was still observed between the extent of reaction in the bottom, middle, and top pellets. Therefore, while it is still possible that there was a temperature gradient that caused some variation

in the pellets, there must be another factor which contributed to the difference in the extent of reaction in the pellets.

Another factor that could have affected the rate of reaction in the pellets was the presence of moisture in the hygroscopic 612 material. It is possible that the presence of oxygen in the form of water vapor in the 612 material could have driven the first proposed reaction to proceed more rapidly. Because the top pellets were closest to the porous W plate, the vacuum pump may have removed water vapor most readily from the top pellets, then the middle pellets, and then the bottom pellets. Therefore, there would have been the least amount of oxygen available to drive the reaction in the top pellets and the greatest amount of oxygen available in the bottom pellets. Assuming that was the case, this would explain why the top pellets reacted to the least extent, while the bottom pellets reacted to the furthest extent. Because it was believed that the top pellets should have been closest to the set point temperature and also should have had the least amount of water vapor present, it was assumed that the quantitative results for the top pellets were the most indicative of the results that would be obtained in a reservoir hollow cathode.

Formation of $BaAl_2O_4$ and Ba_2CaWO_6 with Time

A plot of the percent $BaAl_2O_4$ formed vs. time at 1200ºC for the bottom, middle, and top pellets is shown in Figure 4.23, and a plot of the percent $BaAl_2O_4$ formed vs. time at 1300ºC for the bottom, middle, and top pellets is shown in Figure 4.24.

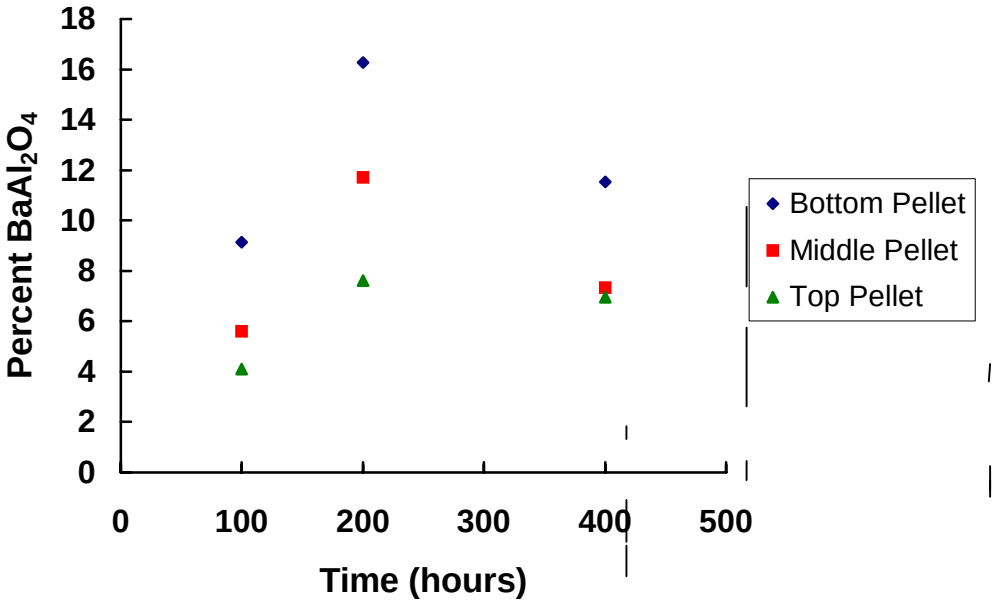

Figure 4.23. Percent $BaAl_2O_4$ Formed vs. Time at 1200ºC.

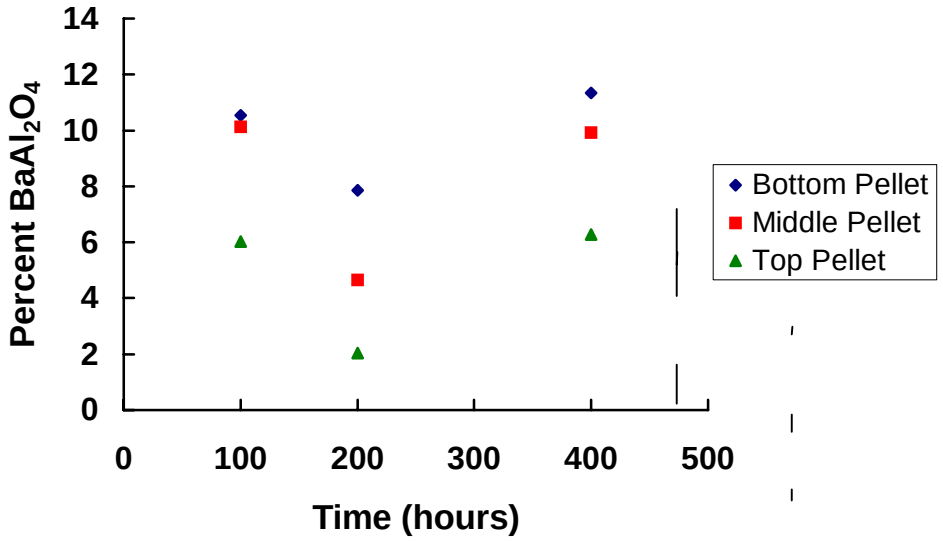

Figure 4.24. Percent $BaAl_2O_4$ Formed vs. Time at 1300ºC.

A plot of the percent Ba_2CaWO_6 formed vs. time at 1200ºC for the bottom, middle, and top pellets is shown in Figure 4.25, and a plot of the percent Ba_2CaWO_6 formed vs. time at 1300ºC for the bottom, middle, and top pellets is shown in Figure 4.26. The percentage of the reaction products $BaAl_2O_4$ and Ba_2CaWO_6 formed in the samples run at 1200ºC increased from 100 to 200 hours and the decreased from 200 to 400 hours. However, the percentage of the reaction products $BaAl_2O_4$ and Ba_2CaWO_6 formed in the samples run at 1300ºC decreased from 100 to 200 hours and then increased from 200 to 400 hours.

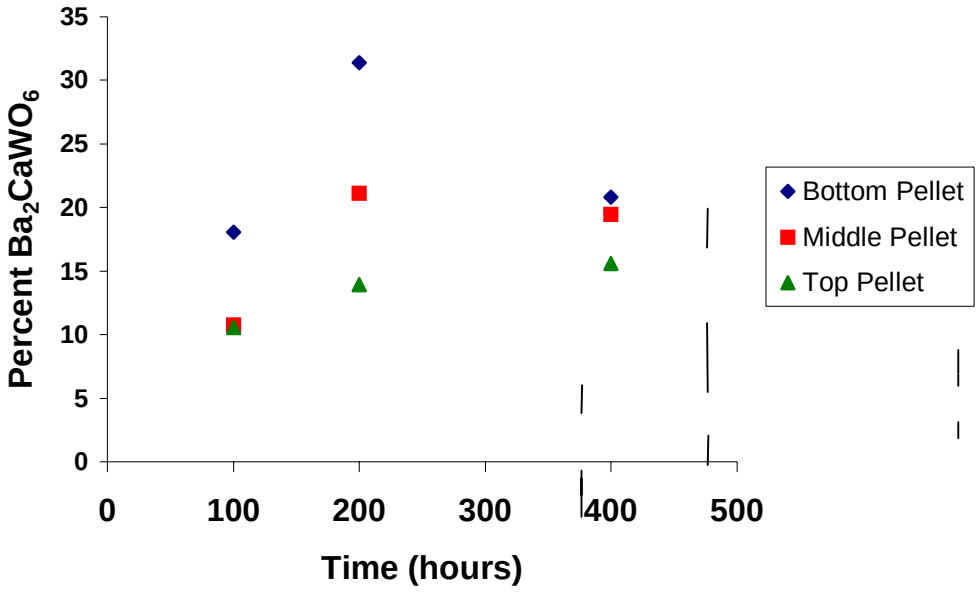

Figure 4.25. Percent Ba_2CaWO_6 Formed vs. Time at 1200ºC.

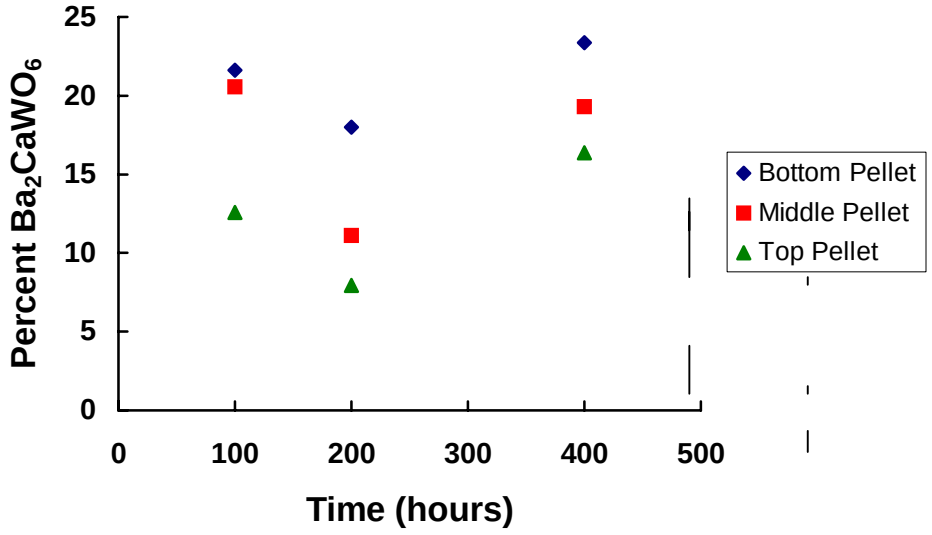

Figure 4.26. Percent Ba_2CaWO_6 Formed vs. Time at 1300ºC.

Because $BaAl_2O_4$ is assumed to be a final reaction product based on the high activation energy of its decomposition reaction, it was expected that the amount of this material formed would increase with time for the samples run at both 1200ºC and 1300ºC. However, neither the samples run at 1200ºC nor the samples run at 1300ºC showed an increase in the formation of $BaAl_2O_4$ with time. With the current amount of experimental data, it is not possible to speculate which data points may be invalid. Further experimental work needs to be done to repeat the measurements at 1200ºC and 1300ºC for 100, 200, 400 hour in order to establish a clearer trend in the data.

The Ba_2CaWO_6 may be an intermediate phase, so it was not clear whether the amount of Ba_2CaWO_6 would increase with time or would initially increase and then decrease as the Ba_2CaWO_6 started to react with W. For the samples at 1200ºC, it is possible that the amount of Ba_2CaWO_6 increased from 100 to 200 hours as the reaction between the 612 material and W progressed, and then the concentration of Ba_2CaWO_6 decreased

from 200 to 400 hours as the Ba_2CaWO_6 reacted with W. However, the results at 1300ºC are not consistent with this trend, and it is not evident why the amount of Ba_2CaWO_6 should have decreased from 100 to 200 hours and then increased from 200 to 400 hours. Again, further experimental work needs to be done in repeating these experiments to learn how the concentration of Ba_2CaWO_6 varies with time.

Semi-Quantitative X-Ray Analysis Results

Semi-quantitative x-ray analysis was performed on the X'Pert HighScore software using the qualitative scans for the samples run at 1200ºC and 1300ºC. The semi-quantitative results are summarized in Table 4.2, and the results for the top pellets at 1200ºC and 1300ºC are plotted in Figures 4.27 and 4.28. The semi-quantitative results are then compared to the quantitative results in Table 4.3.

Table 4.2. Semi-Quantitative Results for the Accelerated Test Samples Run at 1200ºC and 1300ºC

Temp. (ºC)	Time (hrs)	Pellet	$\%B_3A_{SS}$	% $BaAl_2O_4$	% Ba_2CaWO_6	%W
1200	100	Bottom	26	11	17	46
		Top	42	6	10	42
1200	200	Bottom	22	10	17	50
		Top	39	3	11	47
1200	400	Bottom	22	9	17	52
		Top	50	3	8	39
1300	100	Bottom	26	6	15	53
		Top	43	6	11	40
1300	200	Bottom	36	6	10	48
		Top	55	3	8	35
1300	400	Bottom	17	10	16	57
		Top	38	3	11	48

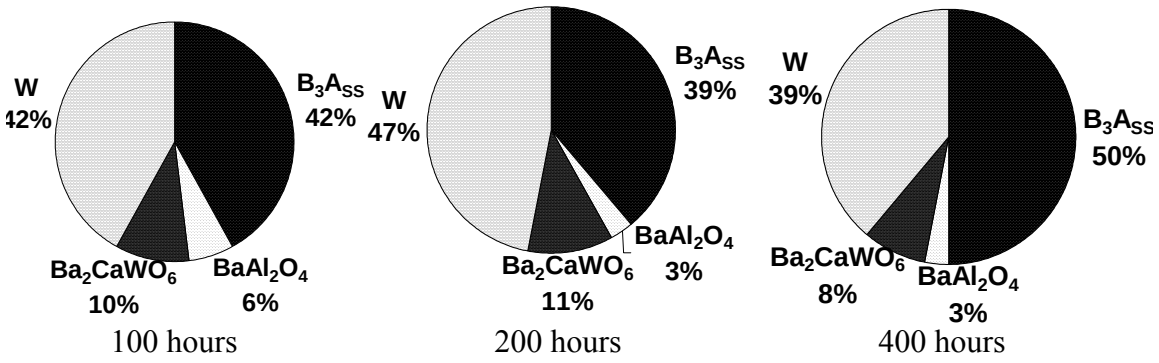

Figure 4.27. Semi-Quantitative Analysis Results for the Samples Run at 1200ºC.

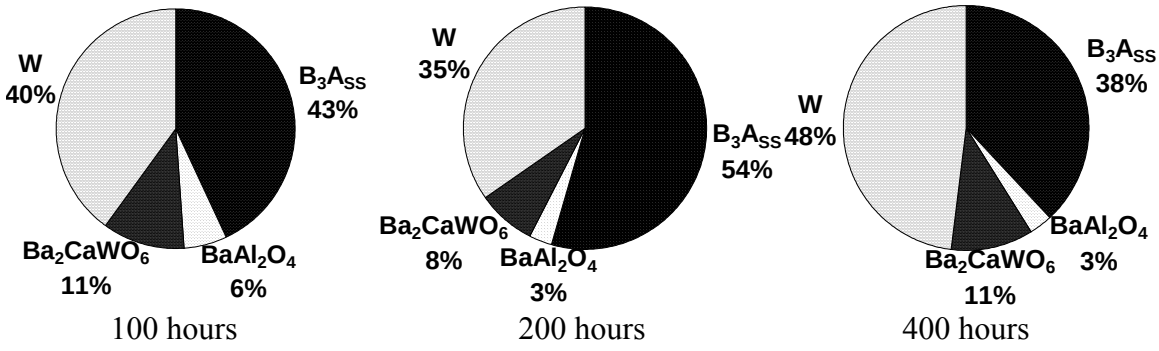

Figure 4.28. Semi-Quantitative Analysis Results for the Samples Run at 1300ºC.

Table 4.3. Comparison Between the Semi-Quantitative Results and the Quantitative Results for the Accelerated Test Samples Run at 1200ºC and 1300ºC

Temp. (ºC)	Time (hrs)	Pellet	$\%B_3A_{SS}$		$\%\ BaAl_2O_4$		$\%\ Ba_2CaWO_6$		%W	
			Quant	Semi-Quant	Quant	Semi-Quant	Quant	Semi-Quant	Quant	Semi-Quant
1200	100	Bottom		26	9.2	11	18.1	17	45.4	46
		Top		42	4.1	6	10.6	10	41.3	42
1200	200	Bottom		22	16.3	10	31.4	17	69.7	50
		Top		39	7.6	3	13.9	11	42.6	47
1200	400	Bottom		22	11.5	9	20.8	17	58.1	52
		Top		50	6.9	3	15.6	8	48.1	39
1300	100	Bottom		26	10.6	6	21.6	15	46.4	53
		Top		43	6.0	6	12.6	11	27.0	40
1300	200	Bottom		36	7.9	6	18.0	10	25.8	48
		Top		55	2.0	3	7.9	8	20.4	35
1300	400	Bottom		17	11.3	10	23.4	16	36.5	57
		Top		38	6.3	3	16.4	11	30.9	48

Quantitative analysis was not utilized to determine the amount of the B_3A solid solution phase present in the samples. As mentioned previously, an initial attempt was made to quantify the 612 material using quantitative analysis, but the peak selected to identify the 612 material corresponded to the B_4A solid solution phase. Because the B_4A solid solution phase reacted very rapidly, the quantitative results indicated that none of the 612 material remained in the samples. Later in the analysis, some of the peaks in the x-ray patterns were determined to correspond to peaks in the B_3A solid solution phase. At this late stage in the project, it was decided to quantify the B_3A solid solution phase using only the semi-quantitative analysis.

Comparing the quantitative and semi-quantitative analysis results for $BaAl_2O_4$, Ba_2CaWO_6, and W, the results for some of the samples appear to be consistent while others do not match very well. It is not evident what factor could have caused this inconsistency in only some of the samples. In general, it is expected that the quantitative analysis results should be more accurate because it measured the peak areas, while the semi-quantitative analysis only used the peak intensities and assumed that the peaks all had the same Full Width and At Half Maximum (FWHM).

It was expected that the amount of B_3A solid solution would decrease with time. This trend was not observed; however, the semi-quantitative analysis results for the B_3A solid solution did appear to be in agreement with the trends observed in the formation of reaction products from the quantitative analysis results. The percent B_3A solid solution remaining the bottom and top pellets of the samples run at 1200ºC is shown in Figure 4.29, and the percent B_3A solid solution remaining in the bottom and top pellets of the samples run at 1300ºC is shown in Figure 4.30.

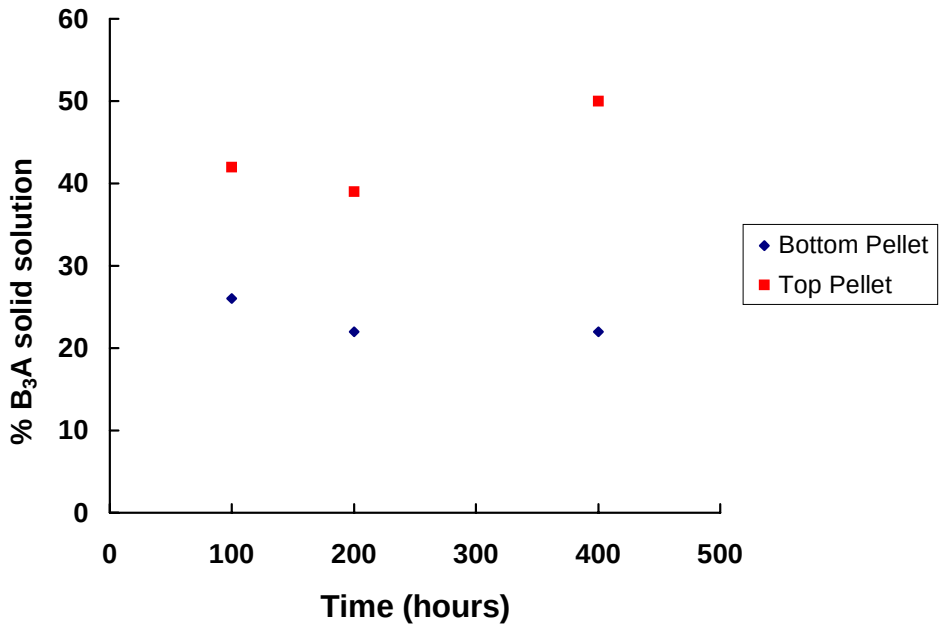

Figure 4.29. Percent B_3A Solid Solution Remaining in the Samples Heated to 1200ºC.

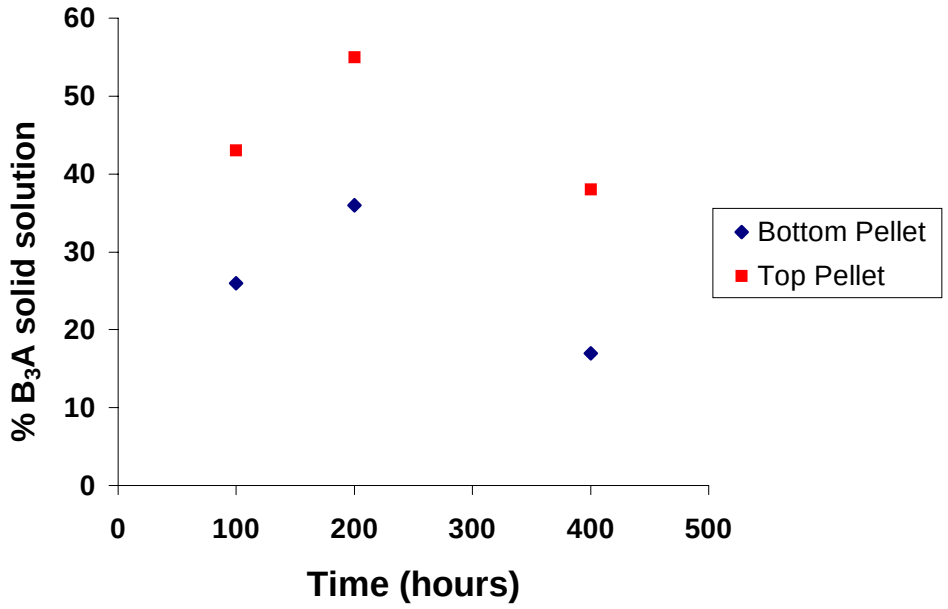

Figure 4.30. Percent B_3A Solid Solution Remaining in the Samples Heated to 1300ºC.

The quantitative analysis results had shown that the percentage of reaction products was higher in the bottom pellets than the top pellets, indicating that the bottom pellets reacted to a further extent than the top pellets. The semi-quantitative analysis results showed that there was a higher percentage of B_3A solid solution remaining in the top pellets than the bottom pellets, confirming that the bottom pellets reacted to a further extent than the top pellets.

Also, the trends observed in the percentage of B_3A solid solution remaining with time in Figures 4.29 and Figure 4.30 match the trends observed in the formation of $BaAl_2O_4$ and Ba_2CaWO_6 with time at 1200ºC and 1300ºC shown in Figures 4.21 - 4.24. While the percentage of the reaction products in the samples run at 1200ºC increased from 100 to 200 hours and the decreased from 200 to 400 hours, the amount of B_3A solid solution remaining decreased from 100 to 200 hours and increased from 200 to 400 hours. Similarly, while the percentage of the reaction products in the samples run at 1300ºC decreased from 100 to 200 hours and the increased from 200 to 400 hours, the amount of B_3A solid solution remaining increased from 100 to 200 hours and decreased from 200 to 400 hours. This consistency between the x-ray results validates the accuracy of the measurement techniques that were used.

The semi-quantitative results for the B_3A solid solution do not fit the predicted trend, as it is believed that the amount of B_3A solid solution should have decreased with time for the samples run at both 1200ºC and 1300ºC. More data points need to be obtained through further experimental work in order to determine what may be causing the inconsistencies in the data and in order to establish a clearer trend of how the concentration of the B_3A solid solution varies with time.

Blum and Li's Reaction Rate Model

According to Blum and Li's[27] reaction rate model, the rate of reaction is best fit to a straight line by plotting xt vs. t. A plot of xt vs. t for $BaAl_2O_4$ for the accelerated reaction test samples run at 1200ºC and 1300ºC is shown in Figure 4.31. In Figure 4.31, it can be observed that the data points for the 1300ºC samples do not appear to fit a straight line. Because the concentration of $BaAl_2O_4$ did not increase with time for the samples at 1300ºC, it was not expected that plotting xt vs. t would fit a straight line. While the data points for the 1200ºC samples do appear to fit a straight line, it is important to remember that there were also some inconsistencies in the formation of $BaAl_2O_4$ with time at 1200ºC.

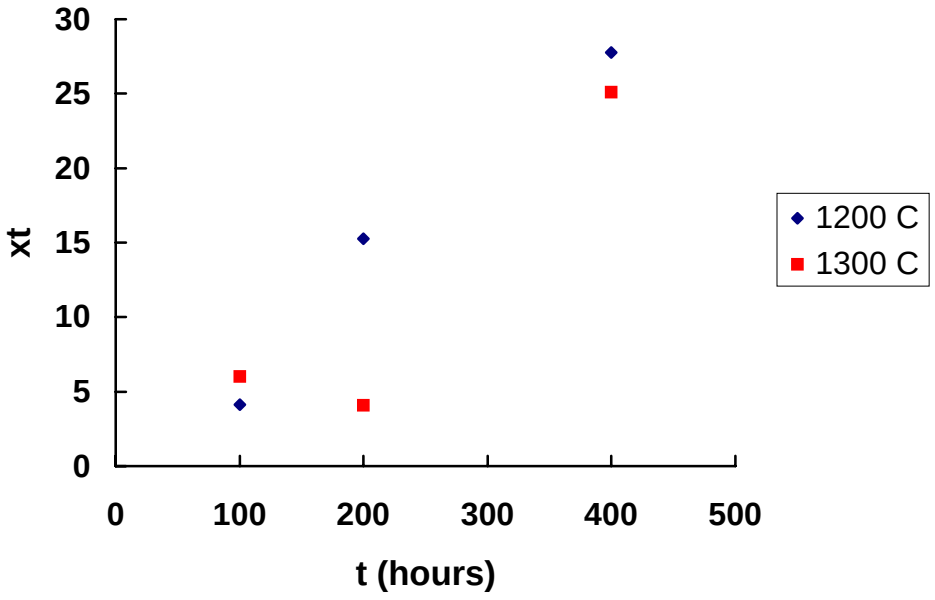

Figure 4.31. Plot of xt vs. t for $BaAl_2O_4$ Formation.

Therefore, although the data does fit a straight line for the 1200ºC samples, it is expected that the slope of a trend line fit through the data points would not accurately model the reaction rates for the 612 material and W. Consequently, it would not be possible to use the slope of the line to accurately predict the fraction of $BaAl_2O_4$ which would exist after a designated operation time of the cathode. Based on the proposed reaction for the 612 material and W, it was calculated that the concentration limit of $BaAl_2O_4$ which could form in the sample would be 24.3 wt%, or x = 0.243.

A plot of xt vs.t for Ba_2CaWO_6 for the samples run at 1200ºC and 1300ºC is shown in Figure 4.32. Similar to the formation of the $BaAl_2O_4$, it appears that the data points for the 1200ºC samples fit a straight line while the data points for the 1300ºC samples do not.

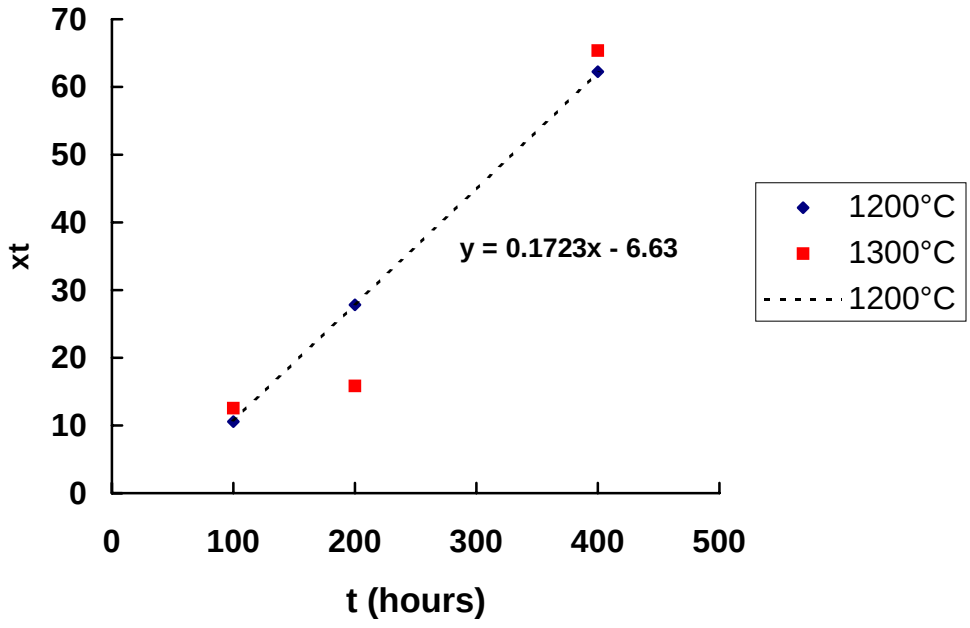

Figure 4.32. Plot of xt vs. t for Ba_2CaWO_6 Formation.

Based on the variation in concentration of Ba_2CaWO_6 with time for the samples at both 1200ºC and 1300ºC, it is not clear whether the amount of Ba_2CaWO_6 should continue to increase with time or should increase and the decrease as the Ba_2CaWO_6 begins to react with W. If the latter is true and the formation of Ba_2CaWO_6 does not increase with time, then it would not be appropriate to try to fit the data for the concentration of Ba_2CaWO_6 to Blum and Li's model. Further experimental data is needed in order to establish a clear trend in the formation of Ba_2CaWO_6 with time.

Scanning Electron Microscopy

The tungsten wires run in the molybdenum capsules at 1200ºC for 100 hours and at 1300ºC for 100, 200, and 400 hours were viewed in the Hitachi S-800 SEM. The formation of a reaction layer on the edge of the tungsten wires was not clearly evident in any of the samples. The diameters of the wires were also measured, but there did not appear to be a clear trend in the variation of the wire size with reaction time for the samples run at 1300ºC.

Vapor Pressure of Ba

The vapor pressure of barium in the cathodes has a significant impact on the rate of reaction, and ultimately on the life of the barium source material. Once the equilibrium vapor pressure of barium is established in a traditional impregnated cathode, the reaction between the source material and tungsten proceeds only to the extent necessary to replace Ba vapor which has diffused through the porous tungsten emitter to the surface. In the reservoir hollow cathodes, it was likewise assumed that the rate of reaction would

significantly decrease once the equilibrium vapor pressure of Ba was established in the reservoir. However, the reactions in the simulated reservoir hollow cathode environment proceeded much more rapidly than had been anticipated, consuming all of the original B_4A solid solution phase in the 612 material in 100 hours or less at 1000ºC. For this reason, it is believed that enough barium vapor did not build up inside the reservoir to establish the equilibrium vapor pressure of Ba and slow down the reaction.

Theoretically, it should only take a small amount of barium vapor to establish the equilibrium vapor pressure of barium in the capsules. Based on the dimensions of the molybdenum capsules, the volume inside the capsules is calculated to be 0.0429 in^3. Assuming that the pellets are 50%-dense, the volume of the pores is estimated to be 0.0215 in^3 or 0.0003523 L. Karmyshin, Totskii, and Shpil'rain[47] developed the following relationship for the vapor pressure of barium: log p (mm Hg) = 6.711 – (7850.5/T). Based on this relationship, the vapor pressure of barium is calculated to be 24.066 mm Hg or 0.03167 atm at 1200ºC. Using this information and the Ideal Gas Law, the mass of barium vapor needed to establish the equilibrium vapor pressure of barium inside the capsules at 1200ºC is 1.268 x 10^{-5} g Ba.

Based on the extent of the reaction, it is apparent that the equilibrium vapor pressure of Ba was not established in the capsules to slow down the reaction. Certainly there was plenty of Ba vapor produced, so therefore it is believed that the barium vapor must have escaped too easily through the pores in the tungsten. The permeability of the porous tungsten must have been high enough to allow the barium to escape not only through diffusion along the surface of the tungsten particles in the emitter but also by Knudsen flow through the pores.

In impregnated dispenser cathodes which have previously been used, the reaction proceeds more slowly because the path for the barium to escape is much more tortuous than in the reservoir hollow cathodes. There is a very dense impregnant in the pores of the W, and the barium can only escape through tiny micro cracks between the impregnant and the walls of the tungsten pores. The reservoir hollow cathodes, however, have approximately 25% open porosity in the tungsten emitters through which the barium can escape.

Surface Area of Tungsten in the Capsules

In addition to the fact that the equilibrium vapor pressure of barium was not established, another factor which could have affected the rate of reaction was the high surface area of the tungsten in the powder mixture. The reservoir hollow cathodes have much higher surface area of tungsten in contact with the barium source material than impregnated dispenser cathodes. In impregnated cathodes where the barium compound is melting into the tungsten matrix, the only tungsten in contact with the barium compound is at the walls of the pores in the tungsten matrix.

It is possible to estimate the surface area of tungsten in an impregnated cathode assuming that the tungsten particles are hexagonally close packed spheres. In this packing configuration, the pores can be visualized as the open space inside the tetrahedral formed by the tungsten particles. Estimating the pore as a sphere, geometry can be used to calculate the radius of the pore to be 0.414 times the radius of the tungsten spheres. Therefore, if the tungsten has a radius of 2.5 μm, the radius of the pore is 1.035 μm. The

surface area of a pore is $4\pi(1.035\mu m)^2 = 13.46\ \mu m^2$. The number of tungsten particles per unit bulk volume, N_p, can be estimated by the equation: [60]

$$N_p = \frac{6(PF)}{\pi a^3},$$

where PF = the packing fraction and a = the diameter of the particles. For a close packed configuration, the packing fraction equals 0.74. Substituting in the packing fraction and diameter of the spheres, the value of $N_p = 0.011306\ \mu m^{-3}$. Each tungsten particle is surrounded by 6 pores, while each pore is surrounded by 4 tunsten particles, so the number of pores can be calculated by multiplying the number of tungsten particles by 6/4. Therefore, the number of pores per unit volume is estimated to be $0.016959\ \mu m^{-3}$ or 1.6959×10^{16} m-^{3}.

The dimensions of the cathode insert are given as follows: OD = 0.25 in, ID = 0.21 in, and length = 1 in. Therefore, the volume of the porous tungsten equals π(1 in)[$(0.125\ in)^2 - (0.105\ in)^2$] = $0.01445\ in^3$ or $2.368 \times 10^{-7}\ m^3$. Considering the number of pores per unit volume is $1.6959 \times 10^{16}\ m^{-3}$, the number of pores in the tungsten insert is 4.016×10^9. Multiplying the number of pores by the surface area of each pore, the surface area of the tungsten in the full-scale impregnated cathode insert is estimated to be $5.405 \times 10^{10}\ \mu m^2$ or $0.05405\ m^2$.

However in the reservoir hollow cathodes, 50 wt% of tungsten powder with a maximum particle size of 5 μm is interspersed with 50 wt% barium compound in the reservoir. Because the particle size of the tungsten powder in the reservoir is very small, it has an extremely high surface area. For the full-scale reservoir hollow cathodes, the volume of the reservoir is $1.74\ cm^3$. Assuming 50% packing density of the powder in the

reservoir, the volume of occupied space is 0.86779 cm^3. While the mixture is composed of 50 wt% of the 612 material and 50 wt% W, this corresponds to 18.6 vol% W and 81.4 vol% of the 612 material. Therefore the volume occupied by W powder in the reservoir is 0.161 cm^3. The volume of one 5 μm W particle is 6.545×10^{-11} cm^3, so the number of tungsten particles in the reservoir is estimated to be 2.46×10^9. Considering the surface area of one particle is 7.854×10^{-7} cm^2, the total surface area of 5 μm tungsten particles in the reservoir is estimated to be 0.1932 m^2. Because 5 μm is actually the maximum particle size of the tungsten powder, this calculated surface area is a minimum value and could actually be substantially larger depending on the particle size distribution of the tungsten powder.

Therefore, the surface area of tungsten in the reservoir hollow cathodes is estimated to be at least four times the surface area of the tungsten in the impregnated cathodes. This significant increase in the tungsten surface area could greatly increase the rate of reaction and decrease the life of the cathode.

2000 Hour Test Cathode

There has been one long-term test of a reservoir hollow cathode filled with the 612 material operated at a discharge current of 25 A for 2,000 hours at NASA's Marshall Space Flight Center in Huntsville, AL. A thermocouple on the orifice plate of the cathode measured the temperature during operation to be ~1050ºC, and therefore the temperature of the cathode insert and the reservoir material were assumed to be very close to 1050ºC.

During the 2,000 hour run, this cathode showed no change in the operating current or voltage, indicating that there was adequate Ba being supplied to the surface of the emitter throughout the test. However, post-mortem analysis of the contents of the reservoir showed that there was no remaining 612 material, and the reaction products were identified as Ba_2CaWO_6, $BaAl_2O_4$, and Ba_3WO_6.

It is interesting to note that Ba_3WO_6 was observed as a reaction product in the 2000 hour test cathode heated to ~1050ºC and the molybdenum capsule heated to 1000ºC for 100 hours, but not in any of the molybdenum capsules heated to 1200ºC or 1300ºC. At higher temperatures, the Ba_3WO_6 is not expected to be as stable, so this may explain why the Ba_3WO_6 formed in the samples run at 1000ºC and 1050ºC, but not in the samples run at 1200ºC and 1300ºC.

Certain aspects of the processing of the 2000 hour test cathode, such as the loading of the cathode reservoir in an open environment, could have increased the O_2 content in the cathode. It is also believed that there was water vapor present in the 612 material in the molybdenum capsule run at 1000ºC, which also formed Ba_3WO_6. Therefore, it may be that this higher supply of O_2 in the system also contributed to the formation of Ba_3WO_6. It is not clear whether the Ba_3WO_6 would have formed at these lower temperatures without the presence of excess O_2.

The following reaction is proposed for the reaction of the 612 material and W at temperatures below 1100ºC in the presence of excess O_2:

$$2Ba_6CaAl_4O_{13} + 3W + 4O_2 \rightarrow 2Ba_2CaWO_6 + Ba_3WO_6 + 4BaAl_2O_4 + Ba(g)$$

As discussed previously, the Ba_2CaWO_6 may continue to react with W to form Ba vapor as proposed by the reaction:

$$Ba_2CaWO_6 + O_2 + W \rightarrow BaWO_4 + CaWO_4 + Ba(g)$$

According to Lipeles and Kan, the activation energy of the decomposition of Ba_3WO_6 is 131.0 kcal/mole over the range of 900 – 1250ºC. Because the activation energy of Ba_3WO_6 approaches that of $BaAl_2O_4$ in this temperature range, it is unlikely to serve as a source of barium vapor in normal operation of the insert. Thus, one might assume that despite exhaustion of the 612 material, the reaction between the Ba_2CaWO_6 and W would continue to serve as a source of Ba to the surface of the emitter. Because x-ray diffraction analysis of the reacted powder showed no evidence of $BaWO_4$ and $CaWO_4$ which are the predicted products, it is likely that the reaction between the Ba_2CaWO_6 and W proceeds very slowly.

SEM analysis of the insert of this cathode supported the hypothesis that a large amount of barium vapor escaped from the reservoir at the beginning of cathode life as a result of the rapid reaction of the 612 material. Energy Dispersive X-Ray Spectroscopy (EDS) was used to analyze the cathode insert, and the results showed a high Ba content on the emitter surface. An SEM image showing the deposition on the surface of the cathode and the EDS results indicating the presence of Ba on the tungsten insert are shown in Figures 4.33 and 4.34.

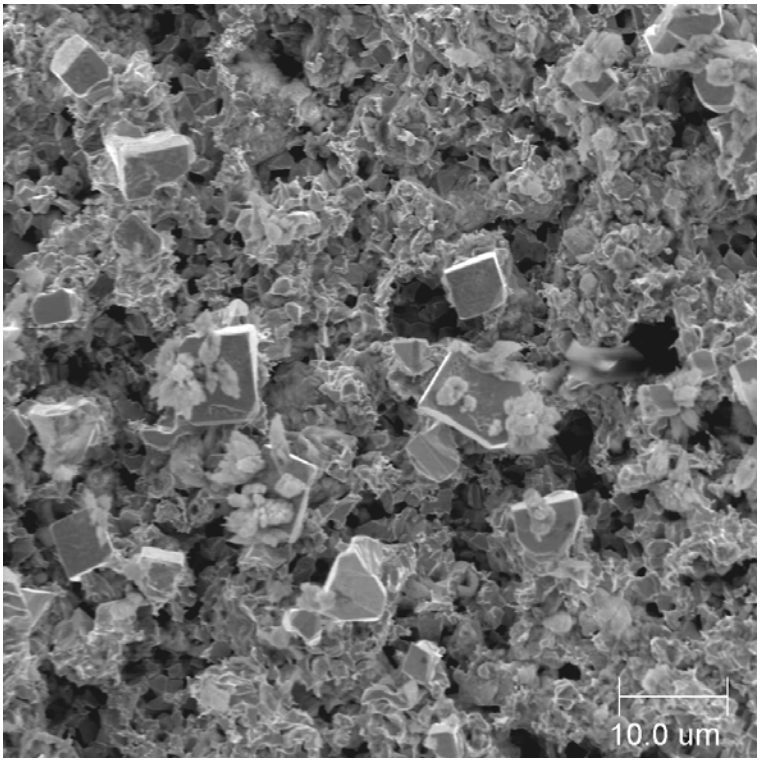

Figure 4.33. SEM Image Showing Deposition on the Tungsten Insert of the 612 2000 Hour Test Cathode.

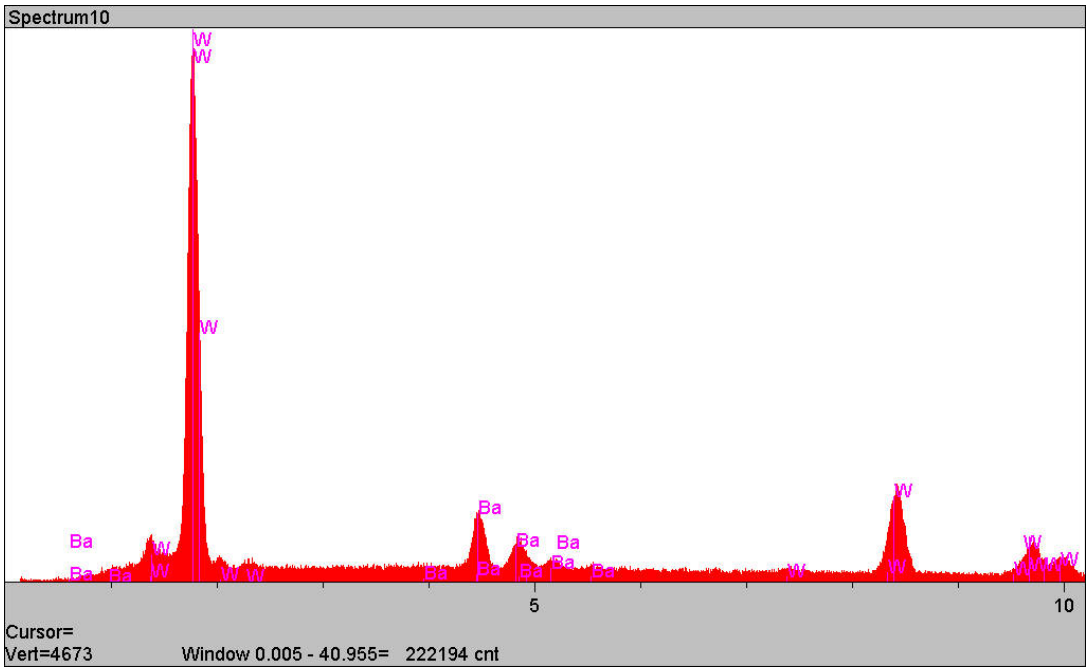

Figure 4.34. Energy Dispersive X-Ray Spectroscopy Results for the 612 2000 Hour Test Cathode Insert.

Unfortunately, the current availability of equipment did not allow x-ray diffraction analysis to be performed on the cathode insert, and without x-ray analysis it is not clear exactly whether this material was BaO, barium hydroxide, or one of the barium tungstates. However, the deposited material did appear to be crystalline, so it is believed that the deposits were most likely one of the barium tungstates.

The fact that this large amount of barium vapor escaped from the reservoir and was carried upstream shows that the vapor pressure of barium did not build up adequately inside the reservoir to slow down the reaction of the 612 material and W. The mass of barium vapor needed to establish the equilibrium vapor pressure of barium inside the reservoir at 1200ºC was estimated to be only 3.12×10^{-5} g Ba. This small amount of barium needed to establish the equilibrium vapor pressure should have been produced very early in the reaction, so it is clear that the high permeability of the tungsten must have prevented the build up of Ba vapor which would have slowed down the reaction.

Predicted Cathode Life Based on Previously Published Ba Evaporation Rates

Based on evaporation rates of Ba from impregnated cathodes published by Zalm and van Stratum[56] and Shroff, et al.,[23] it was possible to predict how long a full-scale reservoir cathode could operate at different temperatures assuming that the all of the barium vapor was being produced by the reaction of Ba_2CaWO_6 and tungsten. From the proposed reaction between 612 and W, it was predicted that each mole of 612 should react to produce one mole of Ba_2CaWO_6. Then based on the second proposed reaction between Ba_2CaWO_6 and W, each mole of Ba_2CaWO_6 should eventually react to produce one mole of Ba vapor. Based on the estimated mass of the 612 material in the full scale cathodes,

3.11 g, the mass of Ba vapor which would be produced by the reaction of Ba_2CaWO_6 with W is calculated to be 0.362 g. This information was used along with the surface area of the tungsten insert, 9.58 cm^2, and the published barium evaporation rates by Zalm and van Stratum (Table 4.4), and Shroff, et al., (Table 4.5), to predict cathode life time.

Table 4.4. Predicted Cathode Life Time Based on Evaporation Rates Published by Zalm and van Stratum.[56]

T (ºC)	Ba evaporation rate ($\mu g\ cm^{-2}\ h^{-1}$)	Time (hours)
927	0.00444	8,502,041
1027	0.02854	1,323,535
1127	0.18335	206,038
1227	1.17776	32,075
1327	7.56565	4,993

Table 4.5. Predicted Cathode Life Time Based on Evaporation Rates Published by Shroff et al.[23]

T (ºC)	Ba evaporation rate ($\mu g\ cm^{-2}\ h^{-1}$)	Time (hours)
927	1.05567	357,839
1027	12.2335	30,879
1127	141.766	2,665
1227	1642.84	230
1327	19037.8	20

Assuming that the actual operating temperature of the cathode insert would be closer to 1127ºC at the desired 35 A discharge current, the cathode lifetime should exceed 200,000 hours based on Zalm and van Stratum's data but only ~3,000 hours based on Shroff et al.'s data. Clearly there is a need for further experimental work to be done in measuring the barium evaporation rates from the actual reservoir hollow cathodes in order to more accurately predict cathode lifetime.

CHAPTER 5

CONCLUSIONS

The results of the environmental studies at a dew point of –15ºC showed that B_3A experienced a weight gain of 1.68% after 60 hours, while the 612, 411, B_4A_{SSL}, and $Ba_3Sc_4O_9$ had all gained less than 0.4% in a similar time frame. After 60 hours at a dew point of 11ºC, the B_3A had gained over 30%; the 612, 411, and B_4A_{SSL} had all gained between 20-25%; and the $Ba_3Sc_4O_9$ had gained less than 1%. These results suggest that B_3A would make a poor candidate as a barium source material from an environmental standpoint; however, the other materials should all be usable if handled appropriately.

After the mixtures of the 612 material and W were heated at 1200ºC and 1300ºC for 100, 200, and 400 hours, qualitative analysis identified the contents of the capsules to be W, $BaAl_2O_4$, Ba_2CaWO_6, and $Ba_{2.6}Ca_{0.4}Al_2O_6$. Ba_3WO_6 was observed as an additional reaction product in the capsule heated to 1000ºC for 100 hours and in the test cathode run at 1050ºC for 2000 hours.

The following reaction was proposed for the 612 material and W above 1100ºC:

$$Ba_{3.4}Ca_{0.6}Al_2O_7 + Ba_{2.6}Ca_{0.4}Al_2O_6 + W + 0.5O_2 \rightarrow Ba_2CaWO_6 + 2BaAl_2O_4 + 2Ba(g).$$

At temperatures below 1100ºC in the presence of excess O_2, the following reaction was proposed for the 612 material and W:

$$2Ba_6CaAl_4O_{13} + 3W + 4O_2 \rightarrow 2Ba_2CaWO_6 + Ba_3WO_6 + 4BaAl_2O_4 + Ba(g).$$

There is anecdotal evidence that Ba_2CaWO_6 will react further with W as proposed in the following reaction:

$$Ba_2CaWO_6 + O_2 + W \rightarrow BaWO_4 + CaWO_4 + Ba(g).$$

The quantitative analysis results showed that the bottom pellets in all the sealed molybdenum capsules reacted to a much further extent than the top pellets. A temperature gradient and excessive moisture in the base of the capsule may have contributed to the increased rate of reaction in the bottom pellets.

While it was expected that the quantitative and semi-quantitative analysis results would show that the concentration of B_3A solid solution decreased with time while the concentration of $BaAl_2O_4$ increased with time, the results did not appear to be consistent for the samples run at the various temperatures. Further experiments need to be done to establish a clearer trend as to how the concentration of the B_3A solid solution and $BaAl_2O_4$ vary with time. Because Ba_2CaWO_6 was considered to be a possible intermediate phase, it was unclear whether the results would show that the concentration of Ba_2CaWO_6 increased with time or that the concentration increased and then began to decrease as the Ba_2CaWO_6 began to react with W. The results did not show any clear trend, and again further experimental work is needed to determine how the concentration of Ba_2CaWO_6 varies with time.

The reactions in the molybdenum capsules proceeded much more rapidly than expected, completely consuming all of the original B_4A solid solution phase in the 612 material in 100 hours or less at 1000°C. There are at least two possible explanations for the accelerated reaction rates. First, it is possible that the permeability of the tungsten closure was too high, which precluded the establishment of equilibrium Ba vapor pressure inside the capsules. Without the equilibrium vapor pressure of Ba established inside the capsules, the reaction proceeded very rapidly. Second, the surface area of tungsten powder in the reservoir hollow cathodes was estimated to be at least four times that of the surface

area of the tungsten matrix in impregnated cathodes. This increased surface area could have substantially increased the rate of reaction in the capsules.

The successful operation of a reservoir hollow cathode filled with the 612 material for over 2000 hours, with no change in operating characteristics, suggests that the reactions occurring in the reservoir were supplying adequate Ba to the surface of the emitter. Because post-mortem analysis of the reservoir showed no evidence of the original phases present in the 612 material, it should be safe to assume that the reaction of Ba_2CaWO_6 with W effectively supplied Ba to the emitter.

Using published Ba evaporation rates from microwave dispenser cathodes and estimating the operating temperature of the reservoir hollow cathode in a full-scale ion thruster, it was possible to estimate the lifetime of the cathode, assuming that Ba was supplied by the proposed reaction between Ba_2CaWO_6 and W. At an operating temperature of 1127°C, the cathode life was projected to be between 3,000 and 200,000 hours, depending on the source of the Ba evaporation data. Clearly, barium evaporation rates from the molybdenum capsules need to be measured in order to more accurately predict cathode lifetime.

CHAPTER 6

RECOMMENDATIONS

In this chapter, several recommendations will be made for future experimental work that could allow for a better understanding of the reactions taking place in reservoir hollow cathodes. First of all, repeating the experiments using shorter reaction capsules could allow for more adequate removal of water vapor from the 612 material and thus reduce the variation observed in the extent of reaction between the 612 material and W along the length of the capsule. Also, additional reaction capsules filled with the 612 material and W could be heated at 1200ºC and 1300º C for times shorter than 100 hours in order to determine how long it takes for the B_4A solid solution phase in the 612 material to react completely with the W.

Similar experiments could also be run with mixtures of Ba_2CaWO_6 and W, and the reaction products could be analyzed in order to evaluate the validity of the proposed reaction between the two materials. If the reaction between the Ba_2CaWO_6 and W proved to proceed slowly and provide an adequate supply of Ba vapor, Ba_2CaWO_6 may be considered as a possible barium source material for the reservoir hollow cathodes.

Modifications could also be made to the reaction capsules in order to reduce the permeability of the porous tungsten and therefore allow the maintenance of equilibrium barium vapor pressure inside of the capsules. First of all, the porous tungsten closure could be made with finer tungsten powders (<1 micron), as the permeability through the material would decrease with particle size. Also, a more dense tungsten closure (84%-

dense) and/or a thicker tungsten closure could be used to reduce the permeability of the tungsten and therefore slow down the reaction.

The surface area of tungsten could also be modified in order to slow down the reaction. The experiments could be repeated using coarser tungsten powders (200 mesh) in the matrix to lower the surface area of the tungsten and reduce the reaction rate.

A mass spectrometer could be used to sample the vapor evaporating from the reaction capsules. Measurements of the Ba evaporation rate could then be used to predict a more accurate lifetime of the cathode. Also, observation of the rate of Ba evaporation with time could be used to evaluate the proposed reaction sequences between the 612 material and W.

APPENDIX A

A summary of the quantitative x-ray diffraction analysis results for each of the pellets are shown below, along with the average values which were reported in the discussion section.

				Quant Program: 612BABW			Quant Program: Ba2CaWO6	Quant Program: W_B3A
Sample	Temp (ºC)	Time (hrs)	Pellet	% 612	% $BaAl_2O_4$	% $BaWO_4$	% Ba_2CaWO_6	% W
1	1300	100	Bottom	0.43	10.41	0.57	22.14	45.76
				-3.52	10.69	0.57	21.07	47.00
			Avg	-1.55	10.55	0.57	21.61	46.38
			Middle	-13.71	12.41	0.53	23.14	56.15
				-7.46	7.84	0.55	18.02	39.65
			Avg	-10.59	10.13	0.54	20.58	47.90
			Top	-71.58	6.75	0.48	13.52	26.97
				-42.66	5.28	0.61	11.64	
			Avg	-57.12	6.02	0.55	12.58	26.97
2	1300	400	Bottom	-8.06	12.67	0.11	23.25	36.48
				-1.57	10.01	0.24	23.51	
			Avg	-4.82	11.34	0.18	23.38	36.48
			Middle	-43.54	9.03	0.26	21.12	54.13
				-37.17	10.81	0.44	17.48	44.75
			Avg	-40.36	9.92	0.35	19.30	49.44
			Top	-28.01	5.98	0.43	17.60	30.94
				-29.78	6.57	0.14	15.10	
			Avg	-28.90	6.28	0.29	16.35	30.94
3	1300	200	Bottom	-87.20	7.91	0.36	18.29	25.83
				-96.12	7.81	0.42	17.71	
			Avg	-91.66	7.86	0.39	18.00	25.83
			Middle	-133.04	4.36	0.48	10.82	32.91
				-152.22	4.91	0.55	11.40	38.85
			Avg	-142.63	4.64	0.52	11.11	35.88
			Top	-57.30	2.09	0.31	8.84	20.38
				-70.13	1.99	0.35	7.02	
			Avg	-63.72	2.04	0.33	7.93	20.38
4	1200	100	Bottom	-12.78	9.13	0.61	19.09	45.39
				-17.71	9.18	0.42	17.02	
			Avg	-15.25	9.16	0.52	18.06	45.39
			Middle	-34.74	6.41	0.65	11.57	29.09
				-19.85	4.80	0.36	9.94	26.47
			Avg	-27.30	5.61	0.51	10.76	27.78
			Top	-82.97	4.64	0.65	12.06	47.22

				-67.85	3.58	0.30	9.09	35.42
			Avg	-75.41	4.11	0.48	10.58	41.32
5	1200	400	Bottom	-25.03	11.60	0.40	21.97	60.80
				-17.49	11.46	0.53	19.70	55.45
				-21.26	11.53	0.47	20.84	58.13
			Middle	-53.46	7.79	0.43	19.73	50.74
				-41.78	6.88	0.59	19.16	48.39
				-47.62	7.34	0.51	19.45	49.57
			Top	-83.70	6.72	0.62	16.11	49.28
				-80.29	7.16	0.58	15.03	46.83
				-82.00	6.94	0.60	15.57	48.06
6	1200	200	Bottom	-10.92	17.96	0.52	33.24	70.64
				-5.72	14.56	0.57	29.55	68.78
			Avg	-8.32	16.26	0.55	31.40	69.71
			Middle	-13.41	13.16	0.59	24.01	59.29
				-9.29	10.28	0.32	18.25	48.77
			Avg	-11.35	11.72	0.46	21.13	54.03
			Top	-52.45	7.26	0.55	12.91	34.93
				-73.27	7.98	0.46	14.94	50.20
			Avg	-62.86	7.62	0.51	13.93	42.57
7	1000	100	Bottom	7.89	5.71	-1.03	10.88	73.02
				-0.45	4.39	-0.74	7.86	61.99
			Avg	3.72	5.05	-0.89	9.37	67.51
			Middle	-2.96	3.61	-0.69	13.04	
				-5.53	5.26	-0.79	12.54	
			Avg	-4.25	4.44	-0.74	12.79	
			Top	10.98	2.66	-0.77	11.36	94.34
				4.08	1.90	-0.65	8.64	72.12
			Avg	7.53	2.28	-0.71	10.00	83.23

APPENDIX B

The APD software was used to obtain quantitative analysis results from the x-ray diffraction scans of selected peaks. The raw data used in these calculations, including the integrated phase intensities and background intensities, along with the corresponding calculated phase percentages are presented below.

Sample	Pellet	.PIO file	Phase	Phase Intensity (counts)	Background Angle (º2θ)	Background Intensity (counts)	Calculated Phase %
1	Bottom	1_612BAB	612	8847	31.1	6440	0.43
					31.8	3500	
			$BaAl_2O_4$	10534	19.5	4580	10.41
					20.2	4580	
			$BaWO_4$	8514	26.2	5075	0.57
					27.0	4850	
			Ag	47638	44.2	24105	
					44.7	7755	
		1_BA2CAW	Ba_2CaWO_6	47389	53.3	12375	22.14
					54.1	6500	
			Ag	47048	44.2	22605	
					44.7	7890	
		1E_W_B3A	W	119068	40.0	15990	45.76
					40.9	8700	
			Ag	38489	44.2	18600	
					44.7	8145	
		1B_612BA	612	7273	31.1	6680	-3.52
					31.8	3220	
			$BaAl_2O_4$	11976	19.5	5280	10.69
					20.2	5060	
			$BaWO_4$	7861	26.2	4525	0.57
					27.0	4500	
			Ag	48080	44.2	19695	
					44.7	9360	
		1B_BA2CA	Ba_2CaWO_6	51211	53.3	12675	21.07
					54.1	6950	
			Ag	48653	44.2	19035	
					44.7	9345	
		1G_W_B3A	W	117959	40.0	16920	47.00
					40.9	7890	
			Ag	38636	44.2	20535	
					44.7	7125	
1	Middle	1H_612BA	612	7934	31.1	11680	-13.71
					31.8	3100	

Sample	Pellet	.PIO file	Phase	Phase Intensity (counts)	Background Angle (°2θ)	Background Intensity (counts)	Calculated Phase %
			$BaAl_2O_4$	12433	19.5	5380	12.41
					20.2	5240	
			$BaWO_4$	7431	26.2	4375	0.53
					27.0	4225	
			Ag	39692	44.2	13770	
					44.7	7395	
		1H_BA2CA	Ba_2CaWO_6	51581	53.3	12100	23.14
					54.1	7050	
			Ag	40684	44.2	13290	
					44.7	7635	
		1H_W_B3A	W	206567	40.0	20700	56.15
					40.9	10440	
			Ag	41759	44.2	13515	
					44.7	7725	
		1I_612BA	612	7892	31.1	10120	-7.46
					31.8	3340	
			$BaAl_2O_4$	11233	19.5	4800	7.84
					20.2	4800	
			$BaWO_4$	7996	26.2	4475	0.55
					27.0	4500	
			Ag	51988	44.2	16035	
					44.7	8550	
		1I_BA2CA	Ba_2CaWO_6	51412	53.3	12325	18.02
					54.1	6800	
			Ag	49881	44.2	15855	
					44.7	8340	
		1I_W_B3A	W	188020	40.0	20250	39.65
					40.9	9510	
			Ag	50913	44.2	15435	
					44.7	8685	
1	Top	1C_612BA	612	13199	31.1	60060	-71.58
					31.8	3100	
			$BaAl_2O_4$	12938	19.5	5920	6.75
					20.2	5720	
			$BaWO_4$	8044	26.2	4450	0.48
					27.0	4600	
			Ag	48595	44.2	8295	
					44.7	7365	
		1C_BA2CA	Ba_2CaWO_6	45063	53.3	9250	13.52
					54.1	5850	
			Ag	49458	44.2	8370	
					44.7	7575	
		1F_W_B3A	W	146382	40.0	15180	26.97
					40.9	7830	
			Ag	48809	44.2	8910	
					44.7	7305	
		1D_612BA	612	9565	31.1	38500	-42.66
					31.8	3020	
			$BaAl_2O_4$	11575	19.5	5380	5.28
					20.2	5220	
			$BaWO_4$	8139	26.2	4425	0.61

Sample	Pellet	.PIO file	Phase	Phase Intensity (counts)	Background Angle (°2θ)	Background Intensity (counts)	Calculated Phase %
					27.0	4375	
			Ag	52628	44.2	10785	
					44.7	6825	
		1D_BA2CA	Ba_2CaWO_6	43343	53.3	9675	11.64
					54.1	5350	
			Ag	54146	44.2	10020	
					44.7	7065	
2	Bottom	2A_612BA	612	7535	31.1	8420	-8.06
					31.8	3660	
			$BaAl_2O_4$	13724	19.5	6060	12.67
					20.2	5840	
			$BaWO_4$	8077	26.2	5025	0.11
					27.0	4925	
			Ag	36999	44.2	10410	
					44.7	6645	
		2A_BA2CA	Ba_2CaWO_6	54061	53.3	12525	23.25
					54.1	6750	
			Ag	37862	44.2	9090	
					44.7	6765	
		2E_W_B3A	W	160193	40.0	17520	36.48
					40.9	8490	
			Ag	43206	44.2	11295	
					44.7	6435	
		2B_612BA	612	6986	31.1	5240	-1.57
					31.8	3420	
			$BaAl_2O_4$	11666	19.5	5180	10.01
					20.2	5160	
			$BaWO_4$	7764	26.2	4775	0.24
					27.0	4600	
			Ag	37253	44.2	11745	
					44.7	5595	
		2B_BA2CA	Ba_2CaWO_6	53750	53.3	13950	23.51
					54.1	6450	
			Ag	37442	44.2	10890	
					44.7	5700	
2	Middle	2G_612BA	612	9345	31.1	29100	-43.54
					31.8	3120	
			$BaAl_2O_4$	11586	19.5	5080	9.03
					20.2	5060	
			$BaWO_4$	7621	26.2	4600	0.26
					27.0	4525	
			Ag	42510	44.2	10335	
					44.7	9255	
		2G_BA2CA	Ba_2CaWO_6	50989	53.3	10950	21.12
					54.1	6925	
			Ag	41582	44.2	9390	
					44.7	9585	
		2G_W_B3A	W	212210	40.0	19890	54.13
					40.9	11640	
			Ag	41507	44.2	9495	
					44.7	9495	

Sample	Pellet	.PIO file	Phase	Phase Intensity (counts)	Background Angle (°2θ)	Background Intensity (counts)	Calculated Phase %
		2H_612BA	612	8631	31.1	27140	-37.17
					31.8	3380	
			$BaAl_2O_4$	13096	19.5	5320	10.81
					20.2	5480	
			$BaWO_4$	8310	26.2	4900	0.44
					27.0	4725	
			Ag	46746	44.2	11655	
					44.7	9150	
		2H_BA2CA	Ba_2CaWO_6	51912	53.3	11450	17.48
					54.1	6550	
			Ag	48811	44.2	11220	
					44.7	9150	
		2H_W_B3A	W	218911	40.0	22590	44.75
					40.9	10860	
			Ag	48869	44.2	10830	
					44.7	9495	
2	Top	2C_612BA	612	9372	31.1	23220	-28.01
					31.8	3460	
			$BaAl_2O_4$	12201	19.5	5840	5.98
					20.2	5740	
			$BaWO_4$	7898	26.2	4625	0.43
					27.0	4475	
			Ag	41906	44.2	6915	
					44.7	7170	
		2C_BA2CA	Ba_2CaWO_6	47363	53.3	10800	17.60
					54.1	6725	
			Ag	39792	44.2	6765	
					44.7	7260	
		2F_W_B3A	W	142193	40.0	14550	30.94
					40.9	7290	
			Ag	41615	44.2	8070	
					44.7	5895	
		2D_612BA	612	9748	31.1	25140	-29.78
					31.8	3820	
			$BaAl_2O_4$	12746	19.5	5900	6.57
					20.2	5940	
			$BaWO_4$	8274	26.2	5100	0.14
					27.0	4975	
			Ag	44430	44.2	7800	
					44.7	7515	
		2D_BA2CA	Ba_2CaWO_6	46699	53.3	10875	15.10
					54.1	6200	
			Ag	45374	44.2	8415	
					44.7	7095	
3	Bottom	3A_612BA	612	17579	31.1	65580	-87.20
					31.8	3420	
			$BaAl_2O_4$	12792	19.5	5740	7.91
					20.2	5800	
			$BaWO_4$	7769	26.2	4475	0.36
					27.0	4600	
			Ag	45110	44.2	6450	

Sample	Pellet	.PIO file	Phase	Phase Intensity (counts)	Background Angle (°2θ)	Background Intensity (counts)	Calculated Phase %
					44.7	12060	
		3A_BA2CA	Ba_2CaWO_6	46093	53.3	9300	18.29
					54.1	6875	
			Ag	42257	44.2	6615	
					44.7	11835	
		3E_W_B3A	W	121134	40.0	12900	25.83
					40.9	7200	
			Ag	44101	44.2	10350	
					44.7	6240	
		3B_612BA	612	17908	31.1	68240	-96.12
					31.8	3360	
			$BaAl_2O_4$	12359	19.5	5560	7.81
					20.2	5680	
			$BaWO_4$	8144	26.2	4625	0.42
					27.0	4850	
			Ag	44141	44.2	6795	
					44.7	12390	
		3B_BA2CA	Ba_2CaWO_6	45147	53.3	8825	17.71
					54.1	6925	
			Ag	43421	44.2	6900	
					44.7	12495	
3	Middle	3G_612BA	612	25715	31.1	116680	-133.04
					31.8	3500	
			$BaAl_2O_4$	11556	19.5	5600	4.36
					20.2	5540	
			$BaWO_4$	8579	26.2	4700	0.48
					27.0	5000	
			Ag	49944	44.2	6930	
					44.7	9660	
		3G_BA2CA	Ba_2CaWO_6	38665	53.3	8625	10.82
					54.1	6200	
			Ag	50642	44.2	6780	
					44.7	9900	
		3H_W_B3A	W	196064	40.0	17730	32.91
					40.9	9810	
			Ag	52916	44.2	8385	
					44.7	7950	
		3I_612BA	612	26763	31.1	134080	-152.22
					31.8	3360	
			$BaAl_2O_4$	11263	19.5	5300	4.91
					20.2	5180	
			$BaWO_4$	8763	26.2	4725	0.55
					27.0	5025	
			Ag	51089	44.2	7065	
					44.7	9660	
		3I_BA2CA	Ba_2CaWO_6	39329	53.3	8375	11.40
					54.1	5800	
			Ag	50401	44.2	6915	
					44.7	9870	
		3I_W_B3A	W	223432	40.0	18270	38.85
					40.9	11850	

Sample	Pellet	.PIO file	Phase	Phase Intensity (counts)	Background Angle (°2θ)	Background Intensity (counts)	Calculated Phase %
			Ag	52169	44.2	6870	
					44.7	9990	
3	Top	3C_612BA	612	13521	31.1	48440	-57.30
					31.8	3780	
			$BaAl_2O_4$	11944	19.5	6320	2.09
					20.2	6400	
			$BaWO_4$	8737	26.2	5075	0.31
					27.0	5225	
			Ag	47297	44.2	9120	
					44.7	6885	
		3C_BA2CA	Ba_2CaWO_6	34506	53.3	8775	8.84
					54.1	6475	
			Ag	53255	44.2	7035	
					44.7	11955	
		3F_W_B3A	W	118234	40.0	13800	20.38
					40.9	7560	
			Ag	51114	44.2	10080	
					44.7	6885	
		3D_612BA	612	18277	31.1	70660	-70.13
					31.8	4580	
			$BaAl_2O_4$	10315	19.5	5240	1.99
					20.2	5480	
			$BaWO_4$	10047	26.2	5775	0.35
					27.0	5925	
			Ag	55529	44.2	8070	
					44.7	9345	
		3D_BA2CA	Ba_2CaWO_6	30903	53.3	8875	7.02
					54.1	6375	
			Ag	53896	44.2	8130	
					44.7	9150	
4	Bottom	4A_612BA	612	9337	31.1	13580	-12.78
					31.8	3240	
			$BaAl_2O_4$	14620	19.5	7220	9.13
					20.2	6440	
			$BaWO_4$	8393	26.2	4750	0.61
					27.0	4825	
			Ag	45777	44.2	17535	
					44.7	6840	
		4A_BA2CA	Ba_2CaWO_6	49172	53.3	13050	19.09
					54.1	6575	
			Ag	45357	44.2	16245	
					44.7	6975	
		4A_W_B3A	W	179248	40.0	20610	45.39
					40.9	8610	
			Ag	45205	44.2	16365	
					44.7	7215	
		4B_612BA	612	9905	31.1	18200	-17.71
					31.8	2960	
			$BaAl_2O_4$	12004	19.5	5220	9.18
					20.2	4960	
			$BaWO_4$	7748	26.2	4475	0.42

Sample	Pellet	.PIO file	Phase	Phase Intensity (counts)	Background Angle (°2θ)	Background Intensity (counts)	Calculated Phase %
					27.0	4475	
			Ag	51067	44.2	15810	
					44.7	10185	
		4B_BA2CA	Ba_2CaWO_6	50320	53.3	10925	17.02
					54.1	7200	
			Ag	52713	44.2	15810	
					44.7	9990	
4	Middle	4G_612BA	612	14846	31.1	35180	-34.74
					31.8	3580	
			$BaAl_2O_4$	15812	19.5	8040	6.41
					20.2	7240	
			$BaWO_4$	9439	26.2	5150	0.65
					27.0	5375	
			Ag	55616	44.2	16050	
					44.7	10845	
		4G_BA2CA	Ba_2CaWO_6	42288	53.3	10500	11.57
					54.1	8075	
			Ag	57615	44.2	15810	
					44.7	11130	
		4G_W_B3A	W	160310	40.0	18450	29.09
					40.9	9960	
			Ag	57308	44.2	15750	
					44.7	10740	
		4H_612BA	612	10584	31.1	21220	-19.85
					31.8	2980	
			$BaAl_2O_4$	9424	19.5	4460	4.80
					20.2	4280	
			$BaWO_4$	7586	26.2	4300	0.36
					27.0	4500	
			Ag	53577	44.2	16455	
					44.7	9120	
		4H_BA2CA	Ba_2CaWO_6	38635	53.3	9875	9.94
					54.1	8225	
			Ag	58269	44.2	15255	
					44.7	11415	
		4H_W_B3A	W	149455	40.0	15840	26.47
					40.9	9420	
			Ag	58708	44.2	15000	
					44.7	11820	
4	Top	4C_612BA	612	20586	31.1	69800	-82.97
					31.8	3500	
			$BaAl_2O_4$	11490	19.5	5680	4.64
					20.2	5520	
			$BaWO_4$	8865	26.2	4650	0.65
					27.0	5200	
			Ag	47373	44.2	9195	
					44.7	9555	
		4C_BA2CA	Ba_2CaWO_6	38217	53.3	8950	12.06
					54.1	6550	
			Ag	47386	44.2	8850	
					44.7	9900	

Sample	Pellet	.PIO file	Phase	Phase Intensity (counts)	Background Angle (°2θ)	Background Intensity (counts)	Calculated Phase %
		4C_W_B3A	W	226425	40.0	19020	47.22
					40.9	11310	
			Ag	47213	44.2	9045	
					44.7	9450	
		4D_612BA	612	23044	31.1	75540	-67.85
					31.8	3560	
			$BaAl_2O_4$	10180	19.5	4920	3.58
					20.2	4780	
			$BaWO_4$	8886	26.2	4875	0.30
					27.0	5500	
			Ag	58959	44.2	9210	
					44.7	12150	
		4D_BA2CA	Ba_2CaWO_6	35778	53.3	7800	9.09
					54.1	6500	
			Ag	57990	44.2	9120	
					44.7	12795	
		4D_W_B3A	W	212759	40.0	17100	35.42
					40.9	11400	
			Ag	57715	44.2	9045	
					44.7	12405	
5	Bottom	5A_612BA	612	11714	31.1	20980	-25.03
					31.8	3480	
			$BaAl_2O_4$	13425	19.5	6020	11.60
					20.2	5760	
			$BaWO_4$	8362	26.2	4875	0.40
					27.0	5025	
			Ag	37966	44.2	9765	
					44.7	7695	
		5A_BA2CA	Ba_2CaWO_6	52175	53.3	10900	21.97
					54.1	9250	
			Ag	38815	44.2	9705	
					44.7	7665	
		5A_W_B3A	W	214662	40.0	22440	60.80
					40.9	11280	
			Ag	37638	44.2	9765	
					44.7	7845	
		5B_612BA	612	10857	31.1	17540	-17.49
					31.8	3620	
			$BaAl_2O_4$	14771	19.5	6540	11.46
					20.2	6360	
			$BaWO_4$	9404	26.2	5525	0.53
					27.0	5400	
			Ag	42751	44.2	12165	
					44.7	7350	
		5B_BA2CA	Ba_2CaWO_6	52869	53.3	11850	19.70
					54.1	10050	
			Ag	42343	44.2	11550	
					44.7	7320	
		5B_W_B3A	W	214344	40.0	22530	55.45
					40.9	10860	
			Ag	40759	44.2	11130	

Sample	Pellet	.PIO file	Phase	Phase Intensity (counts)	Background Angle (°2θ)	Background Intensity (counts)	Calculated Phase %
					44.7	7575	
5	Middle	5E_612BA	612	11685	31.1	35880	-53.46
					31.8	3240	
			$BaAl_2O_4$	11711	19.5	5400	7.79
					20.2	5380	
			$BaWO_4$	7800	26.2	4500	0.43
					27.0	4600	
			Ag	39732	44.2	8475	
					44.7	8595	
		5E_BA2CA	Ba_2CaWO_6	48186	53.3	9475	19.73
					54.1	7700	
			Ag	40056	44.2	8340	
					44.7	8655	
		5E_W_B3A	W	197910	40.0	18330	50.74
					40.9	10560	
			Ag	39535	44.2	8070	
					44.7	8640	
		5F_612BA	612	10713	31.1	30880	-41.78
					31.8	3480	
			$BaAl_2O_4$	11468	19.5	5380	6.88
					20.2	5200	
			$BaWO_4$	8451	26.2	4700	0.59
					27.0	4875	
			Ag	42339	44.2	9135	
					44.7	8055	
		5F_BA2CA	Ba_2CaWO_6	47731	53.3	9750	19.16
					54.1	7775	
			Ag	40673	44.2	9315	
					44.7	8175	
		5F_W_B3A	W	190966	40.0	19650	48.39
					40.9	9990	
			Ag	40271	44.2	9450	
					44.7	8025	
5	Top	5C_612BA	612	18663	31.1	67680	-83.70
					31.8	3240	
			$BaAl_2O_4$	12569	19.5	5940	6.72
					20.2	5660	
			$BaWO_4$	8445	26.2	4675	0.62
					27.0	4725	
			Ag	45921	44.2	7815	
					44.7	9660	
		5C_BA2CA	Ba_2CaWO_6	44676	53.3	8500	16.11
					54.1	6750	
			Ag	43972	44.2	7500	
					44.7	9390	
		5C_W_B3A	W	225393	40.0	17910	49.28
					40.9	11730	
			Ag	44570	44.2	7740	
					44.7	9270	
		5D_612BA	612	18002	31.1	67660	-80.29
					31.8	3160	

Sample	Pellet	.PIO file	Phase	Phase Intensity (counts)	Background Angle (°2θ)	Background Intensity (counts)	Calculated Phase %
			$BaAl_2O_4$	12327	19.5	5520	7.16
					20.2	5460	
			$BaWO_4$	8220	26.2	4400	0.58
					27.0	4725	
			Ag	47584	44.2	8010	
					44.7	9345	
		5D_BA2CA	Ba_2CaWO_6	45212	53.3	8700	15.03
					54.1	7200	
			Ag	46466	44.2	7965	
					44.7	9330	
		5D_W_B3A	W	229573	40.0	18270	46.83
					40.9	11190	
			Ag	47403	44.2	8175	
					44.7	9510	
6	Bottom	6A_612BA	612	9794	31.1	12000	-10.92
					31.8	3320	
			$BaAl_2O_4$	15357	19.5	6540	17.96
					20.2	6300	
			$BaWO_4$	7954	26.2	4725	0.52
					27.0	4600	
			Ag	37442	44.2	11745	
					44.7	9180	
		6A_BA2CA	Ba_2CaWO_6	59479	53.3	10500	33.24
					54.1	11575	
			Ag	36234	44.2	11895	
					44.7	9195	
		6A_W_B3A	W	214910	40.0	20940	70.64
					40.9	12510	
			Ag	37566	44.2	12015	
					44.7	9480	
		6B_612BA	612	8956	31.1	9680	-5.72
					31.8	2920	
			$BaAl_2O_4$	12250	19.5	5020	14.56
					20.2	4800	
			$BaWO_4$	7489	26.2	4275	0.57
					27.0	4350	
			Ag	39632	44.2	11835	
					44.7	9450	
		6B_BA2CA	Ba_2CaWO_6	60239	53.3	10600	29.55
					54.1	10300	
			Ag	39908	44.2	11715	
					44.7	9960	
		6B_W_B3A	W	221183	40.0	20970	68.78
					40.9	11790	
			Ag	39689	44.2	12240	
					44.7	10095	
6	Middle	6E_612BA	612	11003	31.1	15380	-13.41
					31.8	3440	
			$BaAl_2O_4$	15043	19.5	6680	13.16
					20.2	6260	
			$BaWO_4$	8587	26.2	4900	0.59

Sample	Pellet	.PIO file	Phase	Phase Intensity (counts)	Background Angle (°2θ)	Background Intensity (counts)	Calculated Phase %
					27.0	4975	
			Ag	42768	44.2	12855	
					44.7	8895	
		6E_BA2CA	Ba_2CaWO_6	53788	53.3	11350	24.01
					54.1	9850	
			Ag	40651	44.2	12525	
					44.7	8955	
		6E_W_B3A	W	215527	40.0	22410	59.29
					40.9	11970	
			Ag	40960	44.2	11925	
					44.7	8910	
		6F_612BA	612	10126	31.1	13240	-9.29
					31.8	3560	
			$BaAl_2O_4$	13365	19.5	5680	10.28
					20.2	5580	
			$BaWO_4$	8418	26.2	5000	0.32
					27.0	4950	
			Ag	48066	44.2	12420	
					44.7	9540	
		6F_BA2CA	Ba_2CaWO_6	52744	53.3	10825	18.25
					54.1	11175	
			Ag	46937	44.2	12270	
					44.7	9780	
		6F_W_B3A	W	211406	40.0	21030	48.77
					40.9	11370	
			Ag	46974	44.2	12300	
					44.7	10125	
6	Top	6C_612BA	612	17024	31.1	49900	-52.45
					31.8	3480	
			$BaAl_2O_4$	15487	19.5	7420	7.26
					20.2	7020	
			$BaWO_4$	9042	26.2	4925	0.55
					27.0	5250	
			Ag	51678	44.2	10200	
					44.7	10740	
		6C_BA2CA	Ba_2CaWO_6	44221	53.3	9025	12.91
					54.1	7625	
			Ag	52477	44.2	9645	
					44.7	10710	
		6C_W_B3A	W	189994	40.0	18660	34.93
					40.9	11490	
			Ag	52456	44.2	9600	
					44.7	10950	
		6D_612BA	612	16436	31.1	62960	-73.27
					31.8	3200	
			$BaAl_2O_4$	12129	19.5	5200	7.98
					20.2	5080	
			$BaWO_4$	8041	26.2	4425	0.46
					27.0	4700	
			Ag	51756	44.2	9015	
					44.7	12030	

Sample	Pellet	.PIO file	Phase	Phase Intensity (counts)	Background Angle (°2θ)	Background Intensity (counts)	Calculated Phase %
		6D_BA2CA	Ba_2CaWO_6	46790	53.3	8400	14.94
					54.1	8200	
			Ag	51112	44.2	8790	
					44.7	12615	
		6D_W_B3A	W	243417	40.0	19590	50.20
					40.9	13470	
			Ag	50257	44.2	9000	
					44.7	12780	
7	Bottom	7A_612BA	612	37060	31.1	35020	7.89
					31.8	4340	
			$BaAl_2O_4$	12148	19.5	6340	5.71
					20.2	6040	
			$BaWO_4$	8058	26.2	4825	-1.03
					27.0	6475	
			Ag	42902	44.2	8610	
					44.7	18780	
		7A_BA2CA	Ba_2CaWO_6	29724	53.3	9650	10.88
					54.1	9200	
			Ag	43399	44.2	8640	
					44.7	19485	
		7A_W_B3A	W	232404	40.0	15660	73.02
					40.9	17010	
			Ag	44043	44.2	8520	
					44.7	19140	
		7B_612BA	612	33337	31.1	34580	-0.45
					31.8	3740	
			$BaAl_2O_4$	11256	19.5	5800	4.39
					20.2	5580	
			$BaWO_4$	8009	26.2	4550	-0.74
					27.0	6600	
			Ag	45819	44.2	9315	
					44.7	14730	
		7B_BA2CA	Ba_2CaWO_6	29511	53.3	11225	7.86
					54.1	8175	
			Ag	46089	44.2	9090	
					44.7	14520	
		7B_W_B3A	W	232438	40.0	18360	61.99
					40.9	13560	
			Ag	45174	44.2	9105	
					44.7	15345	
7	Middle	7E_612BA	612	31495	31.1	33020	-2.96
					31.8	4120	
			$BaAl_2O_4$	11401	19.5	5940	3.61
					20.2	6120	
			$BaWO_4$	8307	26.2	4825	-0.69
					27.0	6400	
			Ag	39778	44.2	8160	
					44.7	15000	
		7E_BA2CA	Ba_2CaWO_6	31696	53.3	9950	13.04
					54.1	8850	
			Ag	37853	44.2	8145	

Sample	Pellet	.PIO file	Phase	Phase Intensity (counts)	Background Angle (°2θ)	Background Intensity (counts)	Calculated Phase %
					44.7	14550	
		7F_612BA	612	32733	31.1	35620	-5.53
					31.8	3880	
			$BaAl_2O_4$	11113	19.5	5720	5.26
					20.2	5600	
			$BaWO_4$	7851	26.2	4575	-0.79
					27.0	6175	
			Ag	39661	44.2	8595	
					44.7	14985	
		7F_BA2CA	Ba_2CaWO_6	32827	53.3	10600	12.54
					54.1	8600	
			Ag	39893	44.2	8505	
					44.7	14580	
7	Top	7C_612BA	612	29406	31.1	25740	10.98
					31.8	4440	
			$BaAl_2O_4$	11704	19.5	6320	2.66
					20.2	6480	
			$BaWO_4$	8578	26.2	5125	-0.77
					27.0	6350	
			Ag	35351	44.2	7095	
					44.7	15510	
		7C_BA2CA	Ba_2CaWO_6	27991	53.3	10000	11.36
					54.1	8925	
			Ag	35077	44.2	7080	
					44.7	14880	
		7C_W_B3A	W	241323	40.0	15210	94.34
					40.9	16020	
			Ag	35142	44.2	6930	
					44.7	14805	
		7D_612BA	612	30210	31.1	28080	4.08
					31.8	4640	
			$BaAl_2O_4$	11255	19.5	6160	1.90
					20.2	6120	
			$BaWO_4$	9077	26.2	5350	-0.65
					27.0	6900	
			Ag	42092	44.2	7890	
					44.7	14505	
		7D_BA2CA	Ba_2CaWO_6	28771	53.3	10500	8.64
					54.1	9200	
			Ag	41001	44.2	7725	
					44.7	14670	
		7D_W_B3A	W	232279	40.0	15720	72.12
					40.9	14310	
			Ag	39932	44.2	7815	
					44.7	14370	

REFERENCES

1. Wartenberg, V.H., and Reusch, H.J., "Schmelzdiagramme höchstfeuerfester Oxyde," Zeitschrift für Anorganische und Allgemeine Chemie, Vol. 207, No. 1, 1932, pp. 1-20.

2. Toropov, N.A., Reports of the Academy of Science, Vol. 1, No. 2-3, 1935.

3. Toropov, N.A., and Galakhov, F.Y., "Diagram of the State of the BaO - Al_2O_3 System," Reports of the USSR Academy of Sciences, Vol. 82, No. 1, 1952.

4. Appendino, P., "Research on the Most Basic Portion of the System Barium Oxide – Alumina," Ann. Chem., Vol. 61, 1971, pp. 822-830.

5. Appendino, P., "Research on the Ternary System CaO-BaO-Al_2O_3", Ceramurgia, Vol. 11, No. 2, 1972, pp. 103-106.

6. Wolten, G.M.,"An Appraisal of the Ternary System BaO –CaO –Al_2O_3," Aerospace Corp. Interim Report #SD-TR-80-67, 1980. Available from: NTIS, Springfield, VA: ADA-091684.

7. Asselanis, D., "Investigation of the Solidus and Liquidus Temperatures for the High Barium Oxide Portion of the BaO–CaO–Al_2O_3 System," Master's Thesis, School of Ceramic Engineering, Georgia Institute of Technology, Atlanta, Georgia, 1979.

8. Tarter, J.O., "Melting Characteristics of Barium Calcium Aluminate Dispenser Cathode Impregnants," Master's Thesis, School of Ceramic Engineering, Georgia Institute of Technology, Atlanta, Georgia, 1982.

9. Hill, D.N., Hann, R.E., and Suitch, P.R., "Thermochemistry of Dispenser Cathode Impregnant Materials: Phase Equilibria in the BaO-CaO-Al_2O_3 System," Rome Air Development Center, Rept. RADC-TR-87-54, 1987.

10. Kwestroo, W., van Hal, H.A.M., and Langereis, C., "Compounds in the System BaO-Sc_2O_3," Materials Research Bulletin, Vol. 9, 1974, pp. 1623-1630.

11. Persianova, S.N., Soloveichik, A.I., and Yudinskaya, I.V., Elektron. Tekh., No. 12, 1968, p. 125.

12. Kovba, L.M., Lykova, L.N., Paromova, M.V., and Kalinina, T.A., "X-ray Diffraction and Thermographic Investigation of Compounds in the BaO-Sc_2O_3 System," Doklady Akademii Nauk SSSR, Vol. 260, No. 4, 1981, pp. 898-900.

13. Magnus, S.H., "An Investigation of the Relationship Between the Thermochemistry and Emission Behavior of Thermionic Cathodes Based on the BaO-Sc_2O_3-WO_3 Ternary System," Doctoral Thesis, School of Materials Science and Engineering, Georgia Institute of Technology, Atlanta, Georgia, 1996.

14. Janowski, M.P., "An Investigation of the High Barium Oxide Portion of the BaO–Sc_2O_3–Al_2O_3 Ternary Phase Diagram," Master's Thesis, School of Materials Science and Engineering, Georgia Institute of Technology, Atlanta, Georgia, 1996.

15. Ohlinger, W.L. and Rebstock, K.M., "Barium Calcium Aluminate Impregnant Materials: Interaction with Sea-Level Ambient Atmosphere and Decomposition Behaviors of Reaction Products," 30th AIAA/ASME/SAE/ASEE Joint Propulsion Conference, AIAA Paper No. 94-3135, June 27-29, 1994.

16. Wallmark, S. and Westgren, A., "X-Ray Analysis of Barium Aluminates,"Arkiv for Kemi, Mineralogi och Geologi, 12B, No. 35, 1937, pp. 1-4.

17. Ahmed, A.H.M. and Dent Glasser, L.S., "Barium Aluminate Hydrates: Part V. $2BaO{\cdot}Al_2O_3{\cdot}2H_2O$ and $2BaO{\cdot}Al_2O_3$," Journal of Chemical Technology and Biotechnology, Vol. 42, 1988, pp. 31-38.

18. Habashy, G.M. and Kolta, G.A., "Thermal Decomposition of the Hydrates of Barium Hydroxide," Journal of Inorganic and Nuclear Chemistry, Vol. 34, 1972, pp. 57-67.

19. Brodie, I. and Jenkins, R.O., "Evaporation of Barium from Impregnated Cathodes," Journal of Electronics, Vol. 2, 1957, pp. 457-476.

20. Kreidler, E.R., "Phase Equilibriums in the System Calcium Oxide-Barium Oxide-Tungsten Oxide," Journal of the American Ceramic Society, Vol. 55, No. 10, 1972, pp. 514-519.

21. Rittner, E.S., Rutledge, W.C., and Ahlert, R.H., "On the Mechanism of Operation of the Barium Aluminate Impregnated Cathode," Journal of Applied Physics, Vol. 28, No. 12, 1957, pp. 1468-1473.

22. Kreidler, E.R., "Phase Equilibria in the System CaO-BaO-WO_3," Journal of The American Ceramic Society, Vol. 55, No. 10, 1972, pp. 514-519.

23. Shroff, A.M., Palluel, P., and Tonnerre, J.C., "Performance and Life Tests of Various Types of Impregnated Cathodes," Applications of Surface Science, Vol. 8, 1981, pp. 36-49.

24. Sarver-Verhey, T.R., "Destructive Evaluation of a Xenon Hollow Cathode After a 28,000 Hour Life Test," 34th AIAA/ASME/SAE/ASEE Joint Propulsion Confer-

ence and Exhibit Proceedings, AIAA Paper No. 98-3482, July 13-15, 1998. Available from: NTIS, Springfield, VA.

25. Jander, W., "Reaction in Solid State at High Temperatures: I, Rate of Reaction for an Endothermic Change," Zeitschrift für Anorganische und Allgemeine Chemie, Vol. 163, No. 1, 1927, pp. 1-30.

26. Kingery, W.D., Bowen, H.K., and Uhlmann, D.R., *Introduction to Ceramics*. New York: John Wiley & Sons, second ed., 1976.

27. Blum, S.L. and Li, P.C., "Kinetics of Nickel Ferrite Formation," Journal of the American Ceramic Society, Vol. 44, 1961, pp. 611-617.

28. Carter, R.E., "Kinetic Model for Solid-State Reactions," Journal of Chemical Physics, Vol. 34, No. 6, 1961, pp. 2010-2015: Vol. 35, 1961, pp. 1137-1138.

29. Ginstling, A.M. and Brounshtein, B.I., "Kinetics of the Reaction of Polydisperse Mixtures of Crystalline Substances," Journal of Applied Chemistry U.S.S.R. (English Translation), Vol. 29, 1956, p. 2009-2011.

30. He, X., Zhang, Q., and Ling, Z., "Kinetics and Magnetic Properties of Sol-Gel Derived NiZn Ferrite-SiO_2 Composites," Materials Letters, Vol. 57, 2003, pp. 3031-3036.

31. Bailey, J.T. and Russell Jr., R., "Sintered Spinel Ceramics," American Ceramic Society Bulletin, Vol. 47, No. 11, 1968, pp. 1025-1029.

32. Suitch, P.R., "Thermochemical Reactions in Tungsten-Matrix Dispenser Cathodes Impregnated with Various Barium-Calcium-Aluminates," Doctoral Dissertation, School of Materials Engineering, Georgia Institute of Technology, Atlanta, Georgia, 1987.

33. Margrave, J.L, "Vapour Pressure," *Physico-Chemical Measurements at High Temperatures*. London: Butterworths Scientific Publications, 1959, pp. 225-246.

34. Ruff and Bergdahl, Zeitschrift für Anorganische und Allgemeine Chemie, Vol. 106, 1910, p. 76.

35. von Wartenberg, Zeitschrift für Elektrochemie, Vol. 19, 1913, p. 482.

36. Langmuir, I., "The Vapor Pressure of Metallic Tungsten," The Physical Review, Second Series, Vol. 2, No. 5, 1913, pp. 329-342.

37. Speiser, R. and Spretnak, J.W., "Determination of the Vapor Pressure of Metals and Alloys," The Ohio State University, Columbus, Ohio (unpublished).

38. Inghram, M.G., Chupka, W.A., and Porter, R.F., "Mass Spectrometric Study of Barium Oxide Vapor," Journal of Chemical Physics, Vol. 23, No. 11, 1955, pp. 2159-2165.

39. Hilpert, K. and Gerads, H., "Mass Spectrometric Investigation of the Vaporization of BaO from Knudsen Cells Made of Mo, Pt, Graphite, and Al_2O_3," High Temperature Science, Vol. 7, 1975, pp. 11-19.

40. Hilpert, K., Beske, H., and Naoumidis, A., "Mass Spectrometric Study of the Vaporization of $Ba_3Al_2O_6$ and $BaAl_{12}O_{19}$," High Temperature Science, Vol. 7, 1975, pp. 159-166.

41. Copland, E.H. and Jacobson, N.S., "Thermodynamic Activity Measurements with Knudsen Cell Mass Spectrometry", The Electrochemical Society *Interface*, 2001, pp. 28-31.

42. Goodrum, J.W. and Siesel, E.M., "Thermogravimetric Analysis for Boiling Points and Vapour Pressure," Journal of Thermal Analysis, Vol. 46, 1996, pp. 1251-1258.

43. Zavitsanos, P.D. (General Electric Missile and Space Division), "The Vapor Pressure of Barium." 1968, Report No. 68SD331. 17 p. Available from: NTIS, Springfield, VA: AD-713715.

44. Ruff, O. and Hartmann, H., "Researches at High Temperatures. XVII. The Vapor Pressures of the Alkaline Earth Metals," Zeitschrift für Anorganische und Allgemeine Chemie, Vol. 133, 1924, pp. 29-45.

45. Hartmann, H. and Schneider, R., "Boiling Temperatures of Magnesium, Calcium, Strontium, Barium, and Lithium," Zeitschrift für Anorganische und Allgemeine Chemie, Vol. 180, 1929, pp. 275-283.

46. Rudberg, E. and Lempert, J., "The Vapor Pressure of Barium," Journal of Chemical Physics, Vol. 3, 1935, pp. 627-631.

47. Karmyshin, Y.V., Totskii, E.E. and Shpil'rain, E.E., "Experimental Study of the Saturated Vapor Pressure of Barium," High Temperature, Vol. 12, No. 3, 1974, pp. 445-449.

48. Jacob, K.T. and Waseda, Y., "The Vapour Pressures of Barium and Strontium," Journal of the Less-Common Metals, Vol. 139, 1988, pp. 249-259.

49. Claassen, A. and Veenemans, C.F., "Dampfdruckbestimmungen von BaO, SrO, CaO und deren Mischungen aus Verdampfungsgeschwindigkeitsmessungen," Zeitschrift für Physik, Vol. 80, 1933, pp. 342-351.

50. Blewett, J.P., Liebhafsky, H.A., and Hennelly, E.F., "The Vapor Pressure and Rate of Evaporation of Barium Oxide," Journal of Chemical Physics, Vol. 7, 1939, pp. 478-484.

51. Newbury, R.S., Barton, G.W., and Searcy, A.W., "Vapor Species of the Barium-Oxygen System," The Journal of Chemical Physics, Vol. 48, No. 2, 1968, pp. 793-800.

52. Lipeles, R.A. and Kan, H.K.A., "Chemical Stability of Barium Calcium Aluminate Dispenser Cathode Impregnants," Applications of Surface Science, Vol. 16, 1983, pp. 189-206.

53. Barin, I. and Knacke, O., *Thermodynamic Properties of Inorganic Substances*, Dusseldorf: Springer, Berlin, and Stahleisen, 1973.

54. Hilpert, K., Naoumidis, A., and Wolff, G. High Temperature Science, Vol. 7, 1975.

55. Resulhina, T.N., Levitskii, V.A., and Frenkel, M. Y.Izv. Akad. Nauk SSSR, Neorgan. Mater. Vol. 2, 1966, p. 325.

56. Zalm, P. and van Stratum, A.J.A., "Osmium Dispenser Cathodes," Philips Technical Review, Vol. 27, No. 3/4, 1966, pp. 69-75.

57. Cullity, B.D., *Elements of X-Ray Diffraction*, 2nd ed. Reading, Massachusetts: Addison-Wesley Publishing Company, Inc., 1978.

58. Doerner, R.P., Baldwin, M.J., Krasheninnikov, S.I., Schmid, K., and Tynan, G.R., "Erosion of Materials at High Temperature," NEXIS Cathode Workshop, Georgia Institute of Technology, Atlanta, GA, June 17, 2004.

59. Hann Jr., R.E., "Phase Equilibria of the High-Baria Portion of the BaO-CaO-Al_2O_3 System," Doctoral Thesis, School of Materials Science and Engineering, Georgia Institute of Technology, Atlanta, Georgia, 1987.

60. Reed, J.S., "Principles of Ceramic Processing." New York: John Wiley & Sons, Inc., 1988.